Cell-laden micropatterns using self-assembled cell-ECM microtissues in soft pectin hydrogels, for skin regeneration

Fábio Jorge OliveiraRangel

Mestrado em Biologia Molecular e Celular

Departamento de Biologia

2014-2015

Orientador

Pedro Granja, Ph.D, Professor Auxiliar, FEUP

Coorientador

Aureliana Sousa, Ph.D, INEB

Todas as correções determinadas pelo júri, e só essas, foram efetuadas.

O Presidente do Júri,

Porto, _____/_____/_____

Dissertação de candidatura ao grau de Mestre em Biologia Celular e Molecular submetida à Faculdade de Ciências da Universidade do Porto.

O presente trabalho foi desenvolvido sob a orientação científica do Professor Doutor Pedro Granja, com co-orientação pela Doutora Aureliana Sousa, no INEB (Instituto Nacional de Engenharia Biomédica), I^3S (Instituto de Investigação e Inovação em Saúde).

Dissertation for applying to a Master's Degree in Cell and Molecular Biology, submitted to the Faculty of Sciences of the University of Porto.

The present work was developed under the scientific supervision of Professor Bruno Silva-Santos, co-supervised by Doutora Auraliana Filipa and was done at INEB (Instituto Nacional de Engenharia Biomédica), I^3S (Instituto de Investigação e Inovação em Saúde

Aknowledgements

First of all, I would like to thank Professor Doutor Pedro Granja. His passion for this work drew me to the field with the feeling that I always belonged there. Thank you for pushing me to do my best.

To the person that contributed the most to my growth, Doutora Aureliana Sousa, thank you for all the knowledge you passed on to me on both the scientifical and personal fields. Thank you for allowing me to fall on my face.

To my collegues in INEB, who welcomed me into the family and helped me whenever I needed.

To my friends, Helena Brigas and Miguel Rocha, who stayed with me and shared their joys and sorows. To Romeu Catarino, Daniela Gonzáles, André Resende, Bárbara Andrade, João Teixeira, André Silva, André Resende e Paulo Neves, who got me out of my house so I can clear my head.

Finally, and foremost, to my family. Thanks to my parents Fatima and Jorge Rangel to always supported me at the economic, emotional and intelectual levels.To my girlfriend, Marta Monteiro who, even when away, gave me strenght to carry on. To my sister Catarina and Daniel who bugged me when I needed to. To Sr. José and Dona Isabel who offered me home and distraction when I needed.

Abstract

Advanced skin regeneration therapies can combine biomaterials, cells, growth factors and advanced biomanufacturing techniques for the fabrication of constructs that will ultimately mimic native skin anatomy. Regardless of the specific tissue-engineering approach for *in vitro* artificial skin substitute production, to engineer functional skin, the formation of an efficient vascular network is required.

Aiming to develop a strategy to improve constructs microvascularization with fibroblasts support endothelial cells in the formation of self-assembled vascular structures, this study allowed the dissection of human umbilical vein endothelial cells (HUVEC) and neonatal human dermal fibroblasts (NHDFs) behavior in a 3D microenvironment. We addressed for the first time the effect of several culture parameters on cells behavior when embedded on RGD-grafted soft pectin hydrogels. Conditions such as media composition, cell density, cell type to type ratio and polymer concentration were optimized on standard 2D culture conditions. The results obtained allowed us to choose the best conditions to proceed into a 3D experimental setup.

A 3:1 ratio of M199 to DMEM media was selected for HUVEC:NHDFs co-cultures and we also determined that low HUVEC to NHDFs ratios, in 2D environments led to NHDFs spreading in detriment of HUVEC proliferation while higher ratios sustained a controlled environment where HUVECs were able to grow and assemble in spider web-like structures. In a three dimensional context, Cell behavior parameters displayed better outcomes for lower hydrogel formulations (1.5% w/v) and higher cell densities ($1.5x10^7$ cells.mL^{-1}).. Fibroblasts formed spheroidss and contracted the matrix, while maintaining the metabolic activity, in a matrix and cell density-dependent way, with 1.5% (w/v) pectin hydrogels embedded with 1x107cells.mL-1 demonstrating microtissues formation.

Based on combination of NHDFs and HUVECs, a cocuture systems were developed in soft pectin hydrogel matrices. Within these, HUVEC survival was increased, and fibroiblast spheroids formation was observed. Although further investigation is needed, we developed a a three-dimensional co-culture system in RGD-grafted soft pectin hydrogel in which fibroblasts support endothelial cells, and established this techniques as a promising strategy for *in vitro* microvascularization towards skin regeneration therapies.

Resumo

As terapias avançadas de regeneração da pele combinam biomateriais, células, fatores de crescimento e técnicas avançadas de biofabrico de estruturas que, em última análise, visam mimetizar a anatomia da pele. Independentemente da abordagem *in vitro* usada em engenharia de tecidos para regeneração de pele artificial, para produzir uma pele funcional, é necessária a formação de uma rede vascular eficiente.

Com o objetivo de desenvolver uma estratégia para melhorar a microvascularização *in vitro*, este estudo visou dissecar o comportamento de células endoteliais da veia umbilical humana (HUVECs) e fibroblastos dérmicos humanos neonatais (HDFns) num microambiente 3D. Abordamos, pela primeira vez, os efeitos de vários parâmetros de cultura no comportamento das células de em cultura em matrizes macias de hidrogéis de pectina modificados com RGD. Condições como a composição do meio, a densidade celular e a proporção entre os tipos de células foram optimizadas em condições de cultura 2D padrão. Os resultados obtidos permitiram-nos escolher as melhores condições para proceder às experiencias em ambientes 3D.

Um meio composto por um rácio de 3:1 de M199 para DMEM, foi selecionado para a a cocultura de HUVEC:HDFns. Determinamos também que, em condições de cultura 2D, um baixo rácio de HUVEC para HDFns levou à proliferação de HDFns em detrimento do crescimento das HUVEC enquanto rácios mais elevados sustentaram um ambiente onde as HUVECs foram capazes de crescer e estabelecer estruturas numa formação semelhante a teias de aranha. Os parâmetros de comportamento celular sobre os quais nos debruçamos exibiram melhores resultados para formulações de hidrogéis com concentrações de pectina menores (1.5% w/v) e concentrações altas de células ($1.5x10^7$ celulas.mL^{-1}). Os fibroblastos, demonstraram-se capazes de formar esferóides e contrair a matriz, mantendo a atividade metabólica, de uma forma dependente da densidade celular e da matriz, verificando-se que, aquando do aprisionamento de $1x10^7$ celulas.mL^{-1} em hidrogéis de pectina com uma concentração de 1.5% (w/v), ocorreu a formação de microtecidos.

Com base na combinação de NHDFs e HUVECs, foram desenvolvidos dois sistemas de cocultura em hidrogéis de pectina macia. Nestes sistemas, a sobrevivência das HUVECs foi aumentada e a formação de esferóides foi observada nos fibroblastos. Embora seja necessária uma investigação mais aprofundada, desenvolvemos um sistema de cocultura tridimensional em hidrogéis macios de pectina transformada com RGD no qual os fibroblastos suportam as células endoteliais. A técnica neste trabalho

estabelecida apresenta-se assim como uma estratégia promissora para a a microvascularização *in vitro* tendo em vista terapias de regeneração da pele.

Table of contents

List of Figures

List of Tables

List of Abbreviations

2D – Two-dimensional

3D – Three-dimensional

bFGF - Basic fibroblast growth factor

Ca^{2+} - Calcium ions

$CaCO_3$ – Calcium carbonate

CD31 - Cluster of differentiation 31

DAPI - 4',6-diamidino-2-phenylindole

DM - Degree of methylation

DMEM - Dulbecco's Modified Eagle Medium

DNA – Deoxyribonucleic acid

dsDNA – Double-stranded Deoxyribonucleic acid

ECGS - Endothelial cell growth supplement

ECM - Extracellular matrix

ECs - Endothelial cells

EDC - (N-(3-dimethylaminopropyl)-N'-ethylcarbodiimide)

EDTA - Ethylenediaminetetraacetic acid

Em - Emission

Ex - Exitation

FBS - Fetal bovine serum

FBs - Fibroblasts

FN - Fibronectin

G4RGDSP - $(Glycine)_4$-Arginine-Glycine-Aspartic acid-Serine-Proline

GAGs - Glycosaminoglycans

GalA - (1–4)-linked-α-D-galacturonic acid

GDL- *D*-glucono-*d*-lactone

NHDFs - Neonatal human dermal fibroblasts

HGA - Homogalacturonan

HM - High methoxyl

HUVECs - Human umbilical vein endothelial cells

LM - Low methoxyl

MES - 2-(N-morpholino) ethanesulfonic acid buffer

PBS - Phosphate-buffered saline

PCL - Poly(e-carpolactone)

PEG - Poly(ethylene glycol)

Pen - Penicillin

PFA – Paraformaldehyde

PGA - Poly(glycolic acid)

pHEMA - Poly(2-hydroxyethyl methacrylate)

PLA - Poly(lactic acid)

PLGA - Poly(lactic-co-glycolic acid)

PMMA - Poly(methyl methacrylate)

PVGLIG - Proline-valine-glycine-leucine-isoleucine-glycine

RFUs - Relative fluorescence units

RGD - Arginine-Glycine-Aspartic acid

RG-I - Rhamnogalacturonan-I

RG-II - Rhamnogalacturonan-II

RPM – Rotations per minute

RT – Room temperature

Strep - Streptomycin

sulfo-NHS - N-hydroxy-sulfosuccinimide

TBS - Tris-buffered saline

TE – Tris-EDTA buffer

UV –Ultraviolet

VE-cadherin (CD144) – Vascular endothelial cadherin

VEGF - Vascular endothelial growth factor

VSMCs - Vascular smooth muscle cells

vWF - von Willebrand factor

α-SMA - α-smooth muscle actin

Introduction

1.1. Skin

Skin is the largest organ of the human body, representing roughly one tenth of the body mass (Metcalfe & Ferguson 2006; Groeber et al., 2011) performing very important functions besides its obvious aesthetical function. Skin performs several functions: acts as a protective barrier, preventing dehydration, limiting organism invasion by potentially noxious agents (e.g. toxins, virus, UV radiation) also by impermeabilizing the body, helps in the thermoregulation of the body, works as a cushion, among others (Metcalfe & Ferguson 2007; Yildirimer et al., 2012; Pereira et al., 2013).

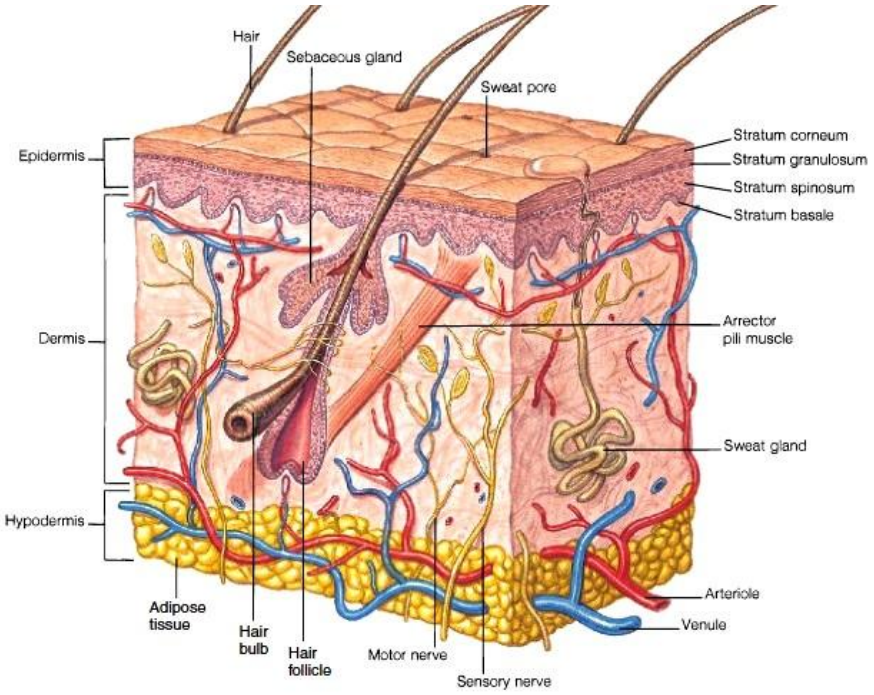

Figure 1. A schematic of the structure of skin. Image from Naturally Healthy Skin (http://www.naturallyhealthyskin.org/anatomy-of-the-skin/the-dermis/dermis-anatomy-of-the-skin/

The skin is composed of three layers: epidermis, dermis and hypodermis (Figure 1) (hypodermis (Groeber et al., 2011; Pereira et al., 2013). The epidermis is thin and totally cellular, mainly composed of keratinocytes but also containing other cell types, such as Langerhans cells and melanocytes. Due to the constant exposure, homeostasis is achieved by constant substitution of the environment-exposed cells by cell migration from the basal layers, which, in turn, are composed of epidermal stem cells able of self-renewal and repair (Alonso et al., 2003; Chunmeng & Tianmin, 2004; Metcalfe & Ferguson 2007; Pereira et al., 2013). In addition, the skin appendages (e.g hair, nails, sweat glands and sebaceous glands) are derived from and linked to the

epidermal layer presenting however deep projections into the dermal layer (Martin, 1997). Situated directly below the epidermis is the dermis. This layer constitutes the bulk of the skin, providing support and nourishment. It contains vascularized extracellular matrix (ECM) rich in collagen, elastin and glycosaminoglycans (GAGs), being responsible for the elasticity and mechanical integrity (Jones et al., 2002; Metcalfe & Ferguson 2007; Groeber et al., 2011). These properties are modulated by fibroblasts, the main cell type in the dermal layer and the the main source of ECM (Berthod et al., 2006). Furthermore, fibroblasts also produce remodeling enzymes, such as proteases and collagenases, playing an important role in wound healing (Ratner et al., 2004). Present in this layer, but in lesser amounts, are also endothelial cells and smooth muscle cells, composing a vascular system, mast cells, which are part of the immune system being responsible for the early recognition of pathogens and cutaneous sensory nerves that pass through dermis into the epidermal layer (Metcalfe & Ferguson 2007; Urb & Sheppard 2012; Pereira et al., 2013). The third layer, the hypodermis, is a well vascularized area mostly composed of adipose tissue, contributing for the mechanical and thermoregulatory properties of the skin as well as acting as an energy source (Metcalfe & Ferguson 2007; Yildirimer et al., 2012; Pereira et al., 2013).

1.1.1 Skin lesions and regenerative medicine

Skin lesions, whether caused by physical/chemical factors (e.g. burns, lacerations, ulcers, acute wounds, surgery, among others) or by chronicle diseases are fairly common (Martin, 1997; Groeber et al., 2011). Upon injury that leads to the disruption of the structure and function of natural tissue, under certain physiological circumstances, skin displays a complex and continuous natural process, overlapping events of hemostasis, inflammation, migration, proliferation and differentiation. These occur due to a constant environmental change that exposes cells to complex molecular patterns which sets off a series of metabolic cascades, propelling the wound through the phases of healing, overlapping events of hemostasis, inflammation, migration, proliferation and differentiation (Figure 2) (Mutsaers et al., 1997; Martin, 1997; Guo & DiPietro, 2010; Häggström et al., 2010).

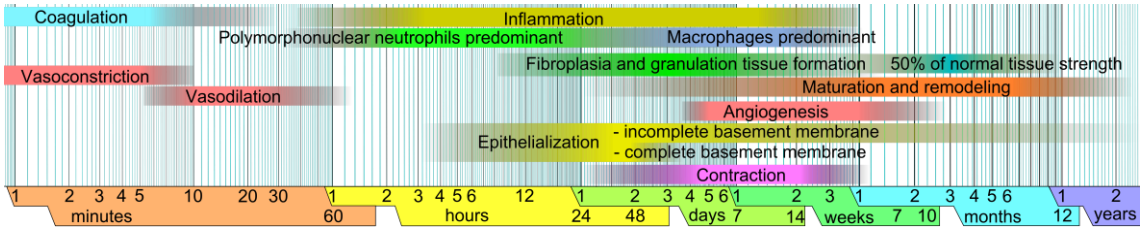

Figure 2. Chronological representation of the phases of wound healing. Adapted from Häggström *et al.*, 2010.

However, depending on the lesion extent, wound environmental exposure can pose a high infection risk that can lead to deeper skin damage, tissue necrosis or, ultimately, death. As such, skin lesions must be treated as a critical issue in healthcare (Zöller et al., 2014). In current medical treatments, clinical strategies rely on the use of closure materials that may act solely as a barrier while natural wound healing occurs or actively contribute for the restoration of the epidermal function while becoming incorporated into the healing wound. Nowadays, it is possible to find several solutions for skin wound treatment (Guo & DiPietro, 2010). Depending on the wound type, depth, extension and the patient, several strategies can be applied. For superficial lesions (mainly affecting the epidermis), creams and ointments are used for disinfection, cleaning, debridement or to help the wound healing process. Although still used, due to their properties their limited permanency in the human body, these solutions have been substituted for more advanced strategies (Boateng et al., 2008). Wound dressings have been widely used due to their low cost and effectiveness. This medical strategy consists in the application of natural or synthetic material over the wound protecting it from the environment. Traditional wound dressings (e.g. bandages, cotton wool, lint and gauzes), covered the wound, keeping the wound dry and preventing the entry of pathogens into the wound (Boateng et al., 2008; Pereira et al., 2013).

Nowadays, accompanying the evolution in the science and technological fields, wound dressings present more advanced solutions for wound healing. Obtained from natural or synthetic sources, modern wound dressings are available as films, foams or gels (Boateng et al., 2008). Based on the concept of creating an optimal environment, which includes an exudation control allowing a moist, non-detrimental environment, effective oxygen circulation aiding the regeneration process, good adhesion to the lesion surface and low pathogen penetration, while minimizing maceration and scar formation, (Stephen-Haynes et al., 2014), several modern wound dressings were developed, as reviewed by Pereira et al. (2013). Moreover, some dressings can even act as drug delivery systems, incorporating the therapeutic agent releasing it in the wound bed (Elsner & Zilberman, 2010; Pereira et al., 2013; Boateng et al., 2015; Momoh et al., 2015). However, due to the complexity of the healing process and the wide variety of

skin wounds existent, no single dress is able to fulfill the requirements for full skin recovery. Notwithstanding the importance of the referred methods for skin regeneration therapies, in cases of severe lesions in the dermis or hypodermis, a complex treatment is required. At the present day, autografts, surgical reconstruction using the patient own skin, are the “gold standard” procedure (Goldberg, 1992; MacNeil, 2007). This strategy however presents limitations depending on the lesion extension and due to the creation of additional surgical sites (Goldberg, 1992). Another solution is the use of allografts, surgical reconstruction using another patient skin. This, however, can pose complication at both ethical and medical levels, as another patient is exposed to a risk situation while also subjecting the wounded patient to a graft that can potentially carry a disease or suffer immunological rejection (Goldberg, 1992).

A potential solution to this problem is to approach this from a tissue engineering–based standpoint for *de novo* organogenesis, using biomaterial scaffolds and a person’s own cells to grow or fabricate skin substitutes (Cuono et al., 1986; Zöller et al., 2014). To date, there are several clinically available skin substitutes, with these being divided into epidermal, dermal, and dermo-epidermal tissue-engineered constructs. As mimicking the extracellular matrix (ECM) structural integrity and function is of key importance, several strategies are revolving around collagen-based matrices (Boyd et al., 2007; Johnen et al., 2008; Cen et al., 2008). Other skin substitute biomaterials used as matrices are chitosan (Mao et al., 2003; Mohd et al., 2013), hyaluronic acid (Park et al., 2004; Wang et al., 2006), among others. Despite recent developments wound healing, the techniques and biomaterials available present significant limitation for skin regeneration. To our knowledge, at the present time, there are no models of skin substitutes that fulfill all the criteria, replicating the anatomical and physiological requirements for biological stability at epidermal and/or dermal. Additionally, available skin substitutes suffer from poor integration, scarring and lack of differentiated structures (e.g. hair and sebaceous glands), contrasting with the aesthetics of uninjured skin (Boateng et al., 2008). Advanced skin regeneration therapies already combine biomaterials, cells, growth factors and advanced biomanufacturing techniques for the fabrication of constructs that mimic skin anatomy. Recently, several methods have been developed to spatially encode local properties to 3D materials-based culture systems. These biofabrication techniques are capable of constructing micropatterned materials, with a high degree of control, by finely tuning and defining material geometries, localization of biomolecular cues, and other mechanical properties, enabling a precise control over the bulk material properties (Nichol & Khademhosseini, 2009; Nikkhah et al., 2012; Pataky et al., 2012; Culver et al., 2012). These are designated bottom up approaches and consist on the formulation of tissue building

blocks with specific microarchitectural features for modular assembly, in an attempt to replicate the heterogeneous nature of endogenous tissues and organs. Another used approach to is to use tissue engineering strategies typically that employs a “top-down” These consist on seeding cells into biomaterial matrices capable of recreating biomimetic structures, exploiting the innate abilities of cells to sense their local environment through cell–cell and cell–extracellular matrix (ECM), self-assembling into complex networks (Dean et al., 2007; Seidlits et al., 2011; Maia et al., 2014). This strategy relies on the ability of the cells to reconstruct the intricate microarchitectural and functional features of natural microenvironments to achieve the desired biological effect. However, for a given skin substitute to attach promptly, a vascularized wound bed is required. Deep wounds that affect the dermal layer constitute a problem. If the skin substitute surpasses a certain thickness nutrient diffusion is limited and the vascularization process is too slow, resulting in necrosis and graft loss. As such, any tissue-engineering constructs that aims to mimic natural tissues and, ultimately, organs, must ideally conjugate all the key components – cells, extracellular matrix (ECM), and vasculature – in precise geometries (Auger et al., 2013; Battiston et al, 2014).

1.2. Vascularization

From the various obstacles for tissue engineered skin substitutes, the inability of the grafts to acquire proper vascularization has been proposed as the most likely reason for deleterious effect on epidermal survival human tissue-engineered skin constructs. The inability to properly assemble a vascular structure within the graft, leads to necrosis at the tissue core, and poor survival due to ischemic injury (Rivron et al., 2008; Auger et al., 2013). Regardless of the specific tissue-engineering approach to create artificial skin any construct that involves living cells needs to fulfill the conditions in which cells are able survive and redeem their biological functions. Reconstructed tissues need to be able to access to oxygen and nutrients, as well as elimination of carbon dioxide and other cellular waste products (Folkman & Hochberg, 1973; Novosel et al., 2011; Auger et al., 2013). It is, therefore, paramount, for the successful transplantation of human tissue-engineered constructs, the formation of a vascular network. At both the stage of in vitro growth and assemble and after the patient implantation of the graft (Rivron et al., 2008; Novosel et al., 2011; Auger et al., 2013).

1.2.1 Endothelial cells

Blood vessels are a multi-cellular system composed of vascular smooth muscle cells (VSMCs), fibroblasts and endothelial cells (ECs) (Ratner et al., 2004). Vascular networks, ranging from large sized vessels, as are arteries and veins, to the micro-sized vasculature networks formed within organs, are lined with a single layer of endothelial cells (ECs), on which one part of the surface defines the lumen while the other is in contact with a highly specialized EC, the basement membrane. In order to sustain their tubular architecture and allow a contractile behavior in these structures, ECs are enveloped by mural cells (e.g. pericytes, VSMCs). EC formation occurs mainly through mesodermal precursor's differentiation of hemangioblasts and/or angioblasts, a critical process in embryogenesis and tumor formation (Augustin et al., 1994; Mani et al., 2008). These cells form a barrier that, due to their capacity of extravasation and high surface-to-volume ratio are capable of actively transport small molecules, macromolecules and hormones, while also performing multiple functions depending on the location and size of the blood vessel that they are lining (Ruoslahti & Rajotte, 2000, Bouis et al., 2001; Pinkney et al., 1997). As such, ECs play an important role mediating many physiological functions such as hemostasis maintenance, vasomotor tone, blood cell trafficking, permeability, proliferation, survival, and innate and adaptive immunity (Aird, 2007).

There are two processes from which neovascularization can take place: angiogenesis, a process through which new blood vessels are formed from preexisting ones, and vasculogenesis, the generation of a new vascular network from endothelial progenitor cells (EPCs) in the absence of preexisting blood vessels (Luttun et al., 2002). These capillary generation events involve a complex sequence of events, which cell adhesion, migration, alignment, protease secretion, and tubule formation. Throughout these, ECs must be exposed to growth factors interaction and mechanical cues as well as cell-cell and cell-EMC interactions all of which must be precisely timed and with the correct concentrations (Yamamoto et al., 2003; Lokmic et al., 2008; Arnaoutova et al., 2009). ECs can be isolated from different endothelium. With proper specific medium supplementation, several ECs population like human umbilical vein endothelial cells (HUVECs) or human dermal microvascular endothelial cells (HDMECs) can be isolated and cultured *in vitro*. Although they possess several common characteristics like cell-cell contact inhibition when confluent, similar morphology and identical expression of cellular markers, choosing the source of ECs is of critical issue. Due to the endothelium

heterogeneity, site specific properties of the ECs could be translated *in vitro*, originating different outcomes when exposed to the same factors. Throughout the years, the phenotypic heterogeneity of the endothelium has been characterized and described recurring lectin staining, immunohistochemistry, in situ hybridization and real-time intravital microscopy, being, nowadays possible to select the most appropriate EC type for each design (Boius, 2001; Aird, 2003; Aird, 2012).

Among these, human umbilical vein endothelial cells (HUVECs) have been of critical importance, largely contributing for scientific knowledge breakthroughs in molecular medicine providing insights over ECs embryogenesis, angiogenesis, vasculogenesis and pathology, at both cellular and molecular levels (Nakatsu et al., 2003; Poliseno et al., 2006; Anand et al., 2010). HUVECs are easily available, free from any pathological process and they are physiologically more relevant than many established cell lines (Cooper & Sefton, 2011).Initial passages of these cells, maintain nearly all of the features of native vascular endothelial cells expressing several endothelial cell specific markers such as: von Willebrand factor a large adhesive glycoprotein that, in the blood, serves as a stabilizing factor for Factor VIII (Zanetta et al., 2000); platelet endothelial cell adhesion molecule-1 (PECAM or CD31), an endothelial specific adhesion molecule (Goldberger et al., 1994); VE-cadherin (CD144), a cadherin expressed in the tight junctions (Esser et al., 1998); and specific signaling pathways receptors markers for vascular endothelial growth factor (VEGF) and fibroblast growth factor (FGF) (Esser et al., 1998; Salcedo et al., 1999). HUVECs have an average life span of 10 serial passages, time after which the cells enter senescence, tending to stop proliferation, form giant multicellular aggregates and dye (Jaffe et al.,1973). Although recovered from a major vessel, HUVECs have been proven capable of forming microvascular structures (Kenneth et al., 2006; Sorrell et al., 2007; Zheng et al., 2012). All summed up, HUVECs 3D culture presents itself as a promising strategy for *in vitro* microvasculature formation and characterization.

To recover functional endothelial cell self-assembled into microvascular structures could presents itself as a major advance in biomanufacturing techniques forthcoming the construction of functional grafts for patient transplantati**o**n.

1.2.2 Vascularization strategies

New vessel formation is essential for wound healing. As such, to culture cells under 3D conditions using a material that can mimic the ECM, and recapitulate some key aspects of the native cellular microenvironment is paramount. Although several 2D

strategies were conducted, in 1983, Montesano et al. (1983) evidenced the importance of culture ECs in a three dimensional environment. Bidimensional environments fail to mimic several cues necessary for the creation of a specific cellular organization. Nowadays, 3D cell cultures stand as essential models for the study of cell biology, as well as support matrices that can incorporate mechanical and biochemical stimuli directly conveyed by the ECM. As such, *in vitro* 3D microvascularization is highly dependent on the composition and properties of biomaterial matrix along with the presence of precisely timed delivery of angiogenic growth factors (Montesano et al., 1983; Nakatsu et al., 2003; Sieminski et al., 2004; Ghajar et al., 2008), being necessary for any attempt that intends to mimic this process, a fine tune of the conditions to which ECs will be exposed. Since the perception that angiogenesis could be achieved, several *in vitro* (Folkman & Haudenschild, 1980), several studies attempted to mimic the natural conditions necessary for this process to occur. Although some single component matrices (e.g. collagen, Matrigel and fibrin), when coupled with specialized growth factors, were able to support tube formation (Montesano et al., 1983; Montesano et al., 1986; Chalupowicz et al., 1995; Bach et al., 1998; Dai et al., 2004; Kleinman & Martin, 2005), attempts to monoculturing ECs on biomaterial matrices for microvasculature formation has not been an effective strategy. In monocultures, ECs seem unable to survive and proliferate and, subsequently, self-assembly into tube-like structures is not archived (Janvier et al., 1997). In addition, it is important, that newly formed structures mature and form stable structures. This implies that the interconnected capillary structures are self-sustained after the initial conditions are not present, which is hard to achieve in monoculture as capillary structural sustainability is dependent on the formation of highly specific bonds between ECs and ECM as well as the envelopment of these cells by mural cells (Ribatti et al., 2011). Although during angiogenesis ECs migrate and make sprouts without mural cells' perivascular cells (PCs) are among the first cells responsible for the invasion of newly vascularized tissues, determining the location of sprout formation and guiding newly formed vessels by interaction with EC via paracrine communication (Ribatti et al., 2011).

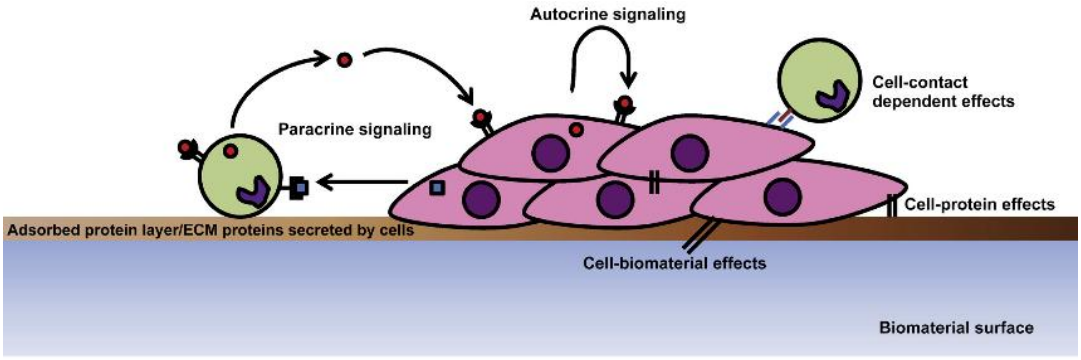

Figure 3. Schematic representation of the dynamics of a co-culture system. Adapted from Battiston et al., 2014

To reproduce this complexity, co-culture systems can be developed to mimic the natural conditions. These involve the culture of two or more types of cells within the same matrix (Battiston et al., 2014). This strategy takes advantage of both the natural cell-ECM interaction and the natural crosstalk between cells, through soluble factors and/or cell-cell interaction and cell-cell contact (Figure 3) (Seghezzi et al., 1998; Grinnel et al., 2000; Saito et al., 2005; Wenger et al., 2005). Co-culture systems are often used with the intent of using one cell type to provide a desired stimulus to a second cell type, presenting a natural, cost-effective strategy for tissue regeneration. This strategy as proven itself effective for ECs tube-like structures formation, as coculturing ECs with fibroblasts (Wenger et al., 2005; Sorrell et al., 2005; Li et al., 2013; Guerreiro et al., 2014; Costa-Almeida et al, 2015), osteoblasts (Hoffman et al., 2008; Grellier et al., 2009; Ghanaati et al., 2011), mesenchymal cells (Wu et al., 2007; Kolbe et al., 2011) and smooth muscle cells (Melero-Martin et al., 2007; Foubert et al., 2008) provides the necessary stimulation for increased ECs survival, proliferation and capillary-like structures assembly that resemble the normal ECs alignment. Human fibroblasts are abundant in the dermis, being the main source of ECM components (e.g. collagen, fibronectin and proteoglycans) and, therefore, modulating mechanical extracellular microenvironment which is critical for vasculogenesis (Berthod et al., 2006). Furthermore, these cells are strongly related to angiogenesis as they infer over the EC behavior through fibroblast-derived proteins (e.g. fibroblast growth factor-2 (FGF-2) and vascular endothelial growth factor (VEGF), the latter a key modulator of normal vessel generation (Seghezzi et al., 1998; Saito et al., 2005), cell-cell dynamics (Wenger et al., 2005) and mechanical extracellular microenvironment contraction (Grinnel et al., 2000), all of which are necessary to modulate EC sprouting and the expansion of capillary-like network (Neufeld et al., 1999; Velazquez et al., 2002; Yamamoto et al., 2003).

However, to build a co-culture system, the physico-chemical properties must be carefully considered as biomaterial will serve as support in the initial stages of the

culture. Matrix dimensionality plays a key role in cell signaling event, affecting, in particular, the way cells experience mechanical stresses and strains (Cukierman et al., 2001; Cukierman et al., 2002; Reilly et al., 2010.), which was proven to have a direct effect on cells' self-patterning (Sieminski et al., 2004; Palama et al., 2012). To engineer a functional tissue, compliant hydrogel matrices with a storage modulus, G' inferior to 1000 Pa (hereafter designated as soft matrices), facilitate different cellular activities, including spreading, proliferation and migration (Bott et al., 2010; Ehrbar et al., 2011; Maia et al., 2014). As Reinhart-King et al. (2011) described endothelial cells communicate through mechanical signals in a stiffness-dependent manner, reacting to strains created by the traction stresses of neighboring cells. In addition, Bott et al. (2010) demonstrated that softer hydrogels matrixes increase fibroblasts spreading and proliferation.

All together, decreasing the substrate stiffness and, therefore, creating a more compliant matrix, while coculturing EC with fibroblasts, presents itself as a promising strategy for the self-assembly of endothelial cells into network-like structures.

1.3. Extracellular matrix

Multicellular organisms are governed by cohesion mechanisms. Among these mechanisms, the matrix adhesiveness is known to be a potent modulator of the architecture and organization of the tissue, playing a key role in cell survival, proliferation, migration and differentiation (Wang et al., 2010; Bowers et al., 2010). The extracellular matrix (ECM) consists in network of proteins and proteoglycans secreted locally and assembled into an organized meshwork. Among the macromolecules that compose the ECM, special attention is given to glycosaminoglycans (GAGs), negatively charged unbranched polysaccharide chains composed of repeating disaccharide units, collagens, which are fibrous proteins, and fibronectin (FN), a glycoprotein (Labat-Robert et al., 1990; Bowers et al., 2010). Different types of collagen provide unique properties the ECM, modeling tensile strength and fibril formation. As such, alterations in the biochemical composition of collagens impose different mechanical properties to the microenvironment (Daley et al, 2008). On the other hand, FN plays crucial role in cell-matrix interactions, serving as a substrate for different adhesion molecules, namely integrins (Romer et al., 2006; Daley et al, 2008). More precisely, FN has been shown to interact with αvβ3 through a small sequence of amino acids, Arginine-Glycine-Aspartate or RGD, mediating cell survival, migration and invasion (Stupack et al., 2003; Yu et al., 2009). This ECM-integrin interaction plays a

key role in cellular fate, providing not only anchorage, but also information concerning their microenvironment (Stupack et al., 2003). Variations in the relative amounts of these macromolecules, coupled with modifications in their organization, provide different patterns of cell adhesion to matrix and growth behavior, leading to *in situ* specific cellular response (Discher et al., 2005; Engler et al., 2006; Li et al., 2010). It is therefore imperative for progress in developmental biology, regenerative medicine, and tissue engineering to provide to the cells the matrix cues necessary for a driven response to the desired effect.

1.3.1 Hydrogels

Biomaterials play a critical role in tissue engineering as they can modulate cell response via different material properties such as surface chemistry and topography, spatial patterning, roughness, mechanical compliance, porosity, isotropy, surface wettability, among others (Ratner et al., 1996; Battiston et al., 2014). Cell-biomaterial interactions affect cell-cell interactions in 3D culture systems, promoting unique behaviors upon interaction with different biomaterials. An ideal biomaterial should able to mimic functionality and complexity of native tissues, providing biospecific cellular adhesion and the subsequent control of cellular functions. Three-dimensional (3D) hydrogels matrixes offer an exciting possibility, capturing many important features of the ECM (Pereira et al., 2013; Drury et al., 2003). Hydrogel matrices are water-swollen crosslinked polymeric networks. These provide a highly hydrated and mechanically compliant environment, permeable to oxygen, nutrients, wastes and water-soluble metabolites (Tibbitt et al., 2009). The microenvironment profile, however, is not only dependent on the biomaterial's properties. By altering the crosslinking reaction scheme, which can be achieved by physical or chemical methods, the gelation reaction kinetics can be tuned and the subsequent hydrogels properties, altered (Yu & Ding, 2008; Neves et al., 2015). Moreover, hydrogels can often be formed under mild conditions, creating the adequate conditions for cytocompatible cell entrapment (Drury et al., 2003). Their delivery can be performed in a minimally invasive manner as several hydrogel matrices can be prepared from soluble precursor's solutions that crosslink in situ (Hall, 2007). As such, hydrogels have been proposed for a myriad functions in the field of tissue engineering, ranging from as space cling agents (Yao & Swords, 2001; Drury & Mooney, 2003; Koran et al., 2007), drug/bioactive molecule delivery (Ribera et al., 2004; Green et al., 2006; Qiu & Kinam, 2012), cell/tissue delivery vehicles (Bidarra et al, 2011; Munarin et al., 2012; Fonseca et al., 2013;

Bidarra et al., 2014) and 3D cellular microenvironments (Seidlits et al., 2011; Fonseca et al., 2011; Neves et al., 2015).

As previously described, hydrogels can be adjusted to fit the demands of each construct. By tuning the biochemical and viscoelastic profile of the hydrogels, it is possible to effectively modulate the process of mechanosensing, promoting, for example, the proliferation and spreading of fibroblasts and favoring endothelial cells network assembly and tubulogenesis (Grinnell & Petroll, 2010; Bott et al., 2010; Bidarra et al., 2011). Naturally derived polymers include components of the extracellular matrix (e.g. collagen, fibronectin, and fibrinogen) or present a chemical structure similar to natural glycosaminoglycans (GAGs) (e.g. alginate, hyaluronic acid, chitosan). Due to this, natural polymers present intrinsic advantages over synthetic ones (e.g. Poly(ethylene glycol) (PEG), Poly(glycolic acid) (PGA), Poly(lactic acid) (PLA); Poly(lactic-co-glycolic acid) (PLGA), Poly(methyl methacrylate) (PMMA), Poly(e-carpolactone) (PCL) (Hoffman, 2012; DeVolder & Kong, 2012). Although some contain cellular binding domains due to their derivation from natural sources, thus allowing cell adhesion, others constitute permissive hydrogels. Notwithstanding that the latter provides a 3D environment for cell culturing, it lacks the ability to promote the specific cell-matrix interactions necessary for cell adhesion and the subsequent physiologic events of anchorage-dependent cells (Munarin et al, 2011). This occurs due to the presence of negatively charged carboxyl groups. To overcome this problem non-adhesive hydrogels can be modified to have a bioactive role by grafting a small oligopeptide sequence that is known to be present in FN, namely, RGD (Stupack et al., 2003; Yu et al., 2009). Incorporating this cell-adhesive peptide (RGD) into the non-adhesive polymer has been shown to significantly improve cell adhesion, growth and differentiation (Rowley & Mooney, 1999; Rowley et al., 2002; Grellier et al., 2009; Bidarra et al., 2011). Furthermore, hydrogels can also be modified with protease-sensitive peptides (e.g. PVGLIG). This allows the matrixes to mimic two key features of the natural ECM: cell-matrix adhesion and cell-driven matrix proteolytic degradation (Raeber et al., 2005; Fonseca et al., 2011).

Three dimensional matrices for cell culture are no longer thought only a structural support to maintain tissue and organ configuration. Nowadays, it is widely accepted that the highly dynamic interactions between cells and the ECM are of key importance in the cellular fate (Berrier & Yamada, 2007). As such, the success of matrices in these roles hinges on finding an appropriate material to address the variables inherent to the desired application. Different biomaterials should be explored to develop new approaches for tissue regeneration therapies, thus providing an insight on the best possible design for each situation.

1.3.1.1. Pectin

A multitude of natural biomaterials has been explored to form hydrogels. Natural polymers possess highly organized structure, being are frequently used in tissue engineering applications as they are either components of or have macromolecular properties similar to the natural ECM (Drury et al., 2003). Due to their tunable characteristics, by grafting of the desired peptides into the biopolymer structure or by controlling their viscoelastic profile through the control of the gelation kinetics (e.g. variations in pH, gelation time, and crosslinking divalent cation), specific tissue engineering matrices can be constructed. Among these, pectin, a complex structural polysaccharide present in the cell walls of higher plants, stand out as an attractive cell carrier. Pectin is a biocompatible anionic polysaccharide that constitutes 30% of the cell wall of plants (Harholt et al., 2010) widely used as thickener, gelling agent, stabilizer, and emulsifier in several food products (Tho et al., 2003). As depicted by Munarin et al. (2012), pectin is mainly extracted from waste products of juice, apples and cider industries through chemical or enzymatic methods. Due to the number of sources and extraction processes that pectin can be obtained from, a wide range of pectin degrees of esterification can be obtained. As such, each batch must be thoroughly characterized for an adequate microenvironment construction and results interpretation (Munarin et al., 1012). Furthermore, the interest in pectin as spread into the pharmaceutical and medical fields (Maxwell et al., 2012) as it has been reported to have multiple positive effects on human health, including lowering cholesterol and serum glucose levels (Mohnen et al., 2008) reducing cancer (Jackson et al., 2007) and stimulating the immune response (Inngjerdingen et al., 2007).

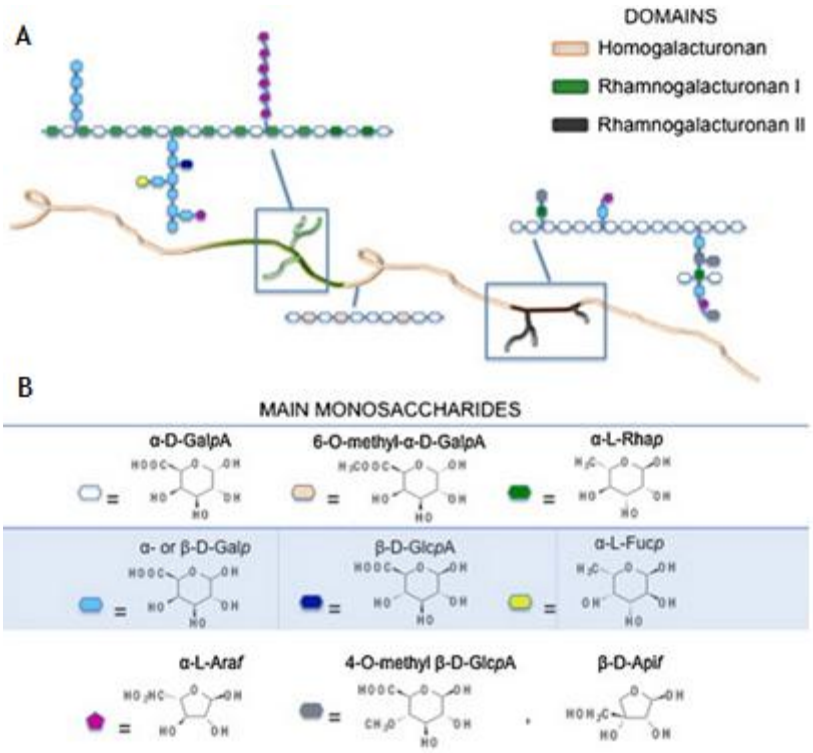

Figure 4. Representation of pectin structure. Adapted from Munarin et al., 2012

Pectin is composed of at least three polysaccharide domains: homogalacturonan (HGA), which is the major component, rhamnogalacturonan-I (RG-I) and rhamnogalacturonan-II (RG-II) (Jarvis, 1984; Mohnen, 2008; Yapo, 2011), forming a branched macromolecule with high molecular weight. The current model proposed, consists of a linear backbone of unbranched HGA residues (“smooth region”) alternately linked to branched RG-I residues (“smooth region-hair region”) (Figure 4). HGA, the major component of pectin polysaccharides (~65%) (Mohen et al., 2008) ,is mainly composed of a homopolymer of (1–4)-linked-α-D-galacturonic acid (GalA) units (Ridley et al., 2001). These units can be partially methyl-esterified on the carboxyl group and sometimes partially acetyl-esterified on the secondary hydroxyls. Based on the ratio of methyl-esterified residues (6-O-methyl-α-D-GalA) HGA backbone to the total carboxylic acid units in their salt form, which defines the degree of methylation (DM), pectins can be classified into two categories: low methoxyl pectins (LM, DE < 50%) or high methoxyl pectins (HM, DE > 50%) (Durand, 1990). These methylation

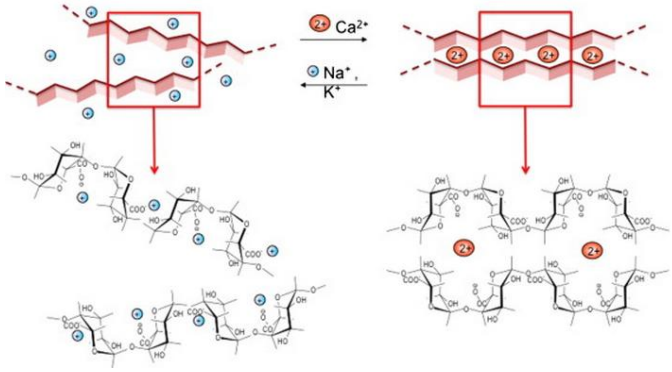

Figure 5. Schematic representation of an "egg box" structure formation in the presence of Ca^{2+}. Adapted from Coimbra et al., 2011

differences provide different properties to the pectin, significantly affecting the properties of the formed gels.

LM pectins, in the presence of strong, positive, divalent metal ions, such as Ca^{2+} ions, establish strong bonds between the carboxyl groups of the HGA pectin backbone leading to the formation of an "egg box" structure. This mechanism involves side-by-side associations of specific sequences of GalA monomer in parallel or adjacent chains linked through electrostatic and ionic bonding of carboxyl groups using the divalent ions, forming a flexible network of polymer chains that can swell but does not dissolve in water (Pérez et al., 2001; Fang et al., 2008) (Figure 5). Furthermore, van der Waals interactions and hydrogen bonds are established within the polymer, stabilizing the egg-boxes formed between neighbored chains (Braccini et al., 1999; Fraeye et al., 2010).The promising aspects of pectin gels for biomedical applications, namely, its easily tunable physical properties, high water content and ability to homogeneously immobilize cells, genes, proteins, drugs or growth factors (Munarin et al., 2010 a; Munarin et al., 2010 b; Munarin et al., 2011; Munarin et al., 2012; Neves e al., 2015), led to a renewed interest on this polymer. Moreover, this biopolymer's solubility can be controlled by quickly displacing the Ca^{2+} ions by monovalent counterions such as Na^{+} or K^{+} (Munarin et al., 2011). Pectin fulfils all of the requirements for hydrogel formation, presenting itself as particularly appealing biomimetic systems providing an adequate microenvironment by simulating the ECM-cell dynamics. Nonetheless, as other natural polysaccharides (e.g. alginate), due to the presence of negatively charged carboxyl groups, pectin presents a hydrophobic nature, resisting to protein adsorption and cell adhesion. To bypass this issue, RGD-containing oligopeptides must be grafted into the pectin backbone, granting the minimal peptide sequence required for the adhesion of integrins to the ECM components (Pierschbacher & Ruoslahti, 1987; Ruoslahti & Pierschbacher, 1987; Yamada, 1997; Giancotti & Ruoslahti, 1999). As for other polymers (e.g. alginate (Bidarra et al, 2011; Fonseca et al., 2011; Fonseca et al., 2013; Bidarra et al., 2014)) RGD-containing

pectin gels present a higher cytocompatibility, cell adhesion and proliferation, improving al the subsequent cellular functions (Munarin et al., 2011; Munarin et al., 2012; Neves e al., 2015). Furthermore, in addition to the structural resemblance between pectin and alginate, allowing into present the same numerous benefits of alginate, pectin stands out as it presents an interesting degradation profile under simulated physiological conditions (Munarin et al., 2012). Finally, more recently, our group explored the potential of the pectin hydrogels crosslinking by internal ionotropic gelation using the slow-gelling calcium carbonate/*D*-glucono-*d*-lactone ($CaCO_3$/GDL) system. Neves e al., (2015) addressed, for the first time, the use of *in situ*-forming pectin hydrogels as skin cell carriers for tissue engineering, providing an ionotropic internal gelation scheme suitable for *in situ* gelling systems.

Although much still remains to be elucidated about this polymer as a biomaterial, the studies found about the easy tunability of this biomaterial for tissue regeneration (Morra et al., 2004; Bussy et al., 2008; Nagel et al., 2008; Munarin et al., 2011; Munarin et al., 2012; Neves et al., 2015), evidence the promising capabilities of pectin hydrogels as a powerful material system for cell delivery, tissue engineering and regenerative medicine applications.

1.4. Main Goals

The incorporation of microvascular networks within the *in vitro* tissue-engineered skin before its transplantation into a patient would be a major contribution, surpassing the need of relying only on the host's system ability to promote vascularization. Although encouraging developments have been made in the field (Rivron et al., 2008; Place et al., 2009), *in vitro* vascularization remains a challenge. In this work, we intend to use a combined approach using the tunable characteristics of soft pectin hydrogel, cells and growth factors to mimic the natural mechanisms involved in the formation of a microvascular network. We aim to construct a three-dimensional, RGD-grafted, soft pectin hydrogel in which fibroblasts support endothelial cells in the formation of self-assembled vascular structures for skin regeneration therapies, while also providing new insights on the biomimetic properties of soft pectin hydrogel's for future tissue-engineering strategies.

Materials and Methods

2.1. Cell Culture

2.1.1 Routine maintenance

Commercial human umbilical vein endothelial cells (HUVECs) (LONZA) and neonatal human dermal fibroblasts (NHDFs, hereafter referred as FBs) (Corriel Institute) were used. HUVECs were cultured in T75 culture flasks, coated with 0.2% (w/v) gelatin from porcine skin (30 minutes at 37 °C, Fluka), with M199 medium (Sigma) supplemented with 10% v/v of inactivated fetal bovine serum (FBS), 1% of antibiotic solution composed of penicillin and streptomycin (Pen/Strep, Gibco) and 0.1 $mg.mL^{-1}$ of heparin (Sigma-Aldrich) with every-other-day medium exchange. Fibroblasts were cultured in T75 culture flasks with Dulbecco's Modified Eagle Medium (DMEM; Gibco) supplemented with 10% (v/v) non heat inactivated FBS (Gibco), 1% (v/v) 1% pen/strep (Gibco) and 1% of antimycotic Amphotericin B solution (Sigma) with no medium changes necessary. The cells were incubated at 37 °C, under a humidified atmosphere of 5% v/v CO_2 in air. Entrapped cells in pectin discs, when in monoculture, were also cultured in the same conditions, with the media being renewed every three days.

After reaching confluence, the cells were trypsinized. For HUVEC trypsinization, the culture medium was removed and the T75s were washed with 5 mL of PBS (NaCl 137 mM, KCl 2.7 mM, $NaHPO_4.2H_2O$ 10 mM, KH_2PO_4 1.8 mM, pH 7.4). The HUVECs were incubated with 2 mL of Trypsin/EDTA in PBS (Trypsin 0.05 % w/v, Sigma; EDTA 0.5 mM, Sigma; pH 7.5) for 5 minutes at 37 °C. The T75s were gently tapped to loosen the cells and 2 mL of M199 were added to inactivate the enzyme. The cells were recovered into a single T75, resuspended to avoid aggregates and 10 µL of the solution were loaded into a Neubauer chamber, where the cells were counted under a microscope. HUVECs where seeded in 0.2% (w/v) gelatin-coated T75 at a density of $6x10^5$ cells/T75 and supplemented with 12 mL M199 with 0.03 $mg.mL^{-1}$ of ECGS. For FBs trypsinization the culture medium was removed and the T75s were washed with 5 mL of PBS. The cells were incubated with 1 mL of Trypsin/EDTA in PBS (Trypsin 0.25% w/v, Sigma; EDTA 2.21 mM, Sigma; pH 7.5) for 5 minutes at 37 °C, after which the flasks were gently tapped to loosen the cells. Neutralization of the trypsin was archived by adding 1 mL of DMEM to each T75 and cells were recovered to a single flask. FBs were resuspended, and cells were counted under the microscope using a Neubauer chamber. FBs were seeded at 5×10^5 cells/T75 and supplemented with 8 mL of DMEM. Both cell types were incubated in the previously described conditions.

For each experiment, HUVECs were used at passages 6-10 and fibroblasts were used at passages 5-10.

2.1.2 Cell thawing

HUVECs and FBs cryovials containing $1x10^6$ cells.mL^{-1} in 10% v/v DMSO in medium, stored in liquid nitrogen, were thawed by immediately placing them in a 37 °C water bath for 1 minute. To the cryovials containing HUVECs or FBs, 1 mL of, respectively, M199 or DMEM was added and a mild up and down was carried out to resuspend the cells. HUVECs were seeded at $6x10^5$ cells/T75 and on supplemented with 12 mL of M199 with 0.03 mg.mL^{-1} of endothelial cell growth supplement (ECGS, Corning), whereas FBs were seeded at $5x10^5$ cells/T75 and supplemented with 8 mL of DMEM. The cells were incubated at 37 °C under a humidified atmosphere of 5% v/v CO_2 in air. Each medium was the next day, for DMSO removal.

2.1.3. Co-culture media selection

In order to select a medium that provides a performance close to the ideal for both cell types, HUVECs and FBs behavior was evaluated in several media, including M199, DMEM (both supplemented as previously described) and a combination of the two in three different ratios of M199:DMEM: 3:1 (M3:1), 1:1 (M1:1) and 1:3 (M1:3). Monocultures of both HUVECs and FBs were carried out on 12-well plates with seeding densities of $3.0x10^4$ (D_1) and $6.1x10^4$ (D_2), which corresponds, respectively, to the relative seeding density per surface area of a T75 and twice as much cells per surface area. For each medium composition, HUVECs were seeded on 0.2% (w/v) gelatin-coated 12-well plates, whereas 1 mL FBs were seeded in uncoated 12-well plates. For HUVECs, each medium composition was supplemented with 0.03 mg.mL^{-1} of ECGS. To evaluate the effect of the different media on cell behavior, three time points were selected (24h, 72h and 120h) and metabolic activity and total double-stranded DNA quantification assays were carried out. Three replicates were conducted for each time point.

2.1.4. HUVECs and FBs density optimization

FBs and HUVECs co-cultures were established with four different cell ratios of 1:1 (R 1:1), 2:1 (R 2:1), 3:1 (R 3:1) and 5:1 (R 5:1) (HUVECs:FBs), at the two seeding densities of D_1 and D_2. Cells were obtained from T75s cultures following the previously described trypsinization methods for each cell type (Section 2.1.1.). After cell count, the different cell ratios were established. Cells were seeded on 0.2% (w/v) gelatin-coated 12-well plates with M 3:1 supplemented with 0.03 $mg.mL^{-1}$ of ECGS. To evaluate the effect of the different ratios on cell behavior, at 24h, 72h and 120h, metabolic activity and total double-stranded DNA quantification assays were carried out. Three replicates were conducted for each time point. At each time point, cells were fixed with 1 mL of 4% (v/v) paraformaldehyde (Merk) in PBS for 20 minutes at room temperature (RT) for phenotype characterization.

2.2. Pectin hydrogel

2.2.1. Pectin purification

Low methoxyl (LM) citrus pectin (Classic CU701), 86% and a DM of 37%, kindly provided by Herbstreith & Fox (Neuenbürg, Germany), hereafter known as RawPec, was purified based on the protocol as described in Neves et al. (2015). A 1% (w/v) RawPec solution was prepared in ultrapure water (18 MU, Milli-Q UltraPure Water System, Millipore). Following complete pectin dissolution, the pH of the solution was measured and adjusted to 6. The 1% (w/v) RawPec solution was submitted to a sequential filtration through decreasing pore diameter filters, namely, 0.80 µm, 0.45 µm, and 0.22 µm filter membranes (mixed cellulose esters, MCE, Millipore). After filtration, activated charcoal (Norit, Sigma-Aldrich, 2% (w/w) were added to the solution, which was stirred for 1 hour at RT. The suspension was centrifuged for 1h at 27 000 rcf at RT. The supernatant was carefully recovered, and submitted to a new centrifugation with the same parameters, to remove the activated charcoal. The supernatant was recovered and submitted to filtration through a 0.22 µm filter membranes. Pectin was then lyophilized and stored at -20 °C until further use.

2.2.2. Carbodiimide RGD-grafting

To surpass the cell-anchorage difficulties imposed by the hydrophobic nature of the hydrogels, biofuncional chemically modified pectin has to be obtained. Pectin was covalently modified with the oligopeptide $(Glycine)_4$-Arginine-Glycine-Aspartic acid-Serine-Proline (G4RGDSP) (GenScript), using aqueous carbodiimide chemistry (Rowley et al. 1998), based on the methods previously described for pectin (Munarin et al. 2011; Munarin et al. 2012; Neves et al. 2015). To minimize carbodiimide chemistry side reactions and provide maximum reaction efficiency, a purified pectin solution (1% (w/v)) was prepared in 2-(N-morpholino) ethanesulfonic (MES) acid buffer (0.1 M MES buffering salt, Sigma, and 0.3 M NaCl), with the pH adjusted to 6.5 using 1 M NaOH at RT, overnight. The solution was divided in two in order to obtain RGD-grafted purified pectin (RGDPec) and a control of unmodified pectin (BLKPec). The covalent pectin-RGD bond is then achieved by adding, water-soluble carbodiimide, 1-ethyl-(dimethylaminopropyl) carbodiimide (EDC), which is used to form amide linkages between amine containing molecules and the carboxylate moieties on the polymer backbone, N-hydroxy-sulfosuccinimide (sulfo-NHS), a co-reactant which stabilizes the reactive EDC-intermediate form against a competing hydrolysis reaction and G4RGDSP, our RGD-containing oligopeptide. To increase efficiency of the amide bond formation, by minimizing COOH on the RGD reaction, these components were added quickly and following the order: sulfo-NHS (N-Hydroxysulfosuccinimide) (Pierce Chemical, 27.40 mg) and EDC (N-(3-dimethylaminopropyl)-N'-ethylcarbodiimide) (Sigma, 48.42 mg), at a molar ratio of 1:2, followed by addition of the oligopeptide (G4RGDSP) (16.70 mg) to the RGDPec, and both solutions were allowed to react for 20 h under constant stirring. The reactions were quenched with hydroxylamine hydrochloride (Sigma, 18 mg per gram of pectin), and dialyzed against decreasing concentrations of NaCl (30 g, 25 g, 20 g, 15 g, 10 g, 5 g) in ultrapure water for the first 2 days and against ultrapure water with 0 g of NaCl on the last day. The membranes stayed in each solution at least 4 hours, remaining at least one night in the ultrapure water. Both RGDPec and BLKPec were treated with activated charcoal (Norit, Sigma-Aldrich, 2% (w/w)) for 1h, at RT with stirring. The suspension was centrifuged for 1h at 27 000 rcf at RT. The supernatant was carefully recovered and submitted to filtration through a 0.22 µm filter membranes. Pectin was then lyophilized and stored at -20 °C until further use.

The success of the immobilization was further confirmed via UV spectra analysis of RGD-pectin. The amount of covalently modified peptide was estimated by successive

dilutions of RGD in 1% (w/v) pectin solutions, measured in a microplate reader (Biotek Synergy MX) with Ex/Em at 530/590 nm

2.3. 3D in vitro cell characterization

2.3.1 Characterization of HUVECs and FBs monocultures behavior within 3D RGD-grafted soft pectin hydrogels

In order to verify the optimal set up for HUVECs and FBs monocultures on soft pectin matrices, six experimental set-ups were tested, consisting on three different cell densities (D_3 = 5 x 10^6 cells.mL^{-1}; D_4 = 1 x 10^7 cells.mL^{-1}; D_5 = 1.5 x 10^7 cells.mL^{-1}) and two RGD-grafted pectin concentrations (1.5% and 2.5% (w/v)), adjusted to 200 µM of RGD).

2.3.1.1. Cell entrapment

The 3D matrices will be prepared by calcium-induced gelation, following the previously described method by Neves et al. (2015).

To obtain the final pectin concentrations of 1.5% and 2.5% (w/v), lyophilized sterile-filtered (0.22 mm) RGDPec was dissolved in 0.9 wt% NaCl (in ultrapure water) at 3% and 4% (w/v), respectively. These precursor solutions were adjusted with sterile-filtered (0.22 mm) BLKPec at the same concentrations in order to obtain a final RGD concentration of 200 µM. To trigger hydrogel formation, based on the stoichiometric considerations from Neves et al. (2015), $CaCO_3$ dissolved in 0.9 wt% NaCl (in ultrapure water) was added and carefully mixed with the pectin solution, followed by the addition of *D*-glucono-*d*-lactone (GDL, Sigma). Each type of cell, previously cultured in T75 was trypsinized, centrifuged and resuspended in 0.9 wt% NaCl (in ultrapure water) and, at the considered densities, mixed with the pectin solution. For the preparation of cylindrical pectin matrices with a height = 0.5 mm, 20 µL of the cell-laden hydrogel was cast onto a teflon plate. 0.5 mm spacers were used and a second teflon plate was applied over the hydrogel. A humidified chamber was prepared and gelation was allowed to occur at 37 °C for 1 hour under a humidified atmosphere of 5% v/v CO_2 in air. After the crosslinking reaction occurred, the cell-laden matrices were transferred to a 24-well culture plate coated with pHEMA (Folkman & Moscona, 1978) and 500 µL of fresh medium was added. To evaluate both the effects of pectin concentration and

entrapping density on cell behavior, four time points were selected (24h, 48h, 96 and 144h) and metabolic activity and total double-stranded DNA quantification assays were carried out. Three replicas were casted for each formulation and time point. At each time point, cell-laden soft pectin matrices were recovered and fixed in a 4% v/v PFA in TBS-Ca, for a phenotype analysis.

2.3.2. HUVEC and Fibroblasts 3D monocultures performance under different culture media

To evaluate the effect of different media on HUVECs and FBs monoculture in a RGD-grafted soft pectin 3D hydrogels, the formulations E_3 and F_3 were supplemented with the medium that presented the closest to ideal performance maintenance in a 2D environment. The embeddings for these formulations were carried out as described in "Characterization of HUVECs and FBs monocultures behavior within 3D RGD-grafted soft pectin hydrogels" and the cell-laden matrices recovered into a 24-well culture plate coated with pHEMA (Folkman & Moscona, 1978) and 500 µL of fresh M3:1 was added. The HUVEC-laden matrices were also supplemented with 0.03 $mg.mL^{-1}$ of ECGS. At each time point (24h, 48h, 96 and 144h) the cell-laden pectin matrices were recovered and fixated in a 4% v/v PFA in TBS-Ca and metabolic activity and total double-stranded DNA quantification assays were carried out. Three replicates were conducted for each formulation and time point.

2.3.3. 3D HUVEC:FB co-culture in soft pectin hydrogels

Co-cultures were established by entrapping the two different cell types (HUVECs and FBs) at a cell ratio of 3:1 (HUVEC:FB) using the formulation: 1.5% (w/v) Pectin with 1.5 x 10^7 $cells.mL^{-1}$ (hereafter described as CC_1). Both cell types, cultured in T75, were individually trypsinized and the ratio was established in a 50 mL Falcon. The cells were centrifuged at 1 200 RPM for 5 minutes at RT and the embedding was carried out as described in "Characterization of HUVECs and FBs monocultures behavior within 3D RGD-grafted soft pectin hydrogels". The resulting cell-laden matrices were transferred to a 24-well culture plate coated with pHEMA (Folkman & Moscona, 1978) and 500 µL the selected medium, supplemented with 0.03 $mg.mL^{-1}$ of ECGS, was added. At each time point (24h, 48h, 96 and 144h) the cell-laden pectin matrices were recovered and fixated in a 4% v/v PFA in TBS-Ca and metabolic activity and total double-stranded

DNA quantification assays were carried out. Three replicates were conducted for each formulation and time point.

2.3.3.1. 3D HUVEC:FB co-culture spatial patterning: Microinjected HUVEC-laden soft pectin on a FBS-laden soft pectin bed

As reviewed by Battiston et al., 2014 an initial spatial patterning of the cells onto the matrix may lead to different outcomes in the co-culture. In this work, a micropatterning technique was used for HUVEC:FB co-culture. Due to time limitations we were only able to carry out a pilot assay. This micropattern was designed to incorporate a HUVEC-laden soft pectin island in the center of an FB-laden soft pectin matrix. Two different independent cell-laden pectin formulations, namely 1.5% (w/v) Pectin with 1.5 x 10^7 HUVECs.mL^{-1} and 1.5% (w/v) Pectin with 1 x 10^7 FBs.mL^{-1} were simultaneously carried out, using the previously described method. When ready, the spatially patterned matrix was constructed by casting 40 µL of F_2 onto a Teflon plate followed by a rapid addition of 10 µL of E_3 in the center of the F_2 matrix using a 10 µL gel micropipette (See figure 6). 0.5 mm spacers were used and a second Teflon plate was applied over the pectin hydrogel. A humidified chamber was prepared and gelation was left to occur at 37 °C for 1 hour under a humidified atmosphere of 5% v/v CO_2 in air. After the crosslinking the cell-laden matrices were transferred to a 24-well culture plate coated with pHEMA (Folkman & Moscona, 1978) and 500 µL of fresh M3:1, supplemented with 0.03 mg.mL^{-1} of ECGS, was added. Cell-laden matrices were maintained at 37 °C under a humidified atmosphere of 5% v/v CO_2 in air, with the media being substituted by the third day.

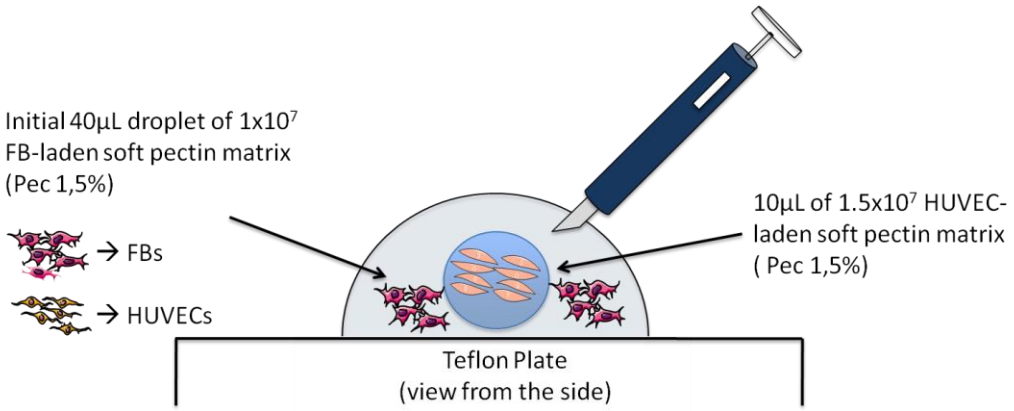

Figure 6. Schematic representation of the 3D HUVEC:FB co-culture spatial patterning embedding process.

2.4. Phenotype characterization

2.4.1. Cell metabolic activity

Cell metabolic activity assessment was performed using a resazurin assay. This assay consists on the bioreduction of the resazurin, which is the oxidized form, to resofurin, which, accordingly, increases the fluorescence. For the 2D resazurin assays, resazurin solution was prepared by dissolution of 10 mg of resazurin (Sigma) in 100 mL of PBS (NaCl 137 mM, KCl 2.7 mM, $NaHPO_4.2H_2O$ 10 mM, KH_2PO_4 1.8 mM, pH 7.4), whereas for 3D assays the solution was prepared in 100 mL of TBS (Tris-buffered saline, 50 mM Tris-Cal, 150 mM NaCl, pH 7,5). After complete dissolution, the solution was sterilized by filtration through a 0.22 µm filter and stored at -20 °C, protected from light until further use. At the designated time points for each experiment, namely, 24h, 72h and 120h for 2D and 24h, 48h, 96h and 144h for 3D, the medium was carefully removed cells were incubated with of 20% v/v of the stock resazurin solution (0.1 $mg.mL^{-1}$, Sigma) in medium for 3 h at 37 °C. Three replicates were monitored for each condition, with three cellular-less replicates serving as control. After the incubation time, 100 µL of the supernatant was transferred to a 96-well black plate with clear bottom (Greiner). Three replicates per well were performed. Fluorescence measurements were carried out using a microplate reader (Biotek Synergy MX) with Ex/Em at 530/590 nm and final results were plotted on Graph Pad Prism 6 software (PRISM).

2.4.2. Total dsDNA quantification

For total dsDNA quantification, the cells used for the resazurin assay were recovered. Regarding the 2D assays, the remaining medium used for the resazurin assay was removed and each well was washed with 1 mL of PBS. Each well was incubated with 250 µL of Trypsin/EDTA in PBS (Trypsin 0.05% w/v, Sigma; EDTA 0.5 mM, Sigma; pH 7.5) for 5 minutes at 37 °C. After incubation, 250 µL of medium was added to the cells and the supernatant was recovered to an eppendorf. For entrapped cells, each matrix was individually recovered to an eppendorf and dissolution was accomplished by incubation with 100 µL of Trypsin/EDTA in PBS (Trypsin 0.25% w/v, Sigma; EDTA 50 mM, Sigma; Glucose 0,1% w/v, Sigma; pH 7.5) for 5 minutes at RT. Cells recovered by centrifugation (10 000 rpm, 5 min), washed with 100 µL PBS, centrifuged again and the pellet was stored at -20 °C until analyzed. Double-stranded DNA (dsDNA) quantification was determined using the Quant-iT PicoGreen dsDNA kit (Molecular Probes, Invitrogen), according to manufacturer's instructions. Briefly the samples were centrifuged (10 000 rpm, 5 min) and the supernatant was removed and cells were lysed using 1% v/v Triton X-100 for 1 h at 400 rpm at 4 °C. Samples were then diluted 1:10 in PBS. For each pool, 10 µL were transferred to a 96-well plate black with clear bottom (Greiner) and in 90 µL of TE buffer was added (200 mM Tris–HCl, 20 mM EDTA, pH 7.5). 100 µL of Quant-iT PicoGreen dsDNA reagent in TE buffer was added and the samples were incubated for 5 minutesat RT in the dark. Fluorescence was quantified using a microplate reader with Ex/Em at 480/520 nm. RFUs were converted into $mg.mL^{-1}$ using a standard curve of DNA in the range of 1-1000 $mg.mL^{-1}$. For each condition n=3 replicates were analyzed.

2.4.3 2D co-culture readouts

After 24h, 72h and 120h, HUVECs:FBs co-cultures seeded on 12-well plates were fixed. The medium of each well was removed and the cells were washed with 1 mL of PBS. Cells were fixed with 1 mL of 4% (v/v) paraformaldehyde (Merk) in PBS for 20 minutes at RT. The paraformaldehyde solution was removed and the cells were washed with PBS for 5 minutes at RT. No staining was conducted. Co-culture's spatial profile and morphology was evaluated using a Carl Zeiss Axiovert inverted microscope. Bright field microscopy images were recovered using a monochromatic camera. Image analysis was performed using the software software ImageJ64.

2.4.4. HUVECs and FBs 3D monocultures and co-culture morphology and spatial distribution

For HUVECs or FBs monoculture analysis, cells were directly assayed within hydrogels (whole mounts).

2.4.4.1 Immunostaining

Cell-laden soft pectin matrices were recovered, washed with 500 µL of TBS-Ca (50 mM Tris-Cl, 150 mM NaCl, pH 7,5 with 7.5 mM $CaCl_2$) and fixed with 500 µL of 4% v/v PFA in TBS-Ca for 20 minutesat RT. The PFA was removed and the matrices were washed with 500 µL of TBS-Ca, for 5 minutes at RT. The matrices were stored at 4 °C in 500 µL of TBS-Ca until further use. For monocultures, F-acting and nuclei immunostaining was performed. F-actin Immunostaining was carried out with Alexa Fluor 488 (Molecular Probes), a toxin with a fluorescent tag that selectively binds to F-actin, whereas the nuclei were stained with DAPI (4',6-diamidino-2'-phenylindole dihydrochloride, Vectashield, Vector), a fluorescent stain that binds selectively to double-stranded DNA. The matrices, stored at 4 °C were recovered, washed with 500 µL of TBS-Ca and permeabilized with 500 µL of 0.1% (v/v) Triton-X 100 (Sigma) for 5 minutes at RT, providing the stains the required access to the inside of the cell. The permeabilized matrices were washed with 500 µL of TBS-Ca for 5 minutes at RT and then blocked with 100 µL of 1% (w/v) Bovine serum albumin (BSA, nzytech) in TBS-Ca for 30 minutes at RT, protected from light. This step is performed in order to prevent nonspecific binging of the fluorescent molecules, providing a higher specificity. The blocked matrices were incubated with 100 µL of Alexa Fluor 488 phalloidin (1:40) in a 1% (w/v) BSA in TBS-Ca, for 1 hour at RT, protected from light. The stained soft pectin matrices were washed with 500 µL of TBS-Ca and stored at 4 °C until further use.

For HUVEC:FB co-cultures analysis, the whole mounts were fixed, stored permeabilized and blocked as described above. Primary antibodies used: rabbit anti-human vWF (1:300; Dako) and mouse anti-human α-smooth muscle actin (α-SMA, 1:100; Dako). These primary antibodies were incubated in 100 µL 1% (w/v) BSA in TBS-Ca, for 16h at 4 °C, protected from light. Following the incubation period, the matrices were washed with 500 µL of TBS-Ca for 5 minutes and incubated with 100 µL of a second solution containing the secondary antibodies, goat anti-rabbit Alexafluor 594 (1:1000; abcam) and chicken anti-mouse Alexafluor 647 (1:1000; abcam), and Alexa Fluor 488 phalloidin (1:40) in a 1% (w/v) BSA in TBS-Ca, for 1 hour at RT,

protected from light. The matrices were washed with 500 µL of TBS-Ca and stored at 4 °C until further use.

2.4.4.2 Image acquisition

Confocal images of monocultures were acquired on a Leica SP2 confocal microscope (LSCM, Leica SP2 AOBS SE; Leica Microsystems). Individually, each matrix was recovered from the TBS-Ca into a support were 6 µL of Vectashield mounting media (Vector) with DAPI was applied onto the matrix. Using the Leica Confocal Software (LCS 2.61, Leica Microsystems), images of the matrices were taken with the objectives HC PLAN APO CS 10x/0.40 and HC PL APO CS 40x/1.25-0.75 Oil. The software was configured to recover the images in a 1024x1024 format, performing each plane sweep with the parameters Line Average and a Frame Average set to 2 and 3, respectively. A sequential scan was performed in each matrix capturing the fluorescence emitted. The distance between each Z plane was set to 5 µm and 2.5 µm, for the 10x and 40x objectives, respectively. Image analysis was performed using the software ImageJ64.

2.4.4.3. Evaluation of the influence of pectin concentration over the ability of FBs monocultures to promote matrix contraction

To verify if the fibroblasts ability to remodel the matrix and microtissue formation, a contraction assay was carried out. 1.5% (w/v) pectin with 1 x 10^7 FBs.mL^{-1} and 2.5% (w/v) Pectin with 1 x 10^7 FBs.mL^{-1} embeddings were carried out as previously described. These conditions were monitored using an inverted light microscope to observe the any matrix diameter change that might occur. Matrices were monitored at 24, 48, and 96 and 144 hours.

2.5. Data treatment

2.5.1. Statistical analysis

Cell metabolic activity and proliferation data was analyzed using GraphPad Prism 6 software (PRISM) Mann-Whitney test, for two unpaired groups. Statistically significant differences were considered when *p* values were lower than 0.05. All data is presented as mean values with ± standard deviation.

2.5.2. Image treatment

Image analysis was performed using the ImageJ64 software. For fibroblast-laden matrices, fibroblast spheroids were counted in the confocal images and the average number of structures was determined by dividing the number of structures by the area (mm^2) of the image. Finally, the area of the spheroid-like structures was also quantified with an n=75 in all images.

Results

3.1 Preparation of 3D biofuncional RGD-grafted pectin

Due to its hydrophobic nature, pectin resists to protein adsorption and cell adhesion (Rowley et al, 1999), which is required for the survival of anchorage-dependent cell, playing a critical role in several physiological events (Dee et al, 1999; Price et al., 1997). The incorporation of the RGD (Arg-Gly-Asp) sequence improves cell adhesion on non-adhesive substrates, providing the minimal peptide sequence required for the adhesion of integrins to the ECM components (Pierschbacheret al., 1987; Ruoslahti et al., 1987; Yamada et al., 1997). In this study, RGD-functionalized pectin was synthesized and further used to prepare hydrogel matrices for culturing HUVECs and FBs under 3D conditions. Based on the method previously described by Neves et al. (2015), pectin was purified and covalently grafted with the oligopeptide $(Glycine)_4$-Arginine-Glycine-Aspartic acid-Serine-Proline (G4RGDSP) (GenScript), using aqueous carbodiimide chemistry (Rowley et al. 1998). The amount of covalently modified peptide was estimated by successive dilutions of RGD in 1% (w/v) pectin solutions.

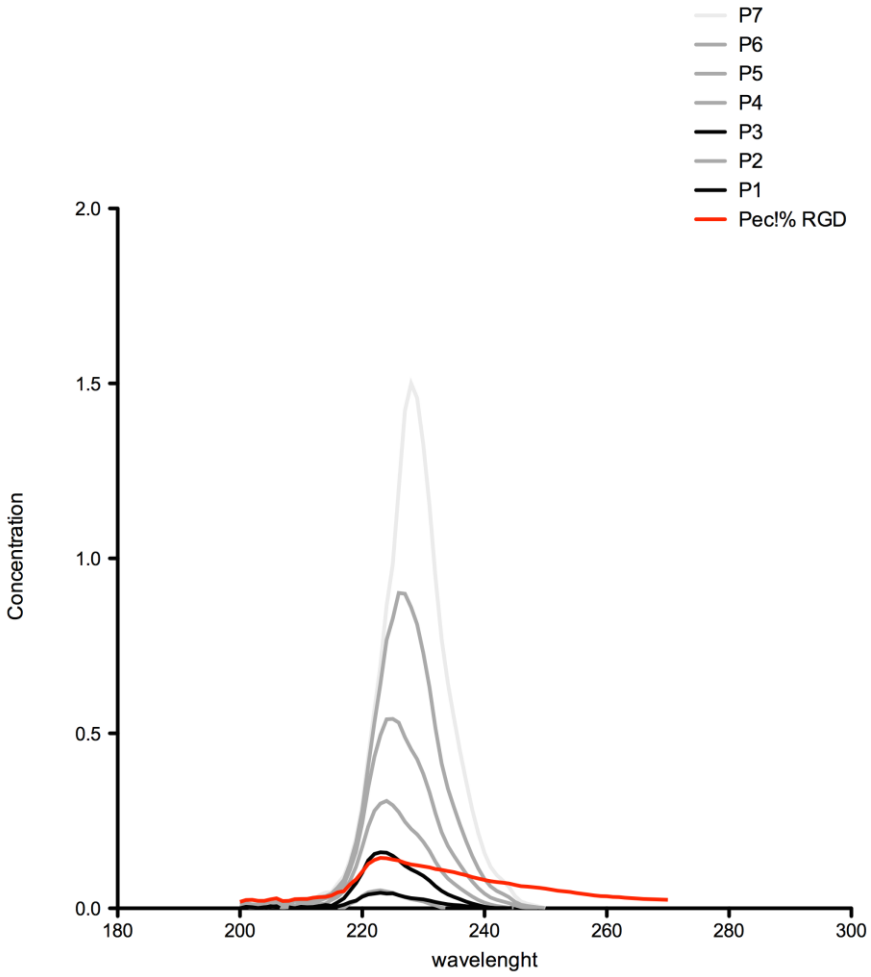

Figure 7. UV spectra of RGD-pectin, soluble RGD peptide and serial dilutions of RGD in a 1% pectin solution

Final approximate RGD content is 18 mg RGD per 1 g of pectin.

3.2. Determination of 2D optimal HUVEC/FB culture media composition

As reviewed by Battiston et al. (2014), a co-culture system involves multiple interactions, presenting several challenges. A correct selection of the base medium is then necessary to optimize growth and cell phenotype. Endothelial cells and fibroblasts will be cultured separately in 24-well culture plates using five different medium compositions. These included M199, DMEM (both supplemented as previously described) and a combination of the two in three different ratios of M199:DMEM: 3:1 (M3:1), 1:1 (M1:1) and 1:3 (M1:3). This experiment was carried out to evaluate the effect of the different media on cell behavior, allowing the selection of the best-suited media for the co-culture of endothelial cells and fibroblasts.

At day 1, HUVECs (Figure 8), at both initial seeding densities (C_1 and C_2) present similar dsDNA yields (Figure 8, a and b). From the start it is possible to observe that despite the dsDNA profiles are not significantly different, significant differences can be found in the metabolic activity (Figure 8, c and d). Three distinct profiles can be perceived whereas M3:1 presents a similar profile to the optimal medium, M199. M1:1 and M1:3 possess similar metabolic behaviors but are already significantly different from the optimal medium. Finally, DMEM presents the lowest metabolic rate. From day 1 to day 3, an increase in the DNA content is observed, accompanied by an increase in the total metabolic activity in all but DMEM supplemented cultures, where these profiles seem to be maintained or decrease. Finally, from day 3 to day 5, we observe a decrease in the total dsDNA and metabolic activity. Despite these fluctuations, the three profiles are maintained and significantly different between them. Throughout the experiment it is possible to observe that the metabolic activity (normalized with the total dsDNA) of HUVECs is maintained.

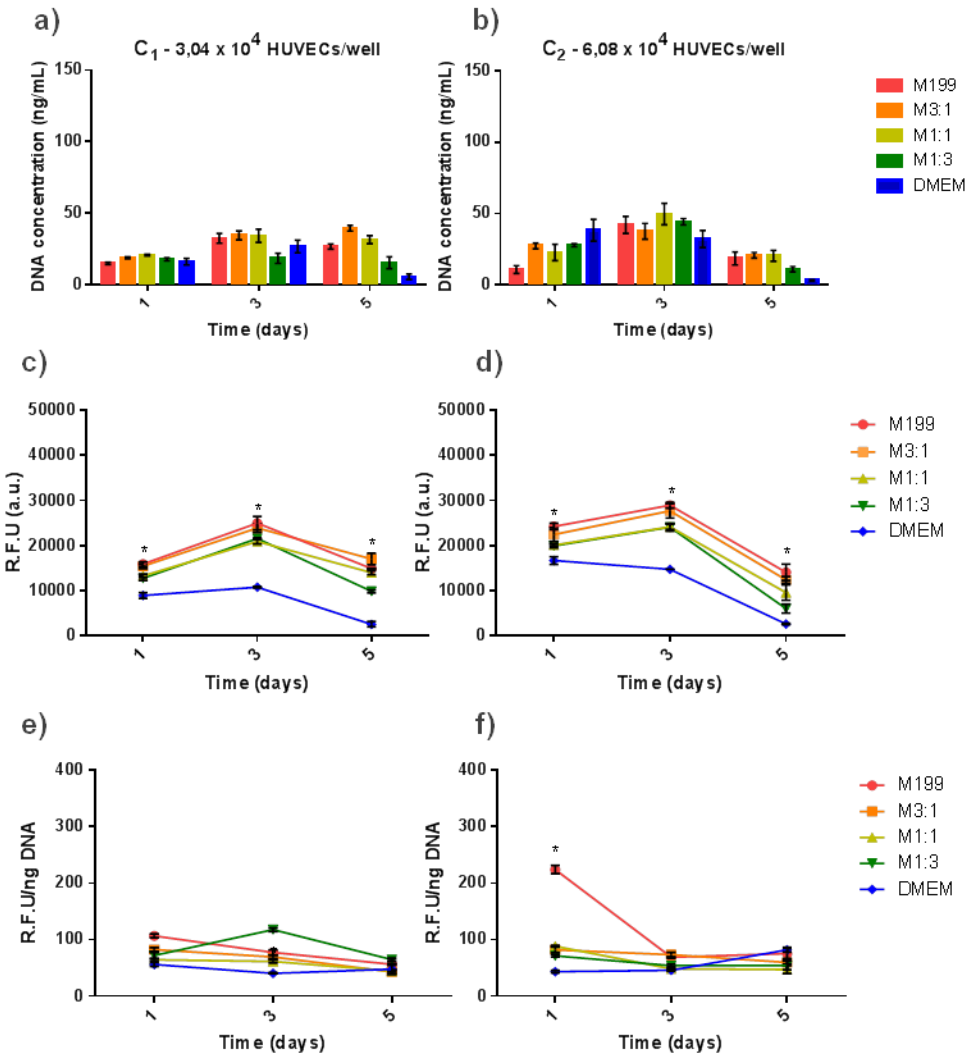

Figure 8. Effect of cell density and medium composition on metabolic activity and proliferation of HUVECs in 2D during 5 days in culture a) and b) total dsDNA (PicoGreen assay), c) and d) metabolic activity (resazurin assay) and e) and f) metabolic activity per nanogram of dsDNA of HUVECs. * denotes statistically significant differences ($p < 0.05$).

Regarding FBs (Figure 9), at day 1, it is possible to see that the different seeding densities are translated into different dsDNA yields (Figure 9, a and b). This difference is also represented in the total metabolic activity (Figure 9, c and d) whereas C_1 presents a lower total metabolic activity than C_2. At day 3, it is observed an increase for both seeding densities in the total DNA content and metabolic activity. By day 5, the total DNA content seems to remain unaltered except for the M199, M3:1 and M1:1 media conditions of C_1, where it increases. Here, we observe a metabolic activity increase for C_1 densities, whereas for C_2 the values remain unaltered for M 3:1, M 1:1 and M 1:3, increasing in DMEM and M199. When normalized, these results point to a constant metabolic activity FBs for seeded at $6.1x10^4$ cell/well throughout the culture

time, whereas for lower seeding concentrations (namely 3.0x10^4 cell/well) it is possible to observe a decrease followed by a slight increase, stabilizing at similar values to C_2.

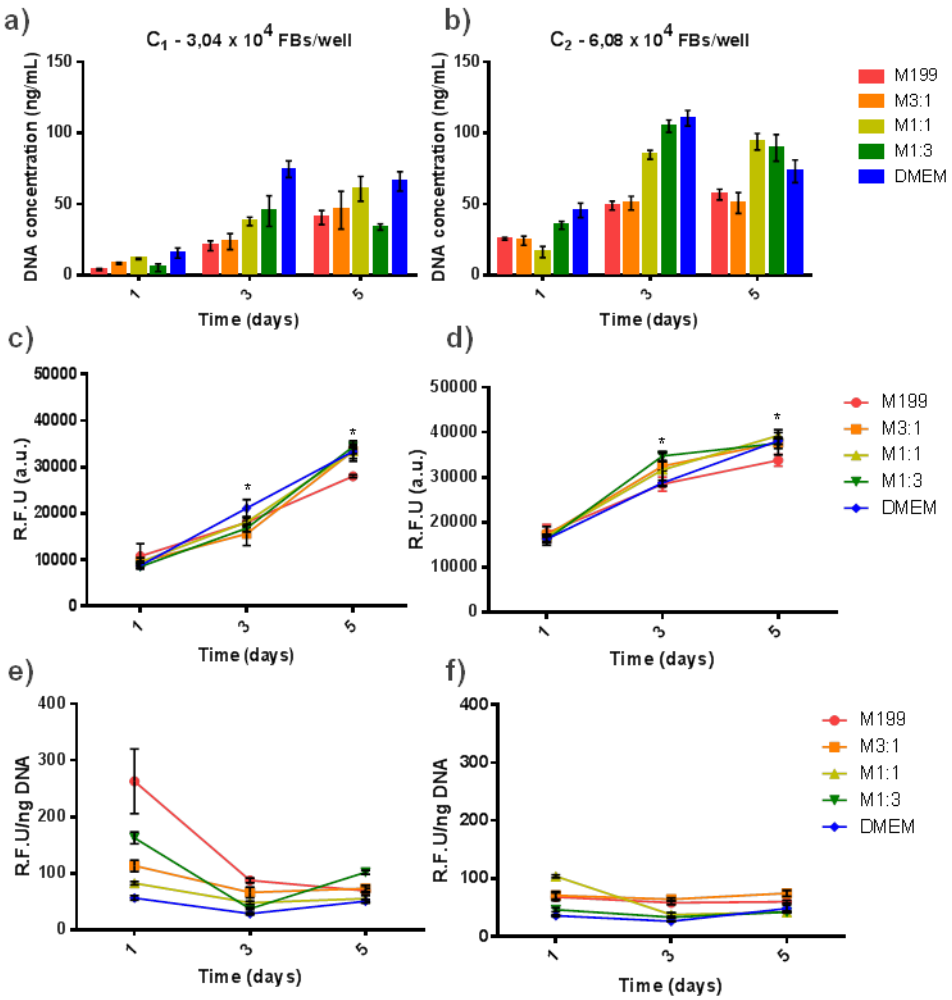

Figure 9. Effect of cell density and medium composition on metabolic activity and proliferation of FBs in 2D within a 5 days culture period. a) and b) total dsDNA (PicoGreen assay), c) and d) metabolic activity (resazurin assay) and e) and f) metabolic activity per nanogram of dsDNA of NHDFs. * denotes statistically significant differences ($p < 0.05$).

Given that, for HUVECs, there are no significant alterations in the metabolic and proliferation profiles alterations when using M3:1 (when compared to M199) and that the same happens to FBs (when compared to DMEM), M3:1 is a suitable candidate for supplementation in a co-culture system.

3.3. Determination of 2D optimal in vitro HUVEC/FB ratio

The majority of natural tissues consist of multi-cellular systems of two or more cell types which interact with each other to facilitate viability, proliferation and differentiation (Nam et al., 2011; Schubert et al., 2008; Traphagen et al., 2013). Blood vessels are a multi-cellular system composed of endothelial cells (ECs), vascular smooth muscle cells (VSMCs), and fibroblasts (Ratner et al., 1996). In tissue engineering, co-culture systems have been increasingly used as it provides simulation of the *in vivo* physical and biological properties. Furthermore, published data indicate that co-culture of ECs with FBs can provide the complex mixture of growth factors, ECM and cell-cell contacts necessary to potentiate tubulogenesis (Berthod et al., 2006; Sorrell et al., 2007; Auger et al., 2013). However, as in natural environments cell distribution is not uniform, for *in vitro* optimal experimental outcomes in co-culture assays it is necessary an optimization of the cell seeding number and ratio. In order to evaluate the effect of FBs on HUVECs capillary-like self-assembly, four our different cell ratios were established, namely, R 1:1, R 2:1, R 3:1 and R 5:1 (HUVECs:FBs) were tested at two seeding densities of $3.04x10^4$ (D_1) and $6.08x10^4$ (D_2). Cells were seeded on a 0.2% gelatin-coated 12-well plate with the selected medium (M 3:1) supplemented with ECGS for five days.

At day 1, the different seeding densities present different DNA content, with higher values for C_2, result of the different densities seeded. Regarding the total metabolic activity, for C_1 all ratios present similar values whereas for C_2 it is possible to observe a pattern where R 5:1 > R 3:1 > R 2:1 > R 1:1, hence presenting higher activities in ratios containing more HUVECs (Figure 10, d), which can also be verified when the values are normalized (using the total dsDNA) (Figure 10, f). By day 3, there are observed increases in the total DNA for C_1 and C_2. However, whereas for C_1 there are no noticeable differences between the different ratios, for C_2, R 1:1 presents higher values than the remainder ratios. This difference is translated in the total metabolic activity where is possible to verify that R 1:1 presented significantly higher metabolic values when compared to the other ratios. Although it is possible to see a decrease in the metabolic activity of the cells (normalized with the total dsDNA) (Figure 10, e and f) it is verified a maintenance of the higher values for endothelial rich ratios (except for R1:1 and R2:1 in C_1 seeding conditions, which can be due to an deficient recovery of the dsDNA, as these also present lower values for total DNA). It is however important to

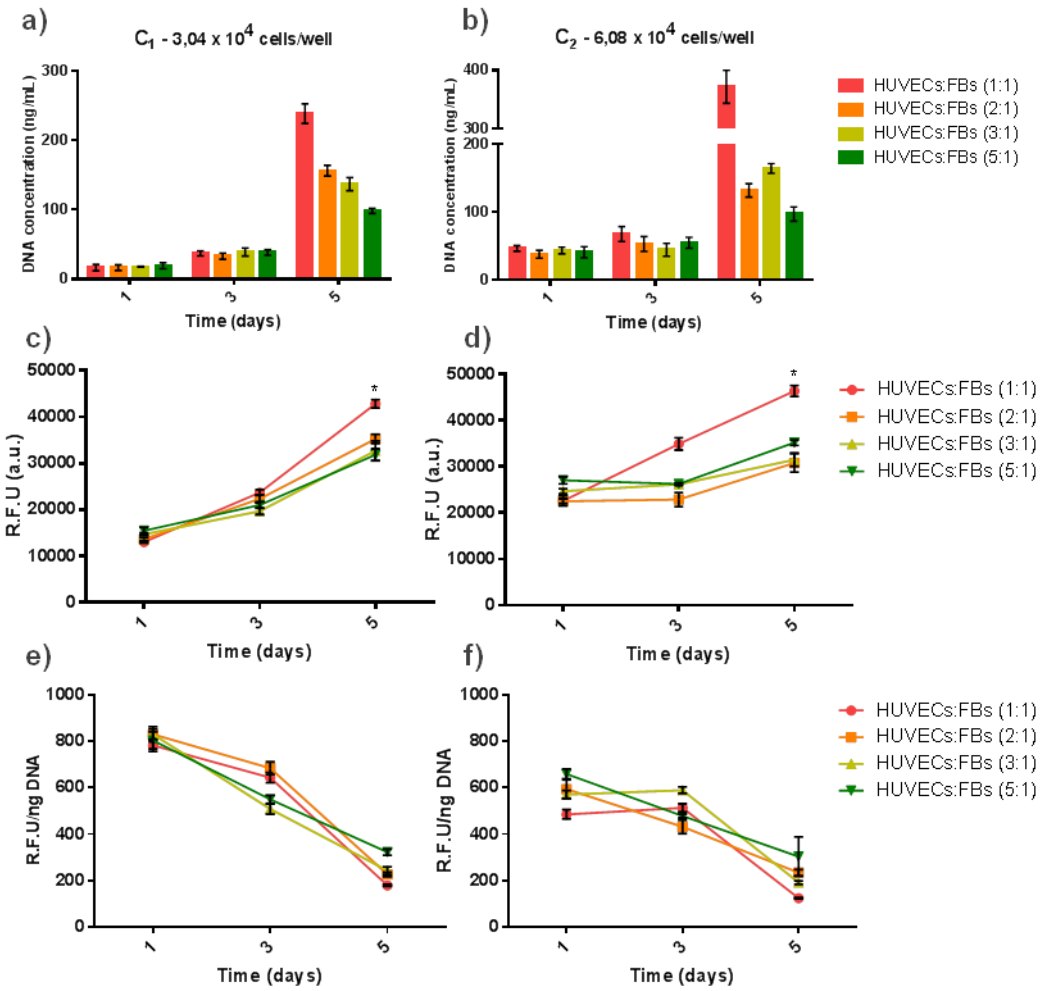

Figure 10. Effect of cell density and cell ratio on metabolic activity and proliferation of HUVEC:FB co-culture in 2D within a 5 days culture period. a) and b) total dsDNA (PicoGreen assay), c) and d) metabolic activity (resazurin assay) and e) and f) metabolic activity per nanogram of dsDNA of HUVEC: * denotes statistically significant differences ($p < 0.05$).

point out that despite this decrease, the cells' metabolic activity is 5 to 6-fold higher than any of the individual cultures. At day 5, the total DNA increases for both seeding conditions, presenting, in all ratios, values superiors to those verified in the monocultures. For C_1 and C_2, in the R 1:1, the ratio containing the highest initial fibroblasts number (presenting however half of those verified in the monocultures), the total DNA content is 3 and 4-fold higher, respectively, when compared to FBs monocultures whereas for R 5:1, an endothelial rich ratio, the total DNA content is 3-fold higher than for HUVEC monocultures. However, regarding the metabolic activity, despite an increase for the total metabolic activity, normalized values show a decrease in the activity of the cells, as it already occurred from day 1 to 3. Nonetheless, the metabolic values are 2-fold higher than individual cell cultures. Putting all together, for a 2D HUVEC:FB co-culture, lower ratios seem to favor proliferation whereas higher ratios seem to favor higher metabolic activities per cell (metabolic activity normalized

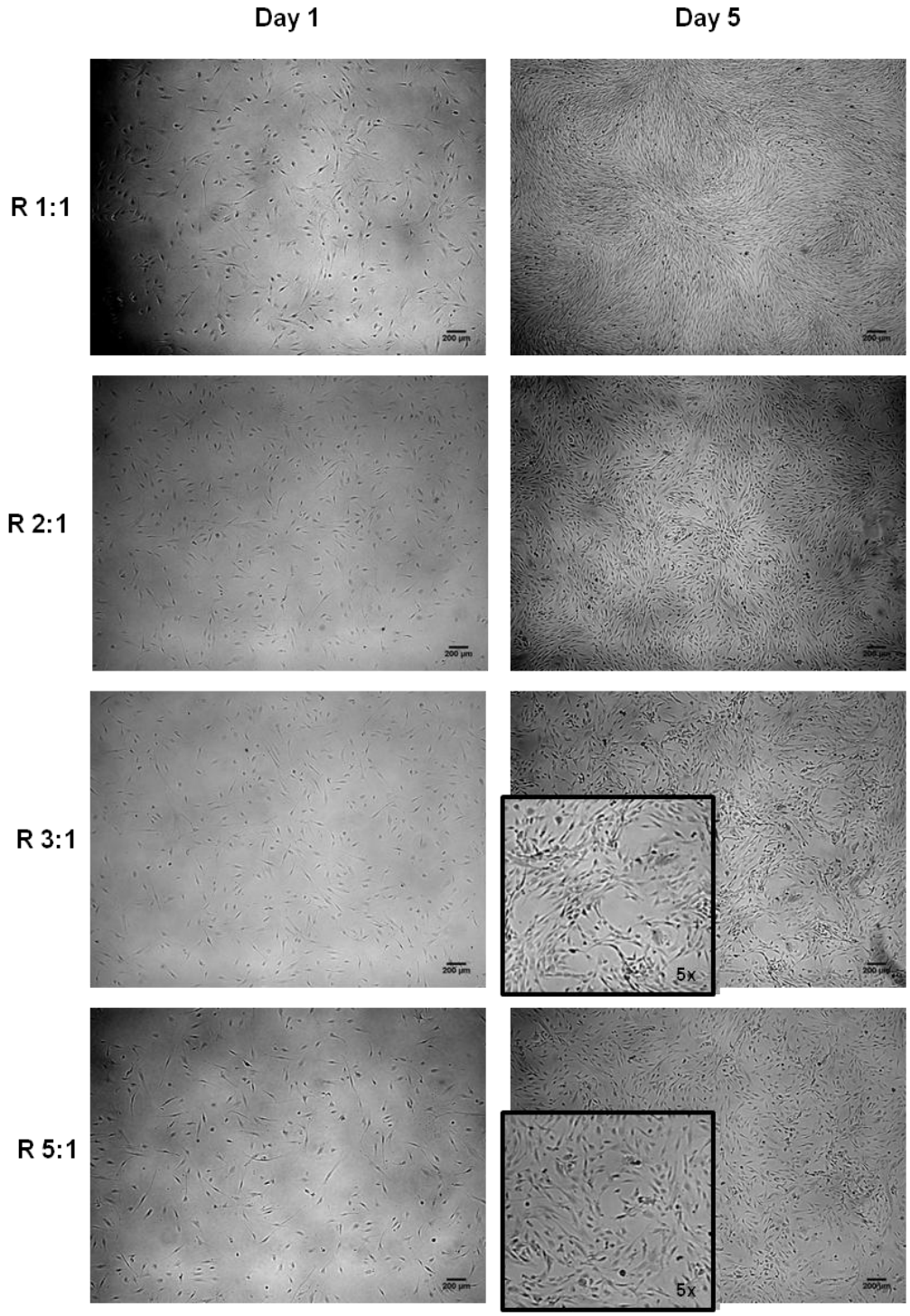

Figure 11. Pictures of HUVEC:FB co-cultures prepared at $6.08x10^4$ cells/well at the different ratios of 1:1, 2:1, 3:1 and 5:1. Images were obtained at the first and last day of 5-days. Scale bars, 200 µm**.**

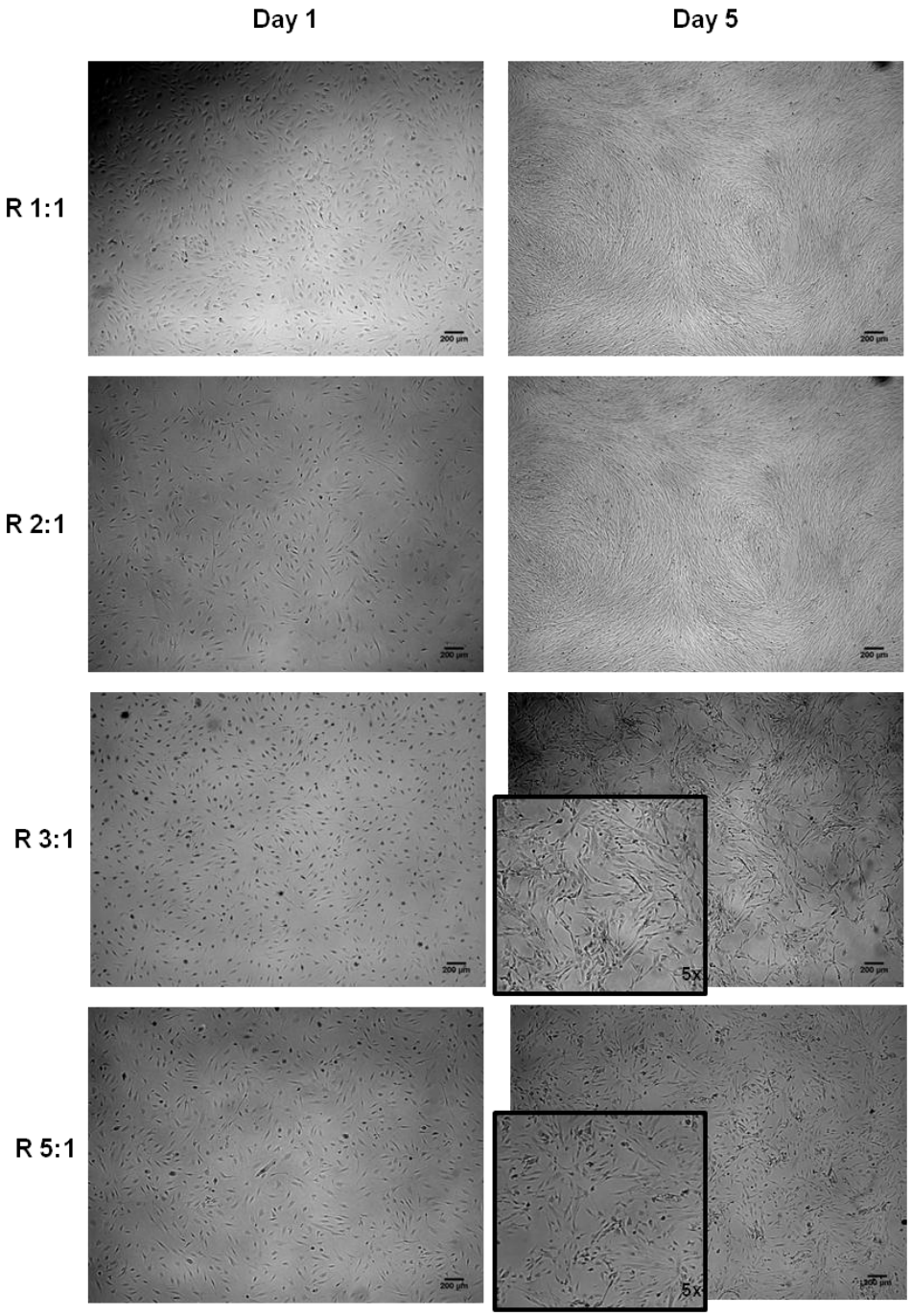

Figure 12. Pictures of HUVEC:FB co-cultures prepared at $6.08x10^4$ cells/well at the different ratios of 1:1, 2:1, 3:1 and 5:1. Images were obtained at the first and last day of a 5. Scale bars, 200 µm**.**

with total dsDNA). For a 5 days culture, the different seeding densities do not seem to influence the final outcome of the culture, affecting however the development of the culture throughout the culture days, as it was also seen for individual cultures.

However, to our purpose, to obtain capillary like structures, metabolic and proliferation studies are not sufficient. In order to properly choose for an adequate ratio, the cell morphology and spatial distribution must be taken into account. To analyze this, we've fixated the different conditions at the different time points and took pictures of the structures formed using an inverted light microscope. The images reveal evident differences between cells organization in different ratios used for HUVEC:FB co-cultures, as can be depicted in the Figures 11 and 12. At lower HUVEC:FB ratios, namely R 1:1 and R 2:1 both cells appeared widely distributed at the cell culture surface throughout the five days, presenting their respective fibroblastic-like and cobblestone-like shapes. At day 5, however, it is observed that these cultures present similar structures to the ones observed in FB monocultures at confluence, hence demonstrating FB dominance in the cell culture surface. At higher ratios, namely R 3:1 and R 5:1, both cell types also archive fibroblastic-like and cobblestone-like shapes. With these ratios, at day 5, it is possible to verify that cells were rearranged in a significantly different manner featuring web-like structures characteristics of tubular-like cellular network formation. All together, high densities with endothelial rich ratios seem more appropriate as 2D co-culture formulations for HUVEC development and capillary-like self assembly.

3.4. Analysis of HUVEC and FB monocultures' behavior in 3D-culture

As depicted in previously, RGD-grafted pectin hydrogels present cytocompatibility, cell adhesion and proliferation characteristics for the improvement of cellular functions (Munarin et al., 2011; Munarin et al., 2012; Neves e al., 2015). As such, pectin stands as a particularly appealing biomimetic material for 3D hydrogel formation for cell culture. For hydrogels, the mechanical performance of a matrix depends on the polymer and crosslinker characteristics, concentration, gelling conditions (e.g. temperature, pH, and gelation time), swelling, and degradation. In turn, these will have an impact in the biomaterial mechanical properties, including elasticity, compressibility, viscoelastic behavior, tensile strength, and failure strain (Anseth et al., 1996). With this in mind, we have followed an already described gelation scheme thoroughly characterized by Neves et al (2015), varying the concentration of the pectin used in the

hydrogels between 1.5% and 2.5% (w/v). These concentrations where used to determine the effects matrix characteristics (e.g. mesh size, mechanical compliance) over the ability of cell to regulate their metabolic activity, alter their morphology, migrate and establish cell-cell contact. Furthermore, to evaluate the effect of cell density on the behavior of cells in 3D environments, cells were entrapped within pectin matrices at different entrapping densities, namely: $D_3 = 5x10^6$ cells.mL^{-1}; $D_4 = 1x10^7$ cells.mL^{-1} and $D_5 = 1.5x10^7$ cells.mL^{-1}. Cell metabolic activity (Resazurin assay), total dsDNA (PicoGreen assay) and morphology (Confocal microscope images) assays were carried out at days 1, 2, 4 and 6.

3.4.1 HUVEC behavioral analysis on 3D soft pectin hydrogels

At day 1, the dsDNA content of the different formulations was proportional to their respective original cell density, presenting however higher values for a 2.5% (w/v) pectin concentration (Figure 13). It is also important to note that the total dsDNA for lowest entrapping density in 1.5% (w/v) pectin hydrogels is nearly inexistent. Regarding the metabolic activity, HUVECs presented higher total metabolic activities in agreement with the previous observations for the total dsDNA. The highest metabolic activity registered was for the $1.5x10^7$ HUVECs.mL-1. When normalized (with total dsDNA), the metabolic results show that for 1.5% (w/v) pectin concentrations all entrapping densities present the same cellular activity, whereas for 2.5% (w/v) lower densities seem to present higher cellular activities. For all the formulations tested (except for 2.5% (w/v) hydrogels with $1x10^7$ HUVECs.mL-1, possibly due to deficient manipulation throughout the experiment), the total dsDNA content gradually decreased along the period of culture, being accompanied by the decrease in the metabolic activity. By day 4, the metabolic activity assay demonstrate close or equal to 0, independently of the content of DNA, which were maintained till day 6.

Regarding the spatial behavior (Figures 14 and 15), for the lowest entrapping density, namely, $5x10^6$ HUVECs.mL-1, the images were not presented as they did not help to elucidate what was happening within the hydrogels. As for $1x10^7$ HUVECs.mL-1 and $1.5x10^7$ HUVECs.mL^{-1} entrapping densities, independently of the pectin concentration, cells seem widely distributed within the matrix. Cells maintained a globular structure, indicative of the lack of adhesion, throughout the experiment. As the total dsDNA and metabolic assays shown very low DNA content and metabolic activity for day 4 and 6, no stains were carried, hence no images are presented.

All together, these results indicate that, independently of the pectin concentration and entrapment densities, monoculturing HUVECs on pectin hydrogels is not an efficient strategy for HUVEC self-assembled tubulogenesis or even maintenance.

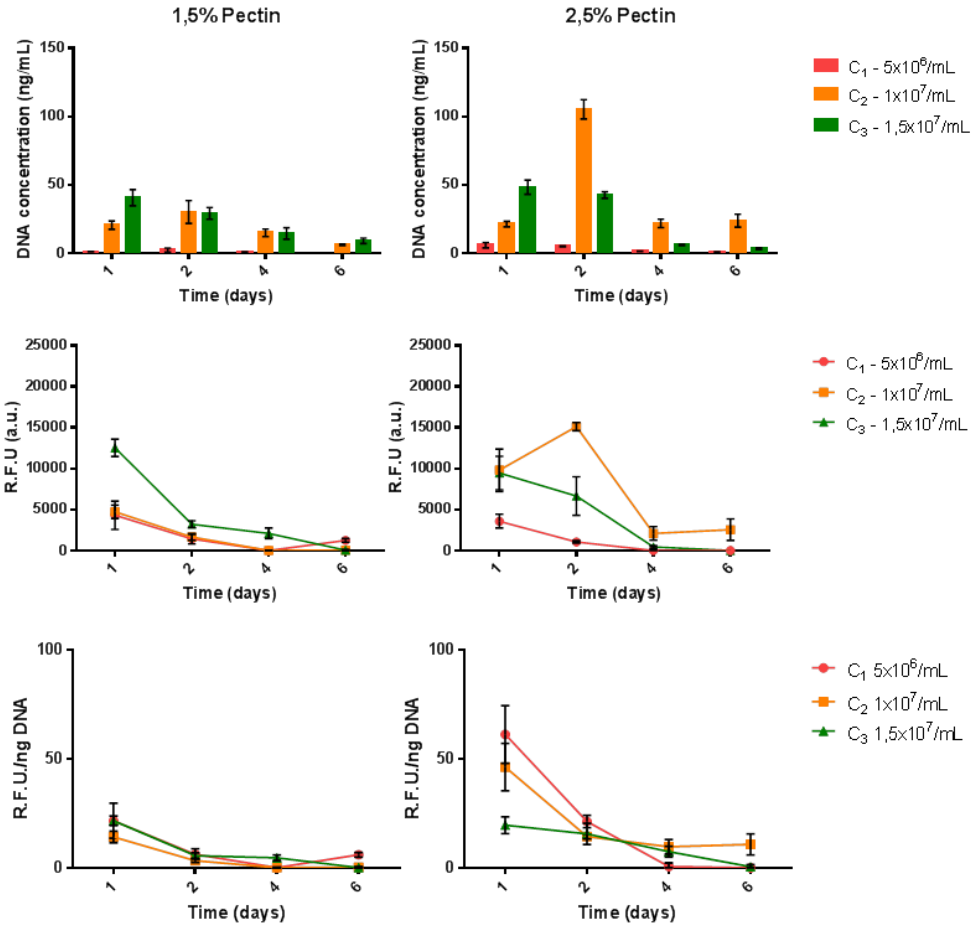

Figure 13. Effect of initial cell entrapment density and pectin concentration on metabolic activity and proliferation of HUVEC in a 3D soft pectin hydrogel within a 6 days culture period. a) and b) total dsDNA (PicoGreen assay), c) and d) metabolic activity (resazurin assay) and e) and f) metabolic activity per nanogram of dsDNA of HUVEC * denotes statistically significant differences ($p < 0.05$).

3.4.2. FBs behavioral analysis on 3D soft pectin hydrogels FBs

As regards to FBs, two significantly different profiles can be observed for different pectin concentrations (Figure 16). For 1.5% (w/v), at day 1, it is possible to verify that the cell-loaded matrix present total dsDNA values in accordance to the initial number of cells entrapped. By day 2, a slight increase in the total dsDNA is observed for the entrapping densities of $5x10^6$ FBs.mL^{-1} and $1x10^7$ FBs.mL^{-1}, which, attending to the remaining profile, could be the result of the total DNA assay manipulation. At day 4, dsDNA seems to slightly decrease, maintaining its values at day 6. Relatively to the

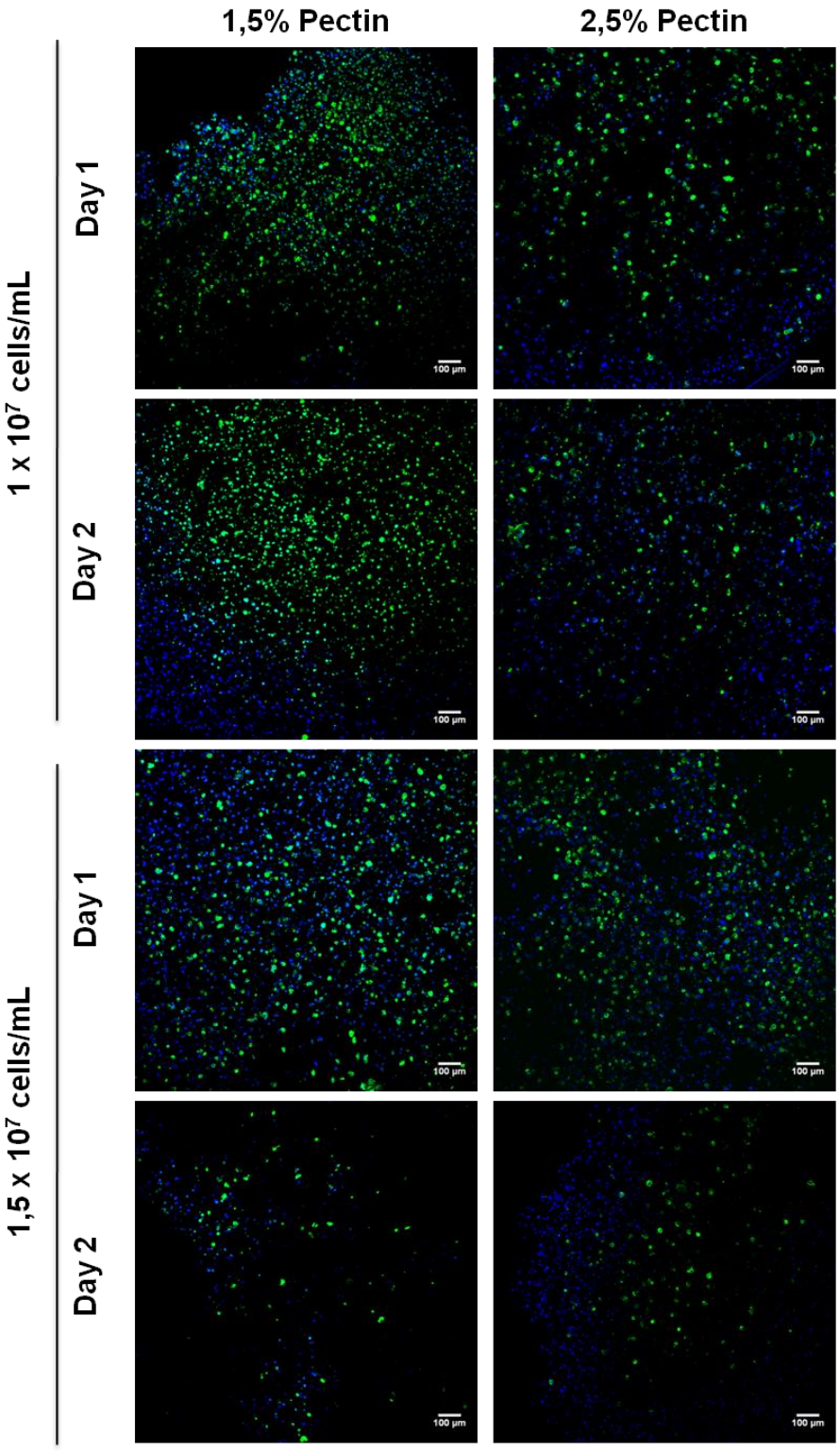

Figure 14. Effect of initial cell entrapping density and pectin concentration on the 3D HUVECs' spatial distribution within a 6 days culture period on a soft pectin hydrogel. HUVECs were stained for F-actin (Green) and nuclei (Blue). Scale bars, 100 µm**.**

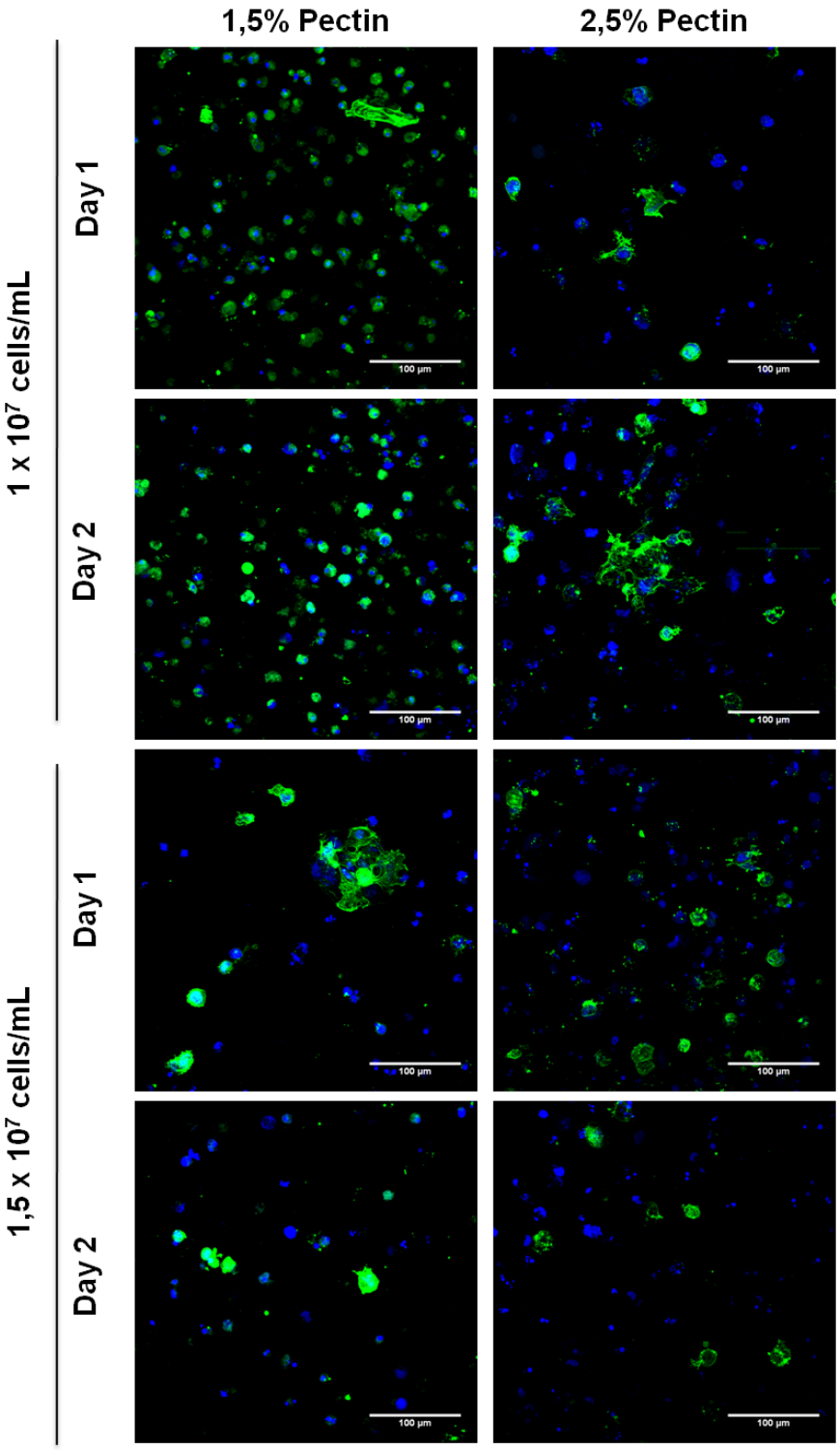

Figure 15. Effect of initial cell entrapping density and pectin concentration on the 3D HUVECs' conformation within a 6 days culture period on a soft pectin hydrogel. HUVECs were stained for F-actin (Green) and nuclei (Blue). Scale bars, 100 µm

.

metabolic activity, FBs, as HUVECs, presented lower metabolic values in 3D matrices when compare to a 2D culture as expected. Regarding 1.5% (w/v) pectin hydrogels, at day 1, total dsDNA contents were in accordance with the entrapping densities, with the metabolic activity in conformity with these entrapping densities. From day 1 to day 2, there is observed a decrease in the $1.5x10^7$ FBs.mL^{-1} entrapping density and an increase in the $5x10^6$ FBs.mL^{-1} $1x10^7$ FBs.mL^{-1} entrapping densities, reaching similar values. From this point onwards, the metabolic activity seems to maintain a steady-state. When normalizing these results, an increase in the cellular metabolic activity is observed between day 2 and 4. To note that, for entrapping densities of $1.5x10^7$ FBs.mL^{-1}, several discs broke from the first day, complicating the manipulation and subsequent recovery of data (both the metabolic and dsDNA assays and image recovery). As for 2.5% (w/v) pectin hydrogels, a different profile is observed. For all the densities tested, the total the total dsDNA content remained constant along the time. However, the total metabolic activity gradually decreased along the period of culture, which, when normalized, translates in a steady decrease in the cellular metabolic activity.

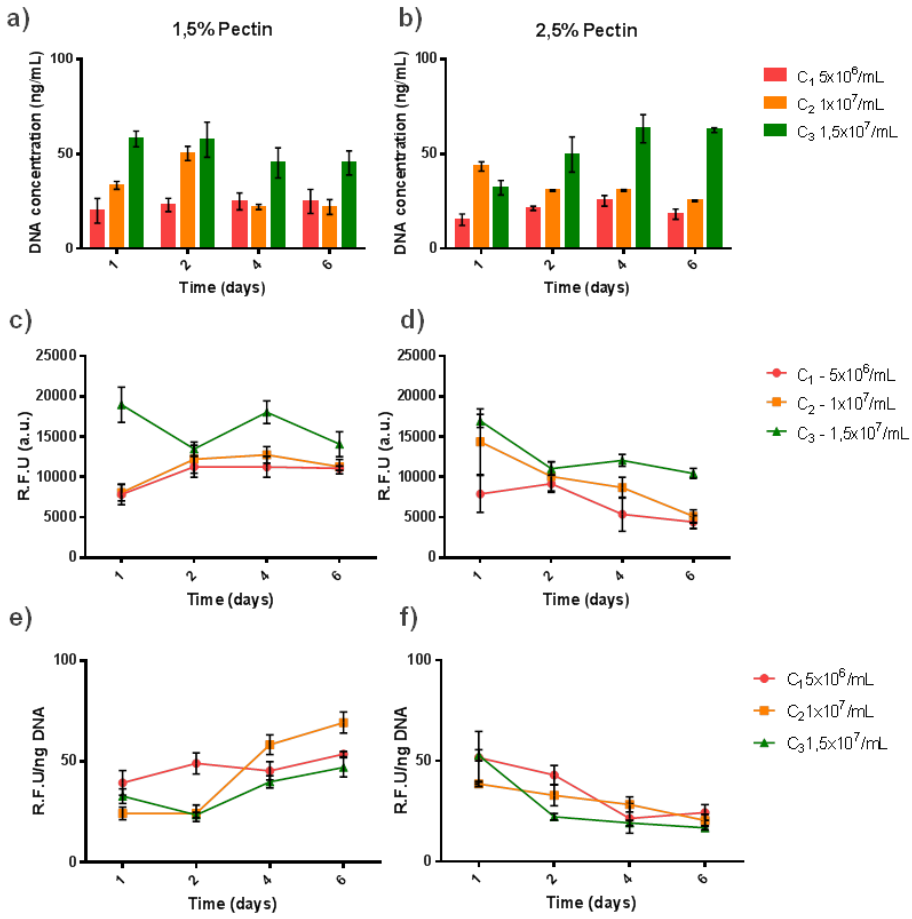

Figure 16. Effect of initial cell entrapping density and pectin concentration on metabolic activity and proliferation of NHDFs in a 3D soft pectin hydrogel within a 6 days culture period. a) and b) total dsDNA (PicoGreen assay), c) and d) metabolic activity (resazurin assay) and e) and f) metabolic activity per nanogram of dsDNA of NHDFs * denotes statistically significant differences ($p < 0.05$) .

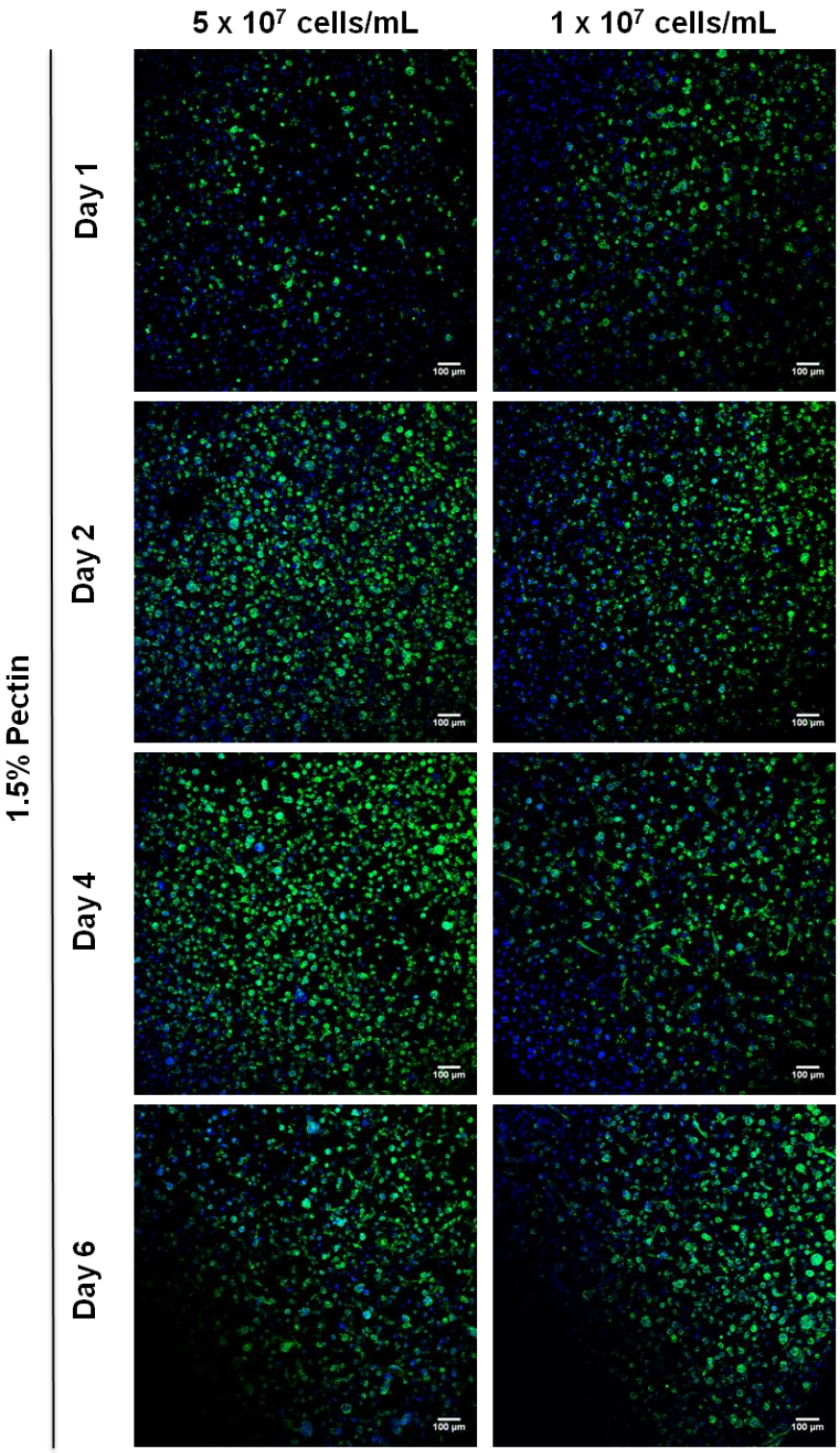

Figure 17. Effect of the initial entrapping density on a 1.5% pectin 3D hydrogel on FBs' spatial distribution within a 6 days culture period. FBs were stained for F-actin (Green) and nuclei (Blue). Scale bars, 100 µm**.**

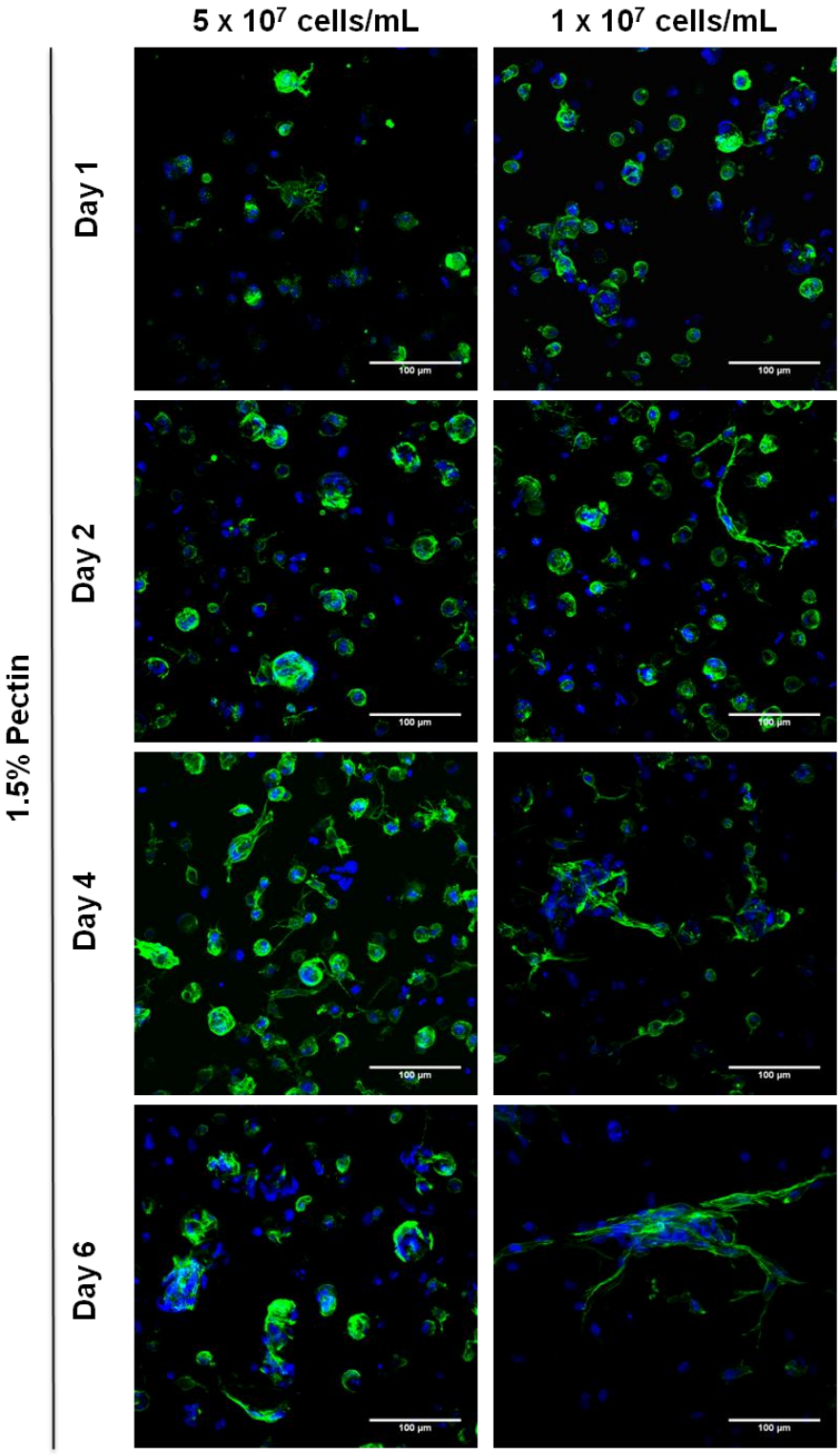

Figure 18. Effect of the initial entrapping density on a 1.5% pectin 3D hydrogel on FBs' conformation within a 6 days culture period. FBs were stained for F-actin (Green) and nuclei (Blue). Scale bars, 100 µm**.**

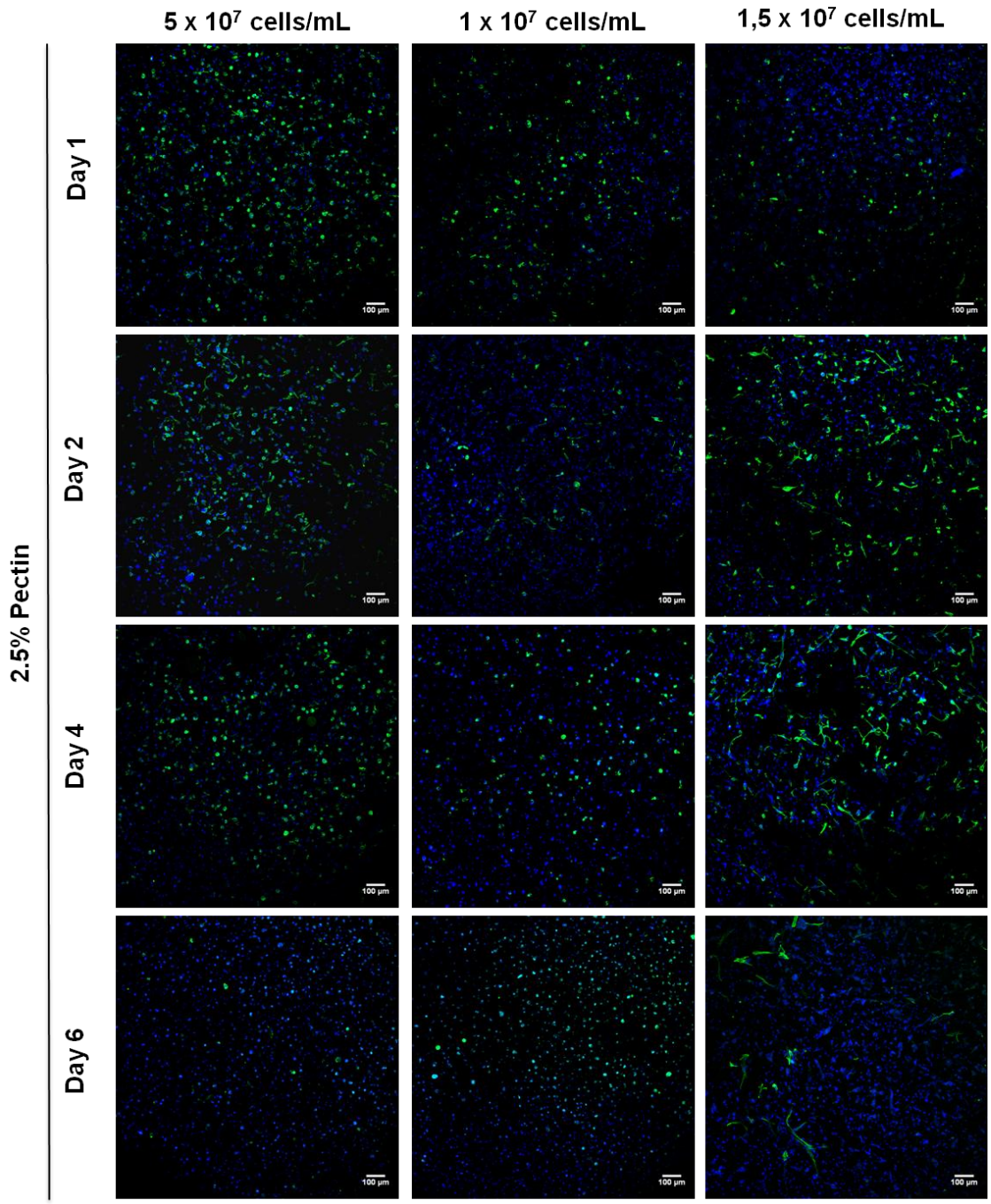

Figure 19. Effect of the initial entrapping density on a 2.5% pectin 3D hydrogel on FBs' spatial distribution within a 6 days culture period. FBs were stained for F-actin (Green) and nuclei (Blue). Scale bars, 100 µm**.**

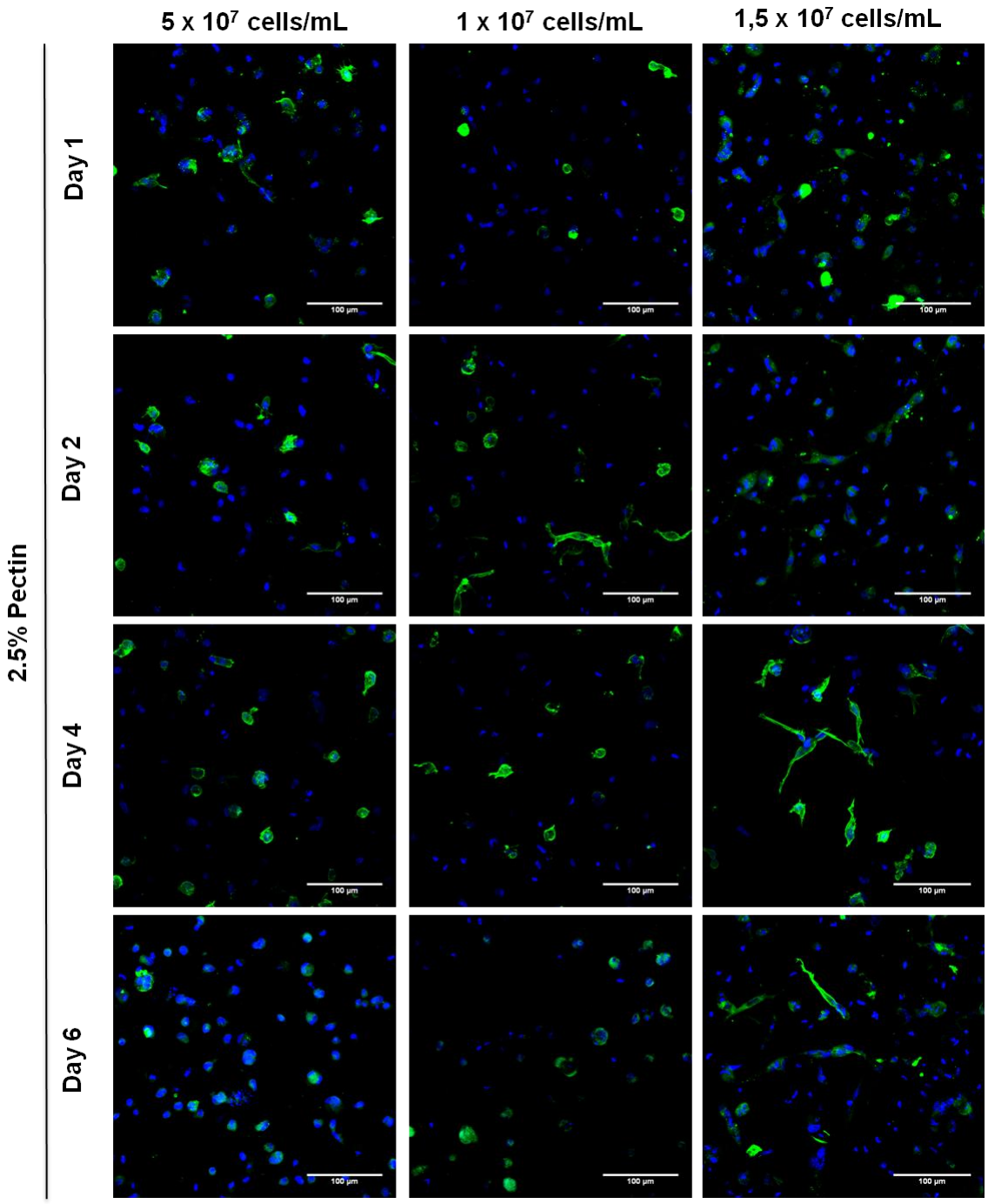

Figure 20. Effect of the initial entrapping density on a 2.5% pectin 3D hydrogel on FBs' conformation within a 6 days culture period. FBs were stained for F-actin (Green) and nuclei (Blue). Scale bars, 100 µm.

Regarding the spatial behavior, accompanying the tendency presented by cell metabolic activity, 1.5% (w/v) pectin hydrogels presented better results when compared to 2.5% (w/v) pectin hydrogels. Within these, as seen in the Figures 17 and 18, cells were widely distributed, being able to adhere, acquiring a fibroblast-like shape. Throughout time, these cells were able to establish cell-cell contacts, forming FB spheroids which increased in number and size, as depicted in Figure 21 and 22 Table 1. These structures presented significantly larger spheroids when compared to the ones formed in 2.5% (w/v) pectin hydrogels. It is also demonstrated that, depending on the initial entrapping densities in 1.5% (w/v) pectin hydrogels, higher entrapping densities favor a significantly larger size of the spheroids (Table 1). However, as stated before, due to degradation of the matrices at $1.5x10^7$ FBs.mL^{-1} (the discs broke and started to decompose). Regarding 2.5% (w/v) pectin hydrogels, independently of the

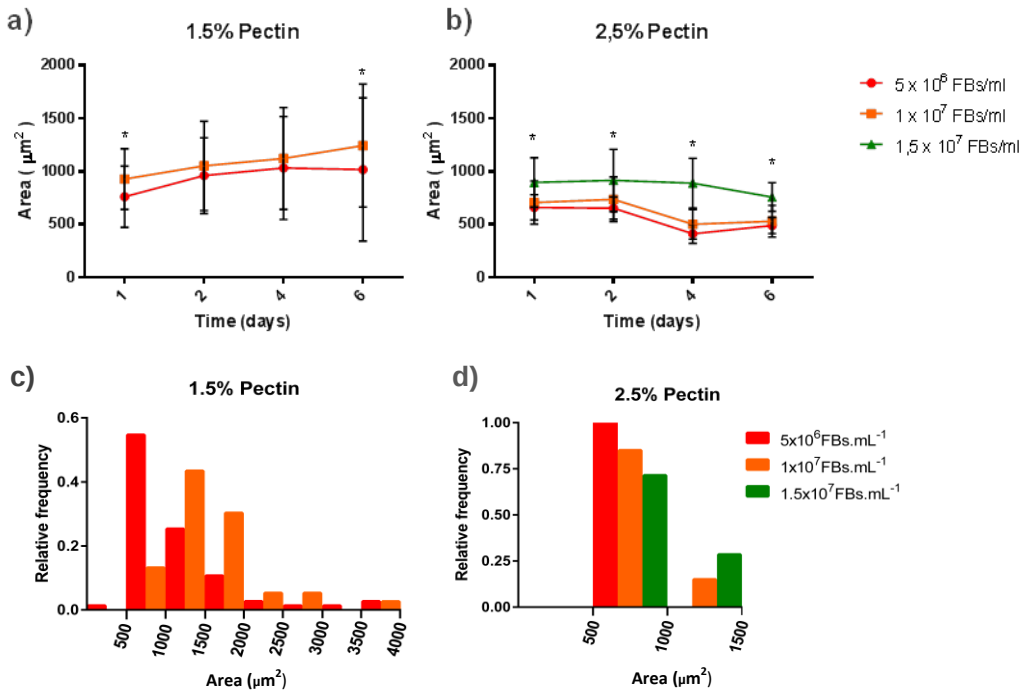

Figure 21. Effect of Initial cell entrapping and pectin concentration over FBs spheroid size. a) and b) spheroids average size throughout the 6 days of culture. c).and d) relative frequency of spheroid size at day 6. * denotes statistically significant differences ($p < 0.05$)) between different entrapping densities on different pectin concentrations.

Table 1. Effect of initial cell entrapping densities and pectin concentration over FBs spheroid size (μm^2) and number. Area means and standard deviation is presented in micrometers. N stands for total number of spheroids. * denotes statistically significant differences ($p < 0.05$) between the same entrapping density on different pectin concentrations. α denotes statistically significant differences ($p < 0.05$) between different entrapping densities on different pectin concentrations.

	Day 1		Day 2		Day 4		Day 6	
1.5% Pectin	Area	n	Area	n	Area	n	Area	n
$5x10^6$ FBs.mL^{-1}	761±288*	37	960±358*	176	1032±486*	261	1017±676*	206
$1x10^7$ FBs.mL^{-1}	927±287*$^{\alpha}$	170	1051±422*	183	1121±481*	291	1244±580*$^{\alpha}$	251
2.5% Pectin								
$5x10^6$ FBs.mL^{-1}	660±120	34	652±105	29	441±90	19	489±77	26
$1x10^7$ FBs.mL^{-1}	705±203	87	735±212	60	500±140	53	528±150	34
$1.5x10^7$ FBs.mL^{-1}	895±232$^{\alpha}$	153	915±294$^{\alpha}$	83	889±235$^{\alpha}$	51	758±136$^{\alpha}$	59

entrapping density, cells exhibit a globular-like shape, with some cells presenting a fibroblast-like shape, mostly observed at the surface (Figures 19 and 20). Although there is possible to observe some spheroids, the number and size is significantly lower than what is observed for 1.5% (w/v) pectin hydrogels. Throughout the period of the culture, 2.5% (w/v) pectin matrices loaded with $1.5x10^7$ FBs.mL^{-1} present significant larger spheroids when compared to the other entrapping densities. However, for all densities, spheroid number and size decreases with time, accompanying the decrease in metabolic activity previously described for these conditions.

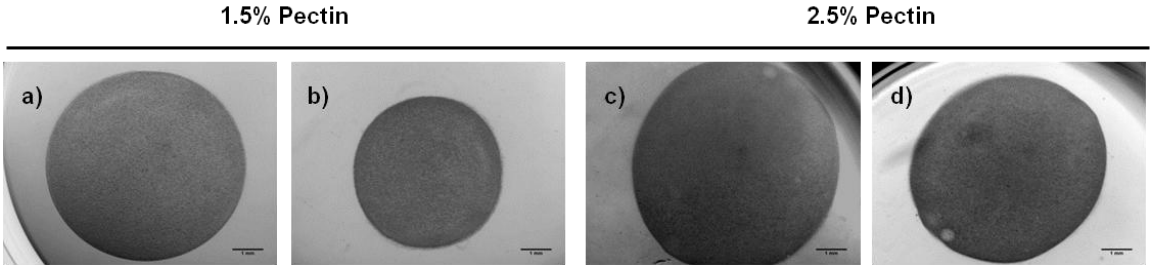

Figure 22. Effect of pectin concentration over the ability of FBs to contract the matrix. Macroscopic differences of 1.5% and 2.5% pectin hydrogels seeded with $1x10^7$ FBs.mL^{-1}. Images were obtained at the first and last day of a 6-days culture using an inverted microscope using a magnification of 16.3 x. a) and b) correspond to 1.5% (w/v) pectin hydrogels at day 1 and 6 respectively. c) and d) correspond to 2.5% (w/v) pectin hydrogels at day 1 and 6 respectively. e) represents the relative size of the pectin matrices when compared to day 1

Table 2. Effect of pectin concentration over the ability of FBs to contract the matrix. Macroscopic differences of 1.5% and 2.5% pectin hydrogels entrapped with $1x10^7$ FBs.mL^{-1}. Areas means and standard deviation is measured in square millimeters

$1x10^7$ cells.mL^{-1}	Day 1	Day 2	Day 4	Day 6
1.5% Pectin	31.95 ± 1.09	21.40 ± 0.04	18.81 ± 0.35	17.58 ± 0.57
2.5% Pectin	38.34 ± 1,09	33.72 ± 0.42	31.46 ± 1.32	29.81 ± 0.12

Another important feature of the gels is the mechanical compliance, which will impact over the cells ability to exert forces to deform the matrices. To test the influence of pectin concentration over the ability of FBs monocultures to promote matrix contraction, macroscopic images of 1.5% and 2.5% (w/v) pectin hydrogels matrices loaded with $1x10^7$ FBs.mL^{-1}, the highest performing comparable density ($1.5x10^7$ FBs.mL^{-1} was excluded as for 1.5% (w/v) pectin matrices were unsuitable to handle), were recovered at day 1, 2, 4 and 6 (Table 2 and Figure 22). At day 1, 1.5% (w/v) pectin hydrogels presented smaller areas than 2.5% (w/v) pectin hydrogels. As these matrices were produced with the same volume (20 µL), this difference indicates that after the initial swelling (verified while manipulating but not measured), from day 0 to day 1 matrices start to contract at lower pectin concentrations. By day 2, 1.5% (w/v) pectin hydrogels presented a 33% matrix contraction when compared to day 1 and by day 6 and 45%. Regarding 2.5% (w/v) pectin hydrogels, for these days, we observe a matrix contraction of 12% and 22% respectively, when compared to day 1. Furthermore, by day 6, 2.5% (w/v) pectin hydrogels are 1.70x larger than 1.5% (w/v) pectin hydrogels.

Summing up, for both pectin concentrations, total dsDNA values remained essentially constant throughout the period of culture, suggesting that the entrapped cells were not able to proliferate, independently of the original cell density. The main differences were found at the metabolic activity and cellular spatial distribution. In 1.5% (w/v) pectin hydrogel matrices, cells were able to adhere to the matrix, acquiring fibroblast-like shape, and establish cell-cell interactions, forming FBs spheroids, while maintaining a steady-state of metabolic activity. In these conditions, higher entrapping densities favored a higher spheroid formation with significantly higher areas. Moreover, for $1x10^7$ FBs.mL^{-1}, macroscopic images of the cell-laden matrices allowed to observe alterations of the construct size, presenting at day 6 to almost half of the size of the one observed at day 1. However, regarding 2.5% (w/v) pectin hydrogels, cells essentially maintained

a globular like shape, exhibiting a fibroblast-like shape mostly at the surface. These results were in accordance to what was expected as 2.5% (w/v) pectin hydrogels are less compliant and provide less free space for cells to spread when compared to 1.5% (w/v) pectin hydrogels (Neves et al., 2015). FBs spheroids were also observed in this construct but with significantly inferior numbers and size. Finally, macroscopic images demonstrate that these matrices maintain a more robust aspect possessing not only, at day 6, 80% of the size when compared to day 1 but also almost a 2-fold increase when compared to 1.5% (w/v) pectin hydrogels. Results obtained by us indicate that cells might be constrained by the polymeric network at higher pectin concentrations, favoring the use of more compliant matrices for FBs culture. Within these (1.5% (w/v) pectin hydrogels), higher entrapping densities seem to stimulate cell-cell contacts and the formation spheroids.

3.5 HUVEC:FB co-culture establishment in 3D soft pectin hydrogels

As previously stated, coculturing ECs with FBs can potentiate tubulogenesis (Berthod et al., 2006; Sorrell et al., 2007; Auger et al., 2013). Nonetheless, great differences can be observed among different matrices, cell type's combinations, entrapping densities and entrapping ratios. As such, it is of utmost importance to optimize these factors for 3D cultures in each specific application design. As documented throughout this thesis, several optimization steps were taken into account in order to choose the coculturing conditions, namely: medium supplementation (through metabolic activity and total dsDNA) and cell ratio (through metabolic activity, total dsDNA and optical microscopy analyzes), in 2D experiments, and polymer concentration and cell entrapping densities (through metabolic activity, total dsDNA and optical microscopy analyzes), in 3D experiments. Aiming to promote the capillary self-assembly of HUVECs in a 3D pectin hydrogel, these were co-culture with FB at a ratio of 3:1 (HUVEC:FB), with an entrapping density of $1.5x10^7$ cells.mL^{-1}. These were cultured in pectin hydrogels with a 1.5% pectin concentration and supplemented with M 3:1 with 0.03 mg.mL^{-1} of endothelial cell growth supplement (ECGS).

3.5.1. Characterization of the influence of M 3:1 supplementation on HUVECs or FB monocultures in 3D soft pectin hydrogels

Preceding the HUVEC:FB co-culture, in order to evaluate the medium influence on the 3D cells behavior, both HUVECs and FBs were loaded in 1.5% (w/v) pectin hydrogels

at the chosen entrapment density namely, $1.5x10^{7}$ cell.mL^{-1}. The behavior was analyzed recurring to metabolic and total dsDNA assays and, as depicted by Figure 23. Throughout the culture period, M3:1 does not present any significant difference displaying very similar profiles when compared to the optimal medium for each cell type, with exceptions made to the metabolic activity of FBs at day 1 for M 3:1 supplementation and dsDNA content for FBs in M3:1 at day 6. The first can be explained due to a faster manipulation of the cell in the entrapment process, leading to a slower loss of activity by the FBs whereas the second, given the metabolic results for the same condition, should be a DNA manipulation error. With this experiment, M 3:1 was successfully tested as a potential candidate for HUVEC:FB co-culture in both 2D and 3D environments.

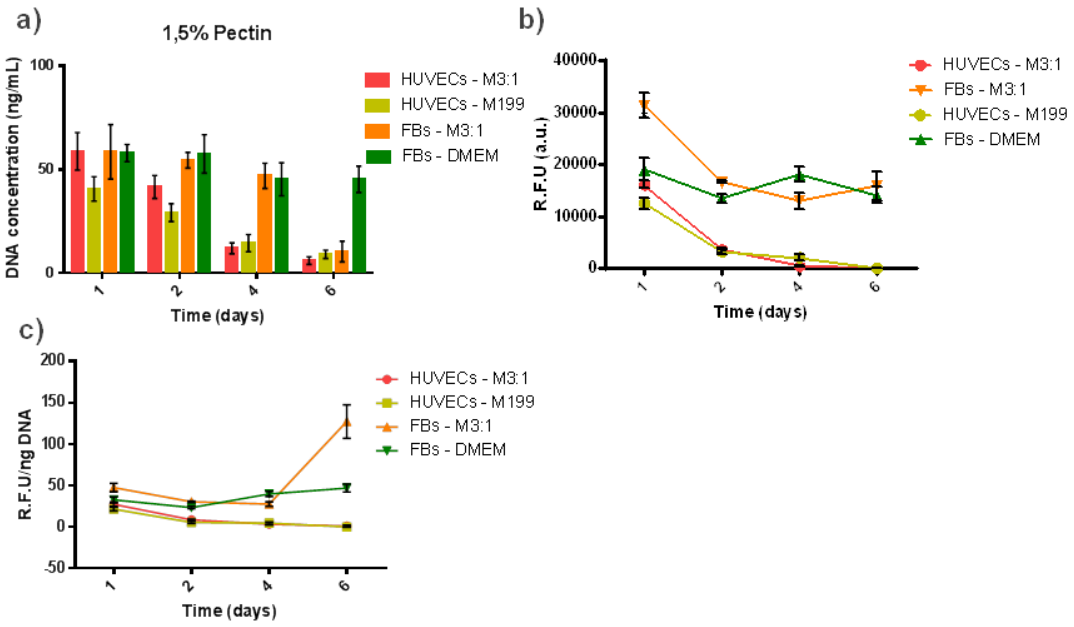

Figure 23. Effect medium composition on metabolic activity and proliferation of HUVECs and FBs in a 3D pectin hydrogel within a 6 days culture period. a) total dsDNA (PicoGreen assay), b) metabolic activity (resazurin assay) and c) metabolic activity per nanogram of dsDNA. * denotes statistically significant differences ($p < 0.05$).

3.5.2. Characterization of HUVEC:FB co-culture behavior in a 3D soft pectin hydrogel

HUVEC:FB co-culture were established by simultaneous entrapment of both cell types in 3D pectin hydrogel, with a entrapping density of 1.5x107 cells.mL-1, at a ratio of 3:1 (HUVEC:FB). To evaluate the behavior of the co-culture, at days 1, 2, 4 and 6, we proceeded to measure the total dsDNA and metabolic activity. These values where then compared to the ones obtained for FBs and HUVECs monocultures in the same conditions.

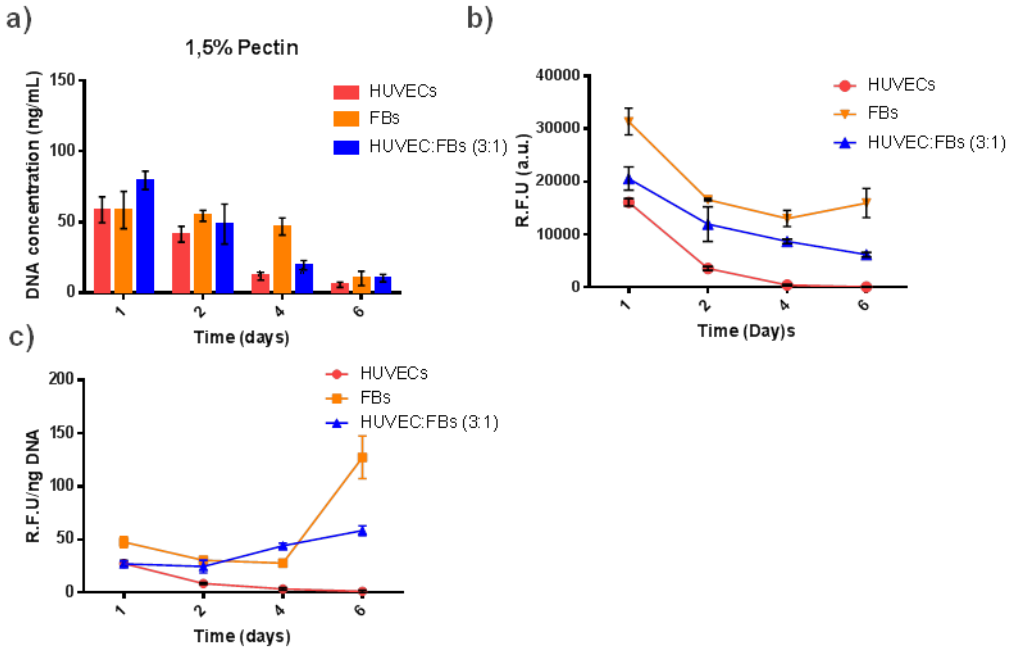

Figure 24. Co-culture of HUVECs and FBs in a ratio of 3:1 (HUVEC:FB) in a 3D pectin hydrogel within a 6 days culture period. a) total dsDNA (PicoGreen assay), b) metabolic activity (resazurin assay) and c) metabolic activity per nanogram of dsDNA

As Figure 24 shows, throughout the culture period co-cultures present a steady decrease in the total dsDNA. This decrease is accompanied by a decrease in metabolic activity. When compared to HUVEC monocultures, at all time points, co-cultures presented higher dsDNA and metabolic values. However, the dsDNA decreasing profile it is similar for both conditions. This could imply that the metabolic differences observed can be a result of a higher cell activity of the cells in a co-culture environment, which is verified throughout the culture period when normalizing the metabolic results with dsDNA content, and/or by the activity of FBs within the matrix. Nonetheless, these results showed that despite the dsDNA loss with time (which represents a cell loss) the culture was able to maintain activity until day 6, which did not happened for HUVEC monoculture.

Cell morphology and re-arrangement within the matrices was analyzed by confocal microscopy. Cell were stained against vWF (Red), an endothelial specific cell marker, α-SMA (Gray) a protein expressed by cell with contractile abilities, F-actin (Green) and nuclei were counterstained with DAPI (Blue) and the merged images were assembled with ImageJ.

At day 1 it is possible to observe a wide distribution of vWF-positive cell, representing HUVECs and vWF-negative cell, which represent FBs (Figure 25 a and d). At this time point images do not show α-sma presence in the cells. Moreover, few FB spheroids are observed, which is probably a consequence of the low number of fibroblasts entrapped

(we previously verified that lower entrapment densities led to fewer and smaller FB spheroids size). Due to experimental problems, as it had already occurred for FB monocultures in 2.5% (w/v) pectin hydrogels, actin staining was not successful, therefore not elucidatory of the shape of the cells. By day 4, it was possible to observe an increase in the number of aggregates in the co-culture, maintaining however widely distributed, unorganized profile (Figure 25 b and e). At this time point there is possible to observe that vWF-negative cells start to express α-sma, which could be indicative of a differentiation of fibroblasts into myofibroblasts. More interestingly vWF-positive cell, namely HUVECs, seem to also be expressing α-sma. Although uncommon, these phenomenon is described in the literature (Lu et al., 2004; Cevallos et al., 2006), indicating a possible differentiation of HUVECs into smooth muscle cells that, in conjugation with myofibroblasts, would fulfill the role of perivascular cells.

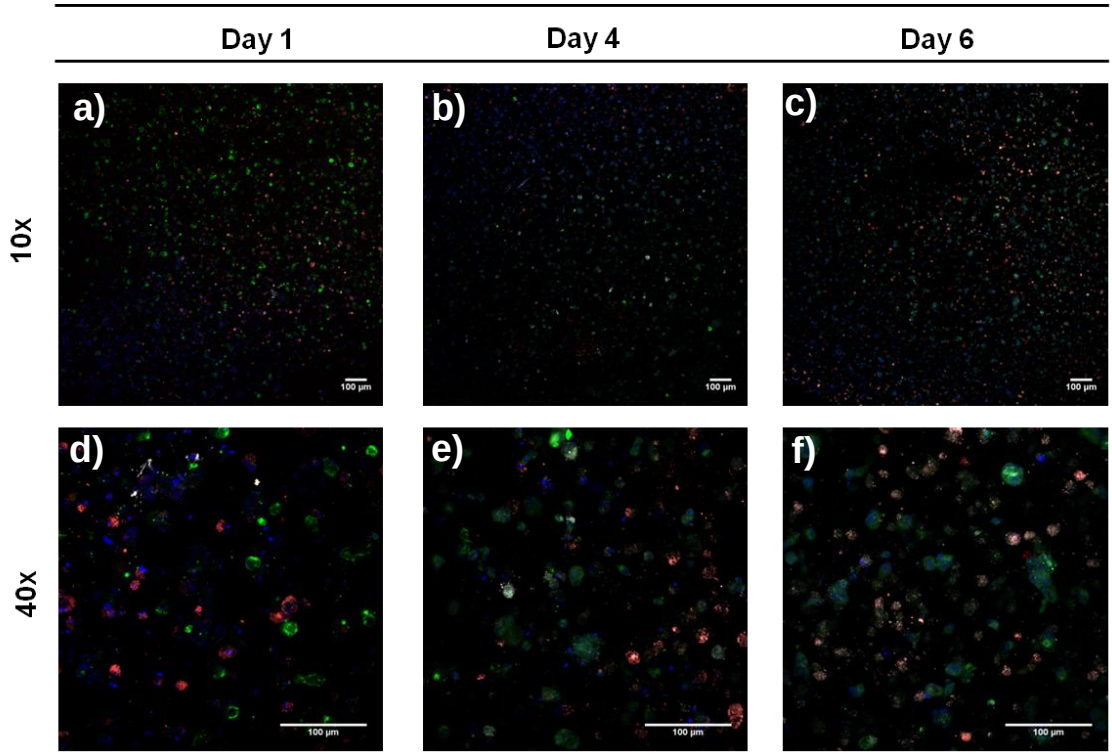

Figure 25. Effect of cell type to type 3:1 ratio on HUVEC:FB co-culture cell morphology and spatial distribution for a 6 days culture period. Cells were stained against vWF (Red) and α-SMA (Gray), for F-actin (Green) and nuclei (Blue). Scale bars, 100 µm

By day 6 (Figure 25 c and f), the expression of α-sma in vWF-positive cell became more evident. Cells remain spread through the matrix, not acquiring any specific organization. All together, these results demonstrate that, in a 6-days culture period, HUVEC self-assembly into tubular-like structure is not favored by the ratio used. Moreover, this ratio seems to promote HUVECs expression of α-sma, promoting their differentiation into smooth muscle cells

3.5.3 Micropatterning

For a different approach on the problem, a micropatterning technique was tested. Micropatterning can be used to control the area on which cell-cell interaction can occur as well as the cell populations that are allowed to interact with one another. Using micropatterning, a HUVEC island was inserted within a matrix of 3D cultured fibroblasts. However, under the light of the previous results for the co-culture experiments, and given the technical implications of this process *in situ* protocol adjustments were performed. As such, the final experimental conditions presented an HUVEC:FB co-culture with a ratio of, approximately 1:3 (more precisely 1:2.66) with an entrapping density of $1.1x10^{7}$ cells.mL^{-1}. This condition was evaluated at the days 1, 2 and 4, using a confocal microscope. For differentiation between the co-cultures, R 3:1 HUVEC:FB co-culture will be depicted as CoHUVECs and the R 1:3 HUVEC:FB co-culture will be depicted as MiHUVECs.

When observed by confocal microscopy, at day 1, under these conditions, it is possible to observe the formation of larger FBs aggregates when compared to the CoHUVECs, with these already express α-sma (Figure 26 a and d). HUVECs where positioned essentially in the center. By day two, it is possible to see the HUVECs rich island from which it is possible to observe that cells are migrating towards the periphery, the FB rich zones. This HUVEC rich island presents several vWF-positive cells that do not express α-sma. In fact, α-sma seems to be expressed in the contact zones between HUVECs and FBs (Figure 26 b). By day 4, HUVECs seem to be more widely distributed, with a mixture of vWF-positive cells that express α-sma and vWF-positive cells that do not. However, at this time point, images are not elucidative on the ability of cells self-assemble into capillary-like structures or even acquiring a spiderweb-like spatial arrangement (Figure 26 c and f), indicative of possible tubular-like formations. Due to the experimental difficulties and time restrains, it was not possible to evaluate this culture behavior at day 6, which could be more elucidative on MiHUVECs ability to promote self-assembled tubular structures.

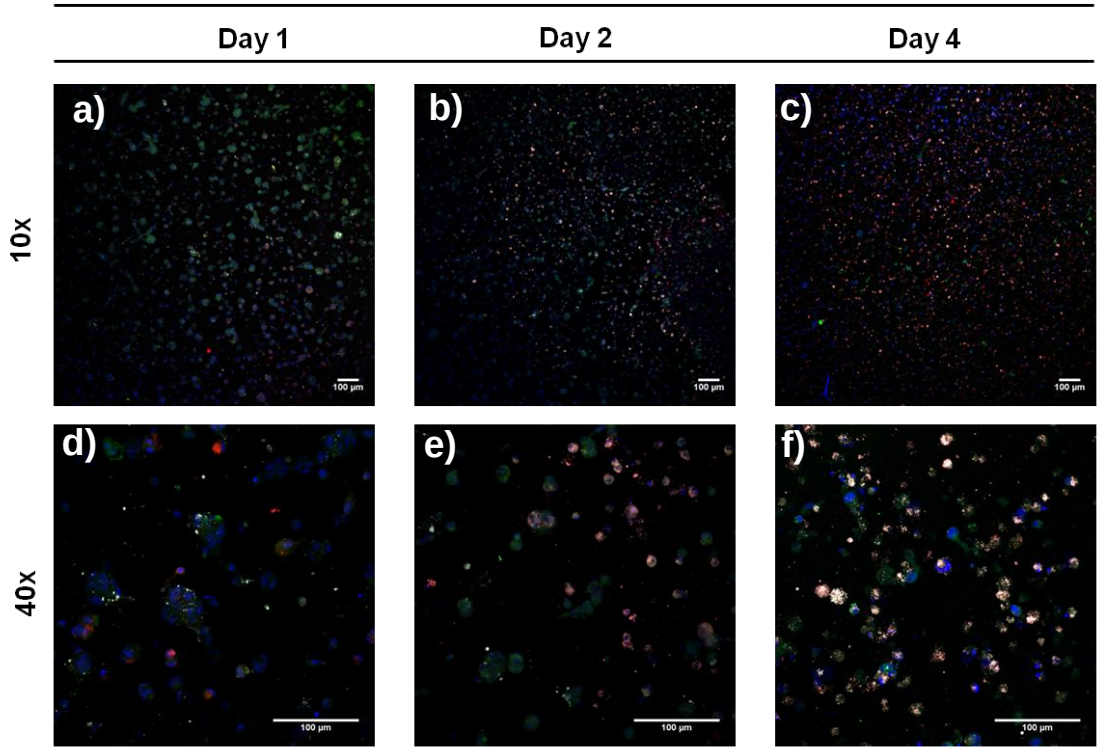

Figure 26. Effect of cell type to type 1:3 ratio on HUVEC:FB co-culture cell morphology and spatial distribution for a 6 days culture period. Cells were stained against vWF (Red) and α-SMA (Gray), for F-actin (Green) and nuclei (Blue). Scale bars, 100 µm

Finally, it is important to note that the *in situ* alterations performed while carrying out the experiment imply that in this construction present three variables when compared to the HUVEC:FB co-cultures previously described: entrapping density, cellular ratio and spatial patterning. Each of these variations should be isolated to properly attend to its influence on HUVECs self-assembly.

.

Discussion

Regardless of the specific tissue-engineering approach, to construct a functional tissue, this must include relevant native or precursor cell types conjugated with the necessary conditions on which these are able to survive and redeem their biological functions. As an organ, skin is not an exception and, in natural tissues, these conditions are proportioned by the extracellular matrix (ECM) which support and modulate cellular development and functions through mechanical and chemical stimuli (Stupack et al., 2003; Discher et al., 2005; Engler et al., 2006; Yu et al., 2009), and by the vascular system that enables access to oxygen and nutrients, as well as elimination of carbon dioxide and other cellular waste products (Rouwkema et al., 2008; Rivron et al., 2008; Auger et al., 2013). This means that, to accomplish this demanding task of biomimicking the functionality and complexity of *in vivo* tissues, all the key components – cells, extracellular matrix (ECM), and vasculature –must be included in *in vitro* systems with precise geometries. Accomplishing a successful co-culture is, however, a daunting task. As reviewed by Bastion et al. (2014) trying to recapitulate cellular cross-talk that occurs *in vivo* with an *in vitro* culture system implies a precise control over the optimal circumstances for the design. The ideal co-culture system is, therefore, an assembly of fine-tuned parameters selected for optimal desired behavior. In this work several parameters were tested: medium selection, cell ratio, cell density and biopolymer concentration.

4.1. 2D characterization of an HUVEC:FB co-culture

Many co-culture systems are conducted under 2D conditions. However, these present limitations when compared to the natural environment as they do not inherently possess several different topographical cues that cells can sense and respond (Ventre et al., 2012; Battiston et al., 2014). In this regard, in order to achieve more relevant physiological results, co-culture of cells in 3D matrices is the step to take, as they better mimic the functionality and complexity of natural tissues (Battiston et al., 2014). Notwithstanding the need of a further 3D parameter analysis, 2D systems could present useful clues, while being less technically challenging. As such, in this work we proceed to the selection of the supplementation medium and cell ratio using 2D cultures.

4.1.1. Characterization of HUVEC and FB 2D monocultures under under different supplementation conditions

Media composition influences cell behavior. Depending on the composition, these can induce different phenotypes. Traphagen et al. (2013) identified that media composition influenced EC invasion due to the conditioning media, the reduction of serum and supplemental growth factor. Kunz-Schughart et al. (2006) demonstrated that the addition of 10 ng/ml VEGF increased EC sprouting. Eckermann et al. (2011) replaced FBS (fetal bovine serum) with human AB serum positively impacting in EC network formation. As such, in a co-culture model, the media must be able to respond to the nutritional demands requires for both cell types, while providing the necessary conditions for the desired phenotype expression. The correct selection of the base medium is then necessary for the optimization of the co-culture system.

In a 2D environment, HUVECs and FBs were cultured in five different medium compositions: M199, DMEM (the optimal media for HUVECs and FBs, respectively) and a combination of the two in three different ratios of M199:DMEM: 3:1 (M3:1), 1:1 (M1:1) and 1:3 (M1:3). As already noted by Bidarra et al. (2011) these media present some major differences in terms of composition. M199 has a higher number of amino acids than DMEM, while also presenting the lowest concentrations on vitamins. On the other hand, DMEM has a higher glutamine concentration, and has sodium pyruvate in its composition, a component that is not found in M199. Regarding the inorganic salts content, no major differences were found. To evaluate the effect of the different media on cell behavior, metabolic activity and total dsDNA quantification assays were carried out. Furthermore, these are supplemented with different serum, being M199 supplemented with 10% v/v of inactivated FBS and DMEM supplemented with supplemented with 10% (v/v) of non-inactivated FBS, which has demonstrated by Shahdadfar et al. (2005), could impact on cell proliferation, differentiation, gene expression, and transcriptome stability. Although not discriminating the cause, in this study a selection of the media was carried out based on the metabolic profile and total dsDNA content. For both cell types, M 3:1 presented similar values to those observed in the optimal medium (Figures 2 and 3). By choosing a mixed medium, cells remain in contact with their optimal media and. Given the ratio, these results show that HUVECs are more strictly dependent of the conditions offered by their routinely used medium and/or serum. This fact is well recognized by other colleagues as several ECs co-cultures are established using ECs monocultures (Stahl et al., 2004; Fuchs et al., 2007;

Unger et al., 2007). However, this is not the ideal situation as co-cultured cells with ECs might experience nutritional deficiencies. In the proposed medium this would be bridged by the presence of a small portion of the routinely used medium and/or serum in FBs monocultures, which as evidenced, seems sufficient for normal FBs biological performance.

4.1.2. Characterization of HUVEC:FB co-culture behavior in a 2D environment, under different seeding ratios

Natural tissues consist in multi-cellular systems composed of different cell types which interact, whether through direct cell-cell contact or paracrine signaling, triggering several genetic pathways that may infer over proliferation (Schubert et al., 2008), migration (Trkov et al., 2010), differentiation (Ratner et al., 1996), growth factors and proteins production (Morita et al., 1995; Sorrell et al., 2007), spatial organization (Janvier et al., 1997), among others. ECs, in three-dimensional monocultures seem unable to survive and proliferate and, subsequently, self-assembly into tube-like structures (Janvier et al., 1997). Co-cultures offer a natural, cost-effective alternative where we take advantage of the natural occurring interaction between cells. These involve the culture of two or more types of cells within the same matrix (Battiston et al., 2014), often with the intention of stimulating a desired effect of focus cell type using a secondary cell type. In this regard, several studies showed that for ECs, co-culture with fibroblasts for capillary-formation is a promising strategy for both 2D and 3D approaches (Wenger et al., 2005; Sorrell et al., 2005; Li et al., 2013; Guerreiro et al., 2014; Costa-Almeida et al, 2015). Whether by matrix deposition (Costa-Almeida et al, 2015), soluble factors production, which are known to be potent angiogenic growth factors with key importance in the regulation of this process (Seghezzi et al., 1998; Saito et al., 2005) or direct cell-cell contact (Korff et al., 2001; Wenger et al., 2005), fibroblast are shown to improve ECs survival, proliferation and promotion of self-assembled capillary-like structures formation. However, shifting the quantitative ratios of EC to other cell types might influence the final phenotype. When cultured with smooth muscle cells altering the ratio between 4:1 and 1:1 can modify VEGF responsiveness (Korff et al., 2001). EC co-cultures with heart fibroblasts stimulate endothelial sprouting and capillary growth at low fibroblasts densities, decreasing with the increase in fibroblasts (Nehls et al., 1998). As such, attending to the final objective, cell ratio must be carefully chosen. In this work, four different cell ratios of HUVECs:FBs were tested: R 1:1, R 2:1 , R 3:1 and R 5:1, all supplemented with the

selected medium. HUVECs growing in co-culture with fibroblasts were able to proliferate and survive throughout the culture period (Figure 4), which in individual monocultures was not verified. Although no distinction between cells was performed (e.g. marker specific staining), by day 5 images demonstrate the presence of two different morphologies, representing FBs and HUVECs (Figure 5a and 5b). However, at lower HUVEC:FB ratios, namely R 1:1 and R 2:1 demonstrate, by day 5, similar structures to those observed in FBs monocultures in confluence. These environmentally FB rich environments present total DNA contents 3 and 4-fold higher than individual FBs monocultures. These results points towards the potential of HUVECs to stimulate FBs proliferation, indicating therefore that a synergetic co-culture, were both cell types stimulate each other, is established. Notwithstanding the increased cell proliferation, these ratios seem inappropriate for co-cultures aiming to promote capillary self-assembled structures formation. Within these, the rapid FBs proliferation might be triggering contact-dependent inhibition that affect HUVECs behavior, as already documented. (Nehls et al., 1998) In fact, cultures that presented lower FBs quantitative ratios, namely R 3:1 and R 5:1, by day 5, demonstrated organized structures composed of both cell types forming a spider-web-like structure, which has already been associated to capillary formation (Niger & Folkman 1989). In these, HUVECs were able proliferate, migrate and self-assemble. As such, these ratios establish favorable environments for 2D HUVECs microvascular self-assembly, seemingly triggered by FB presence through one or several of the factors previously mentioned (e.g. ECM deposition, growth factors release, cell-cell direct contact). Summing up, for an efficient HUVEC:FB co-culture, one must attend to the benefits of the natural occurring phenomena between these cell types that promote capillary formation, not overcrowding the environment with FBs which, as shown, has a negative impact on HUVECs self-assembly.

Together, the aforementioned cultures allowed a characterization of individual two-dimensional cultures for HUVECs and FBs, as well as several co-culture designs. Moreover, these granted a weighted selection of the medium supplementation for HUVEC:FB co-cultures and the selection on an adequate ratio for two-dimensional co-cultures. The criteria established which will be followed in our 3D HUVEC:FB co-culture.

4.2 HUVEC and FB monocultures' behavior in 3D-culture

Evaluation of cell behavior within a 3D microenvironment is a multifactorial task that has to take into account cell-ECM interaction as well as both the soluble and direct cell-cell contact signaling. For each specific matrix construct, several specific parameters should be taken into account. ECM-cell interaction plays a key role in cellular fate, providing cells important information concerning their microenvironment (Stupack et al., 2003). As such, matrix characteristics as porosity, diffusion rates, surface, roughness, mechanical compliance, among others should be carefully chosen (Ratner et al., 1996; Lee et al., 2008; Battiston et al., 2014). In fact, nowadays there is a multitude of biomaterial available, both natural and synthetic, which in addition to their unique properties, can be tailored to present the desired characteristics. These techniques include the fine-tuning their viscoelastic profile and mesh size by polymer and crosslinker characteristics, concentration, gelling conditions modulation (Anseth et al., 1996; Neves et al., 2015), modification of their adhesiveness profile through manipulation of the total RGD content and disposition (Discher et al., 2005; Engler et al., 2006; Li et al., 2010), increase of their protease sensitivity by modifications of the polymer (Bussy et al., 2008; Siboni et al., 2008; Fonseca et al., 2011; Fonseca et al., 2013), among others.

In the present work, pectin, a natural polysaccharide, was explored as a potential biomaterial for hydrogel formation aiming to form self-assembled microvascular structures. Pectin fulfils all of the requirements for hydrogel formation presenting all the numerous benefits of other polymers (e.g. alginate) while also possessing an interesting degradation profile under controlled stimulation (Munarin et al., 2010 a; Munarin et al., 2010 b; Munarin et al., 2011; Munarin et al., 2012; Neves e al., 2015). However, as other natural biomaterials, pectin does not intrinsically possess cell adhesive clues, which, coupled with the presence of negatively charged carboxyl groups, grants an hydrophobic nature to the polysaccharide, making this polymer resistant to protein adsorption and cell adhesion (Ridley et al., 2001). RGD (Arginine-Glycine-Aspartate) is a small oligopeptide sequence present in FN. (Stupack et al., 2003; Yu et al., 2009), is known to interact with endothelial cells via integrins $\alpha_v\beta_3$, being a requirement for angiogenesis (Bayless et al., 2000; Petrie et al., 2006; Serini et al., 2006). Furthermore, studies demonstrated that variations in RGD peptide surface density and spatial arrangement as an impact over the biomaterial's cytocompatibility, triggering adhesion-dependent cell responses (e.g. migration, proliferation, differentiation), improving al the subsequent cellular functions (Discher et al., 2005;

Engler et al., 2006; Li et al., 2010; Munarin et al., 2011; Fonseca et al., 2011; Munarin et al., 2012; Fonseca et al., 2013; Neves et al., 2015). As such, to bypass the adhesiveness issue of the polymer, a system based on the combination of RGD-modified pectin was attempted by grafting RGD-containing oligopeptides into the pectin backbone using aqueous carbodiimide chemistry (Rowley et al. 1998), based on the methods previously described for pectin (Munarin et al. 2011; Munarin et al. 2012; Neves et al. 2015). Another factor taken into account was diffusion. Diffusion is crucial to attend the cell nutritional requirements, metabolic wastes, and soluble molecules, being a critical issue in microscale designs. Diffusion is dependent on the distance that a molecule as to travel. As such, smaller matrices facilitate diffusion as the center of the matrix is within a more reachable distance, easing the cell's effort to obtain nutrients and deplete wastes. Furthermore, pectin microsphere studies demonstrated that diameters ranging from 300-500 μm were suitable to convey the incoming flow of oxygen and the outgoing of catabolites, as cells maintained their viability for 29 days (Munarin et al., 2011). Attending to these factors, in this work we've used 500 μm cylindrical pectin hydrogel matrices modified with controlled final RGD concentration of 200 μM. Within these, the mechanical influence was tested through the use of different polymer concentrations (1.5% and 2.5% (w/v)). Moreover, in 3D matrices cell-cell interactions are directly influence by the cell entrapment density (Maia et al., 2014). To address this, different entrapment densities were also tested to fibroblasts and endothelial cells do study their cell-cell implications on the behavioral development within the hydrogels.

To achieve the desired in a 3D environment studies suggest that are required strategies to overcome the physical impediments posed by the matrices, which include: growth arrest; stimulating cell senescence and favoring a quiescent-like state (Bott et al., 2010). As evidenced for HUVEC monocultures (Figure 6), all the conditions established, the total dsDNA content gradually decreased along the period of culture, being accompanied by the decrease in the metabolic activity. Endothelial cells are typically "quiescent" (the average lifespan of an EC is more than 1 year) (Aird, 2007). As such, and given the favoring of a quiescent-like state by 3D matrices, proliferation was not expected. However, in addition to the lack of proliferation, cell loss is observed throughout the experiment, with lower dsDNA values being obtained in 1.5% (w/v) pectin hydrogels in the first 2 days. A possible explanation for this is the pore size of the matrices. As depicted by Neves et al. (2015), the initial mesh size of pectin hydrogels is higher for the 1.5% (w/v) hydrogels when compared to the 2.5% (w/v) hydrogels (707 nm vs 380 nm). Experimental observations show that, after medium addition to the matrices, pectin hydrogels swell, as other authors already verified

(Sriamornsak et al., 2007). As water migrates to the matrix, pores and channels are created (Liu et al., 2003). Given that HUVECs are cells with measured sizes of 14-15 µm, cells might be escaping the matrix (or even dying) before being able to establish the necessary integrin-RGD adhesive interactions, being the loss faster in bigger size pore matrices. Furthermore, this loss might also impact over the already adhered cells as cellular critical densities values for cellular development might not be achieved and subsequently promote cell detachment. In fact, for 3D environments, at lower entrapment densities, cell–cell interactions may be easily hindered, and, as consequence, a decrease in the biological performance can be noted (Cukierman et al., 2001). Among others factors, paracrine signals, as vascular endothelial growth factor (VEGF) (Silva & Mooney, 2010) and basic fibroblast growth factor (bFGF) (Edelman et al., 1991) have been linked with better proliferation, migration and viability results for ECs. The lack of these soluble factors in out constructs can be another of the limiting factor. As such, although described in the literature that lower stiffness materials favor endothelial self-assembly and tubulogenesis (Saunders & Hammer, 2010; Bidarra et al., 2011; Maia et al., 2014), for pectin, in these conditions HUVEC monoculture is not sustainable. Any further attempt at HUVEC monoculture designs using pectin hydrogels must attend to the initial pectin swelling and soluble factors presence issues. Possible solutions for these must be attended through chemical modifications of the polysaccharide and/or different gelation strategies (Liu et al., 2003) and addition of the factors through exogenous addition or co-culture systems (Eckermann et al., 2011). Furthermore, despite these issues, aiming microvasculature formation *in vitro,* 1.5% (w/v) pectin hydrogels use should be prioritized as, as demonstrated by Saunders & Hammer (2010), more compliant matrices (Young modulus of 140-1000 Pa) promote network formation, whereas stiffer matrices (Young modulus > 1000 Pa) do not.

Regarding FB monocultures, the present results showed that entrapped FBs were metabolically active throughout culture time within all pectin hydrogels, although no stimulation of cell proliferation is observed (Figure 8). Better results were however observed in 1.5% (w/v) hydrogels were cells presented a steady-state of metabolic activity throughout the 6 days, whereas for for 2.5% (w/v) hydrogels it was verified a decrease along time. In 1.5% (w/v) hydrogels, fibroblasts were able to spread and establish cell-to-cell contacts inside the RGD-grafted pectin hydrogels, leading to the formation of multicellular aggregates, which was not observed for 2.5% (w/v) hydrogels where cells remained round and dispersed. As previous 1.5 % (w/v) pectin hydrogel mesh size is larger, forming a polymeric network that is less dense that those presented by 2.5% (w/v) matrices. Pore size is of critical importance, affecting not only

the diffusion process and well as the cell migration, cell differentiation and cell distribution, by altering perception of the environment by the cells (Lee et al., 2008; Choi et al., 2010; Bergmeister et al., 2013). As such, within the first days (before the matrix contract), less dense matrices may lead to enhancement of the biological performance, a factor which was already proposed by other authors (Zhang et al., 2011; Bidarra et al., 2013; Neves et al., 2015). Moreover, 1.5 % (w/v) pectin hydrogel present softer microenvironments. Coupled with the pore size, these matrices present more compliant environments that allow cells to exert “tracking” forces to deform the surrounding matrix, and, thus, migrate and aggregate. Moreover these microscopic observations (aggregates formation, Figure 9), when coupled with the macroscopic evidences (matrix contraction, Figure 11) suggest tissue formation, which is evidenced to be dependent on mechanical input to the cells, as also observed in other studies (Butler et al., 2000; Drury et al., 2003; Reinhart-King et al., 2008; Reinhart-King, 2011). To note that, for 2.5% (w/v) hydrogels, although the documented internal behavior presented mostly round cells, a similar effect to the one documented by Maia et al. (2014) for 2 (w/v)% alginate hydrogels when compared to 1% (w/v) for hMSCs. However, in our matrix surface appeared populated by stretched cells, able to establish cell-cell contacts and forming cellular networks. (See annexes Figure 1.). These results show that, independently of the selected pectin concentration, by taking advantages of the mechanical compliance posed by pectin, FBs were able to migrate outwards the matrix, populating the surface and forming aggregates within the hydrogels, which was already demonstrated for Neves et al. (2015) regarding hMSCs. Given that the dsDNA analysis demonstrated steady values for the period of culture, one can speculate that these were formed through self-assembly rather than clonal expansion. Nonetheless, to provide an insight over the origin of these aggregates, a KI-67 test should be conducted.

Cell density directly influences cell–cell signaling. Therefore, the initial seeding densities will impact on the 3D cellular behavior presented by the cells in a co-culture. In 2D environments, cellular densities are well studied. In these, higher cell densities are known to promotes cell-to-cell contact, which can lead to contact inhibition (cell cycle arrest and thus proliferation inhibition) (Puliafito et al., 2012), stimulate cellular differentiation (Hohn et al., 1996), among others. For 3D environments, these effects were also verified, whit higher cell densities promoting clusters formation (Zhang et al., 2011), differentiation (Mudera et al., 2010) and ECM production (Huang et al., 2008; Talukdar et al., 2011; Maia et al., 2014; Neves et al., 2015). In this work, higher entrapment densities promoted FB clusters formation, with significant differences in relation to lower densities. It is however important to note that 1.5% (w/v) pectin

hydrogel with 1.5 x 10^7 FBs.mL^{-1} construct were not able to sustain FB development due to matrix decomposition. In one hand, as exposed by Neves et al. (2015), the crosslinking times are slightly affected when cells are present within the hydrogel (~5 minutes for 1,5% (w/v) and ~3 minutes for 2.5% (w/v)), more specifically with 8x10^6 cells.mL^{-1}. In our work, the highest used density was almost 2-fold higher, being 1.5 x 10^7 FBs.mL^{-1}. Therefore, the cross-linking reaction could have been significantly altered leading to a more sensitive matrix. In addition, the high porosity present in 1,5% (w/v) matrices sacrifices mechanical properties by reducing the amount of material present in the matrix (Lee et al., 2008). On the other hand, in 3D cell culture, the matrix must withstand cell attachment forces (Lee et al., 2008), which at higher cell densities are expected to be greater. All together, we suggest that the matrix degradation might be a physical impediment of the matrix, inefficient cross-linking reaction and/or high porosity, when exposed to high densities contractile cell embedding. Finally, although our work only establishes a comparison between polymer concentrations, other studies demonstrated that the final maximum force produced is dependent on the number of cells within the matrix (Eastwood et al., 1994).

To sum up, these results demonstrate a matrix and cell density-dependent 3D cell behavior, suggesting a potentiated response for lower stiffness and higher cell entrapment, where FBs tend to aggregate into “tissue-like” structures. The metabolic results, coupled microscopic (aggregates formation) and macroscopic (matrix contraction) evidences, suggests microtissue formation, with possible ECM deposition and angiogenic growth factors production, in lower pectin hydrogels concentrations (1.5% (w/v)), being the best result, for FBs, the 1.5% (w/v) pectin matrices with 1 x 10^7 FBs.mL^{-1} construct.

Fibroblast microtissue formation is of utmost importance for the optimization of a co-culture system. In skin, FBs are the main responsible for ECM modulation. FBs have the ability of remodeling the elasticity and mechanical integrity of matrix, by producing enzymes, such as proteases and collagenases (Ratner et al., 2004). This ability is also observed in in vitro conditions were FBs, under controlled conditions, are able to produce natural ECM proteins such as FN, collagen, GAGs, tenascin-C, and others (Dzamba & Peters, 1991; Korducki et al., 1992; Berthod et al., 2006; Soucy & Romer, 2009; Costa-Almeida et al., 2015). Among these FN stands out as it is significantly stronger than than the RGD peptide alone. FN presents a native tertiary structure that favors the specific angiogenesis-dependent integrin interactions (Petrie et al., 2006). Moreover, additional peptide sequences present in the polymer (e.g. PHRSN) enhance the $\alpha_5\beta_1$ integrin binding to the FN-RGD motif, which are also liked to be a requirement for angiogenesis (Aota et al., 1994; Laurens et al., 2009). Besides matrix

deposition, fibroblasts are also strongly related to angiogenesis as they infer over the EC behavior through fibroblast-derived proteins, namely fibroblast growth factor-2 (FGF-2) and vascular endothelial growth factor (VEGF), the latter a key modulator of normal vessel generation (Seghezzi et al., 1998; Saito et al., 2005). Furthermore, deformations of the matrix suggest that fibroblasts may be producing smooth muscle α-actin (α-SMA), a fibroblasts contractile marker. This indicates that fibroblasts are going through differentiation into myofibroblasts, which are involved in wound contraction and remodeling wound healing processes, on which vascularization is potentiated (Darby et al., 1990; Arora et al., 1999). ECs in compliant matrices are shown to communicate through mechanical signals, perceiving and reacting to tension dependent stresses of neighboring cells (Reinhart-King et al., 2008; Reinhart-King, 2011). Through traction forces, interactions between endothelial cells and ECM, for example, regulate bFGF and subsequently, capillary development (Ingber & Folkman, 1989). All together, the use of a co-culture system using ECs and fibroblasts to test biomaterials biocompatibility and their influence in *in vitro* angiogenesis assays is the logical step to follow.

In the present study, to achieve *in vitro* microvascularization, we purposed to integrate cellular, biochemical, and biophysical cues biomaterials, taking advantage of the natural crosstalk between cells, through soluble factors and/or cell-cell interaction and the mechanical compliance demonstrated in 1.5%(w/v) pectin hydrogels. This strategy as proven itself effective for ECs tube-like structures formation, as coculturing ECs with fibroblasts (Wenger et al., 2005; Sorrell et al., 2005; Li et al., 2013; Guerreiro et al., 2014; Costa-Almeida et al., 2015). Here, we intend to take advantage of the FBs documented ability to produce natural ECM (Costa-Almeida et al., 2015; Berthod et al., 2006) and soluble factors (VEGF and bFGF) (Seghezzi et al., 1998; Saito et al., 2005) to, through a natural and cost-effective way , potentiate angiogenesis. Furthermore, as critical cell density was showed to be needed for network formation (Saunders & Hammer, 2010), to surpass the HUVEC loss by our results evidenced, the highest cell density was chosen. Finally before proceeding to the 3D HUVEC:FB co-culture, M 3:1 efficiency for HUVEC and FB supplementation was tested. Therefore, two additional conditions were tested using identical monoculture conditions to those chosen for co-culture (medium type, biomechanical stimulation, cell densities, culture substrate, among others). With this, we intend to address the data interpretation issue, distinguish between the relative contributions of cell-cell interactions versus cell-biomaterial interactions, aiding to determine effects of the cells compared to how they are stimulated by the biomaterial substrate alone. As demonstrated by Figure 12, the monocultures cultured in the selected medium, M 3:1, presented identical profiles to

the ones cultured in the optimal medium. This result indicates that this medium is suitable for both 2D and 3D HUVEC and FB co-cultures. These results will serve as a standpoint for co-culture comparison, and, if differences exist, this indicates that they will be most likely due to cell-cell interactions.

4.3 HUVEC:FB co-culture establishment in 3D soft pectin hydrogels

Tissue architecture and function are closely interrelated. Blood vessels consist of multi-cellular system with 3 distinct layers of endothelium, smooth muscle, and connective tissue. More precisely, these are lined by a longitudinally oriented single layer of ECs, which defined the lumen, followed by circularly oriented smooth muscle layer (pericytes) and outer connective tissue layers (Ratner et al., 2004). As such, the formation of mature and functional vascular networks requires the cooperation of endothelial cells (ECs) and perivascular cells, with cell-cell direct contact and paracrine signaling interactions being of utmost importance for the sustainability of mature microvasculature (Auger et al., 2013; Battiston et al., 2014). As previously pointed out, until this point, this study focused on the use optimization of the conditions for the establishment of a HUVEC:FB co-culture. We are specifically interested in addressing this subject in context of microvascularization inclusion in *in vitro* self-assembled artificial skin for skin regeneration therapies. As described throughout this work, *in vitro* self-assembled capillary formation is dependent on EC lining for lumen formation (Ratner et al., 1996; Ratner et al., 2004; Koh et al., 2008). For this, several cues provided by ECM-cell, cell-cell and cell-growth factor interactions play key roles in this process, all of which were demonstrated, by our and other works, to be present in FB cultures capable of forming tissue like structures (Seghezzi et al., 1998; Saito et al., 2005; Reinhart-King et al., 2008; Soucy & Romer, 2009; Reinhart-King, 2011). As such, through weighted selection based on observed result and current literature, a co-culture was established under the following conditions: 1.5% (w/v) pectin hydrogels seeded with $1.5x10^7$ cells.mL^{-1} with a 3:1 ratio favoring HUVECs. This was supplemented with a mixture medium composed of M199:DMEM in a 3:1 ratio. The results were evaluated through metabolic and total dsDNA assays as well as staining against anti-α-SMA and anti-vWF, respectively, a contractile marker characteristic (but not exclusive) of myofibroblasts and a endothelial-specific marker.

As depicted by (Figure 13), throughout the culture period co-cultures present a steady decrease in the total dsDNA, accompanied by a decrease in metabolic activity. This profile is similar to HUVEC monocultures. However by day 4 and until day 6, unlike

monocultures, co-cultures maintained metabolic activity. Furthermore, when normalized (by the total dsDNA) these results show an increased cell metabolic activity with time (Figure 13). As such, the establish co-culture seem to present a mix of the characteristics presented by HUVEC and FB monocultures, namely, a HUVEC-like cell loss profile (total dsDNA and metabolic activity decrease) and a FB-like positive response to the mechanical compliance of the matrix. However these results do not positively distinguish between cell types. As such, to provide more insight on the implications of the co-culture in HUVECs behavior, spatial arrangement was analyzed through immunostaining techniques. As showed in Figure 14, the main objective was not achieved as no tube-like structures are observed. Nonetheless, by 6 it is still possible to verify a prominent demarcation of HUVECs by anti-vWF (Figure 14. Image c), indicating FB co-culture had a positive impact over HUVECs, increasing their survival. However, as mentioned, our HUVEC:FB did not support capillary which was already verified in other studies (Wenger et al., 2005; Sorrell et al., 2005; Soucy et al., 2009; Eckermann et al., 2012; Guerreiro et al., 2014). As it is known VEGF, a fibroblast-derived protein, is a potent and key mediator for angiogenesis (Seghezzi et al., 1998; Korff et al., 2001; Saito et al., 2005; Silva & Mooney, 2010; Eckermann et al., 2011). The effects of this growth factor over EC are, dose-dependent (Conn et al., 1990), gradient dependent (Gerhardt et al., 2003) and time-dependent (Silva & Mooney, 2010), with the best results optimal results being obtained with high VEGF levels (50 $ng.mL^{-1}$) at early time points and constant presence over time (Nakatsu et al., 2003 ;Silva & Mooney, 2010). Moreover VEGF is also linked to present a potent synergetic effect with bFGF (also known as FGF-2) for angiogenesis induction (Pepper 1992). In fact, bFGF, whether released by fibroblasts or EC (Schweigerer, 1987), induces VEGF expression in endothelial cells, leading to capillary formation (Seghezzi et al., 1998). However, we constructed a co-culture with a low FB density in the culture which could result in low growth factor concentrations values and, consequently, weaker stimulation of the HUVECs. In fact, low FB density could suitable, yet untested, explanation for our results as another density-dependent phenomena might not occur. For example, higher ECM deposition rates within cellular aggregates, which have been linked with higher cell densities (Maia et al., 2014). Among the proteins secreted releases FN, stands out as it is significantly stronger than than the RGD peptide alone, by promoting multiple integrin potentiated in interaction with FN-RGD (Aota et al., 1994; Laurens et al., 2009; Petrie et al., 2006; Soucy & Romer, 2009). In our co-culture, as Figure 14, shows it is verified few FB clusters are observed with relatively small sizes. As such, these may not have reached the critical conditions for a physiologically relevant matrix deposition for HUVEC self-assembled capillary formation. Finally, the

mechanical modulation impact on ECs behavior cannot be disregarded as it has the potential to promote endothelial cell expression of bFGF and promote angiogenesis (Ingber & Folkman 1989; Berthod et al., 2006; Reinhart-King et al., 2008; Reinhart-King, 2011). The magnitude of the exerted forces is not only dependent on matrix stiffness (Sieminski et al., 2004) but is also modulated by cell density. (Eastwood et al., 1994). Our results show that, despite the low FBs densities, FBs were able to express α-SMA by the 4th day, suggesting that myofibroblasts differentiation occurred and that a contractile phenotype was achieved. However these in these densities, the mechanical tension forces applied showed might have not been able to reach the critical values for angiogenesis stimulation. All in all, although no certain confirmation was obtained in this study, we postulate that one of the possible reasons for HUVEC microvascular unsuccessful self-assembly was the low FB density.

Furthermore, it is important to note that HUVECs phenotype suffers alterations through time. At day 1, HUVECs are characterized by a red phenotype indicating the presence of vWF, an endothelial specific marker (Zanetta et al., 2000). However, throughout our culture period, the cells progress from red to orange, being this difference more pronounced by day 6. This indicates a progressive expression of α-SMA, which, as we already noted, is a contractile marker. Although, to our knowledge, this phenotype is not commonly expressed in ECs, in some cases it might be observed. Through Jagged1-Notch interaction, endothelial cells are shown to undergo endothelial-mesenchymal transdifferentiation, leading to the expression of α-SMA (Noseda et al., 2004; Noseda et al., 2006). Cevallos et al. (2006) demonstrated that cyclic strain induces expression of specific smooth muscle cell markers in human endothelial cells. This is however a situation that requires a deeper insight on the mater. In the future would be interesting to stain HUVEC monocultures against anti-α-SMA, allowing the distinction between whether this phenotype is a consequence of cell-cell or cell-ECM interactions. Furthermore stain of anti-α-SMA against HUVEC monocultures should be carried out against M199 or m 3.1 supplemented conditions, evaluating the effect of the media/serum on this phenotype, which were already demonstrated to impact over several cell biological functions (Shahdadfar et al., 2005; Kunz-Schughart et al., 2006); Eckermann et al. 2011; Traphagen et al., 2013).

4.4 3D HUVEC:FB co-culture spatial patterning: Microinjected HUVEC-laden soft pectin on a FB-laden soft pectin bed

Attending to the issues verified in the co-cultures a spatial patterning approach was attempted. As HUVEC cell loss was one of the main concerns, we embedded a HUVEC island in the center of a FB-laded 1.5(w/v) pectin matrix. By doing so, we intended to use peripheral FB-containing matrix as a net, trying to prevent HUVEC loss. Furthermore, do protocol adjustment on the course of the experiment, allowed us to increase the initial FB entrapment density from the $3.75x10^6$ cells.mL^{-1} verified in the 3:1 (HUVEC:FB) ratio to $8x10^6$ cells.mL^{-1}, altering the ratio to approximately 1:3 (HUVEC:FB). This FBs density was closer to the optimal FB density for microtissues formation ($1x10^7$ cells.mL^{-1}). From day 1, FB presented more clusters with larger sizes. Furthermore, α-SMA is expressed in the fibroblasts from day 1, which was not observed in our initial co-cultures (Figure 15 a and d). By day 2, HUVECs already presented a phenotype similar to the one in day 6 of our co-culture, expressing both α-SMA and vWF (Figure 15 b and e). More importantly, these images may provide an insight on why the HUVECs are expressing α-SMA. In the Figure 15 b) it is possible to observe the HUVEC island, at the right side of the image, and the fibroblast rich zones. The orange phenotype resulting of the simultaneous expression of α-SMA and vWF occurs mainly in the fibroblast contact zones. As previously mentioned, Notch signaling has been implicated in the transdifferentiation of ECs to smooth muscle cells, leading to the production α-SMA through a Jagged1-Notch interaction (Noseda et al., 2004; Noseda et al., 2006). Notch receptors are membrane-tethered receptor that mediates cell-cell receptor-ligand interactions. As such, in these conditions, we hypothesize that, through cell-cell direct contact mechanisms, FBs are recruiting HUVECs to a transdifferentiation into smooth muscle cells through a Jagged1-Notch interaction. Nonetheless, as aforementioned, media supplementation and cell-ECM influences on HUVEC phenotype should be performed to better infer on this phenomenon. Finally, by day 4 Figure 15 c) show a mixture of FBs, α-SMA positive HUVECs and α-SMA negative HUVECs, which seem to be acquiring a spider web-like pattern.

The variations imposed between or 3:1 (HUVEC:FB) co-culture and our spatially patterned co-culture seem to favor spatial arrangement in HUVECs suggesting tubular formation. However, to confirm HUVEC self-assembly in these conditions, a prolonged experience time in needed, which, due to the technical difficulties imposed during this embedding protocol and time limitations, was not possible. Furthermore, matrix

deposition and growth factor detection assays should be conducted for FBs monocultures and both co-cultures for an accurate description of the FB environmental remodeling, providing better insights on data interpretation.

All in all, notwithstanding the fact that no clear evidence for tubular formation was presented, our results offer promising expectations for future experiments under similar conditions.

Conclusions and Future Remarks

Independently of the specific tissue-engineering approach for *in vitro* artificial skin regeneration, the biologic complexity must be redeemed through a combination of biomaterials, cells, growth factors and advanced biomanufacturing techniques (Stupack et al., 2003; Discher et al., 2005; Engler et al., 2006; Yu et al., 2009; Battiston et al., 2014). Moreover, for the successful transplantation of human tissue-engineered constructs is of utmost importance the formation of a vascular network (Rivron et al., 2008; Novosel et al., 2011; Auger et al., 2013). As such, it is important to use conditions that will not merely generate capillaries but also lead to the formation of mature and stable structures that will be sustained once the initial conditions are no longer present.

In this thesis, recognizing the media/serum importance in a cell culture (Shahdadfar et al., 2005; Kunz-Schughart et al., 2006; Eckermann et al. 2011; Traphagen et al., 2013), HUVEC and FB monocultures where characterized for five different media supplementation. We have demonstrated that the ideal medium for a HUVEC:FB co-culture scenario is a mixture, of the two routinely used media for HUVEC and FB culture (M199 and DMEM, respectively) in a 3:1 ratio (M199:DMEM). Furthermore, four different cell ratios were assessed. Varying cell ratios in a co-culture could significantly vary the outcome (Nehls et al., 1998; Korff et al., 2001). This work demonstrated that, in a 2D context, low HUVEC:FB ratios favor FB proliferation in detriment of HUVEC proliferation and self-assembly, while higher HUVEC:FB ratios appeared more prone to HUVEC and FB structural formation.

In addition, in a 3D context, pectin's ability as a soft hydrogel matrix for cell culture was successfully asserted, leading to the formation of microtissues in FB cultures and the construction of viable co-cultures of HUVECs and FBs in 6-days culture periods. To our knowledge, this was the first study demonstrating the potential of soft pectin hydrogel matrices for FBs microtissues self-assembly. However, regarding to co-cultures with a 3:1 (HUVEC:FB) ratio, results were not promising due to severe cell loss and lack of structures formation. As such, the results selected from a 2D culture were not translated into a 3D environment. Instead, an antipodal result closer to the results desired, pointing to structural organization and tube formation within the matrix. These results difference happen because 3D environments inherently possess several clues that are not present in two-dimensions, promoting different responses (Ventre et al., 2012; Battiston et al., 2014). In the future, in order to better understand the underlining processes for these phenomena, matrix deposition (e.g collagen, fibronectin) and growth factor (e.g. VEGF, bFGF) quantifications should be carried out, allowing further optimizations to be made. Finally, as vasculogenesis is greatly affected by matrix deposition and growth factors presence we propose a two-stage approach: 1.

Promotion of self-assembled cell-ECM microtissues in soft pectin hydrogel matrices. 2. Biofabrication of cell-laden micropatterns using self-assembled cell-ECM microtissues in soft pectin hydrogel.

References

Aird, W. C. (2003). Endothelial cell heterogeneity. *Critical care medicine*, *31*(4), S221-S230.

Aird, W. C. (2007). Phenotypic heterogeneity of the endothelium I. Structure, function, and mechanisms. *Circulation research*, *100*(2), 158-173.

Aird, W. C. (2012). Endothelial cell heterogeneity. *Cold Spring Harbor perspectives in medicine*, *2*(1), a006429.

Alonso, L., & Fuchs, E. (2003). Stem cells in the skin: waste not, Wnt not.*Genes & development*, *17*(10), 1189-1200.

Anand, S., Majeti, B. K., Acevedo, L. M., Murphy, E. A., Mukthavaram, R., Scheppke, L., ... & Cheresh, D. A. (2010). MicroRNA-132-mediated loss of p120RasGAP activates the endothelium to facilitate pathological angiogenesis. *Nature medicine*, *16*(8), 909-914.

Anseth, K. S., Bowman, C. N., & Brannon-Peppas, L. (1996). Mechanical properties of hydrogels and their experimental determination. *Biomaterials*,*17*(17), 1647-1657.

Aota, S. I., Nomizu, M., & Yamada, K. M. (1994). The short amino acid sequence Pro-His-Ser-Arg-Asn in human fibronectin enhances cell-adhesive function. *Journal of Biological Chemistry*, *269*(40), 24756-24761.

Arnaoutova, I., George, J., Kleinman, H. K., & Benton, G. (2009). The endothelial cell tube formation assay on basement membrane turns 20: state of the science and the art. *Angiogenesis*, *12*(3), 267-274.

Arora, P. D., Narani, N., & McCulloch, C. A. (1999). The compliance of collagen gels regulates transforming growth factor-β induction of α-smooth muscle actin in fibroblasts. *The American journal of pathology*, *154*(3), 871-882.

Auger, F. A., Gibot, L., & Lacroix, D. (2013). The pivotal role of vascularization in tissue engineering. *Annual review of biomedical engineering*, *15*, 177-200.

Augustin, H. G., Kozian, D. H., & Johnson, R. C. (1994). Differentiation of endothelial cells: analysis of the constitutive and activated endothelial cell phenotypes. *Bioessays*, *16*(12), 901-906.

Bach, T. L., Barsigian, C., Chalupowicz, D. G., Busler, D., Yaen, C. H., Grant, D. S., & Martinez, J. (1998). VE-Cadherin Mediates Endothelial Cell Capillary Tube Formation in Fibrin and Collagen Gels 1. *Experimental cell research*,*238*(2), 324-334.

Battiston, K. G., Cheung, J. W., Jain, D., & Santerre, J. P. (2014). Biomaterials in co-culture systems: towards optimizing tissue integration and cell signaling within scaffolds. *Biomaterials*, *35*(15), 4465-4476.

Bayless, K. J., Salazar, R., & Davis, G. E. (2000). RGD-dependent vacuolation and lumen formation observed during endothelial cell morphogenesis in three-dimensional

fibrin matrices involves the α v β 3 and α 5 β 1 integrins. *The American journal of pathology*, *156*(5), 1673-1683.

Bergmeister, H., Schreiber, C., Grasl, C., Walter, I., Plasenzotti, R., Stoiber, M., ... & Schima, H. (2013). Healing characteristics of electrospun polyurethane grafts with various porosities. *Acta biomaterialia*, *9*(4), 6032-6040.

Berrier, A. L., & Yamada, K. M. (2007). Cell–matrix adhesion. *Journal of cellular physiology*, *213*(3), 565-573.

Berthod, F., Germain, L., Tremblay, N., & Auger, F. A. (2006). Extracellular matrix deposition by fibroblasts is necessary to promote capillary-like tube formation in vitro. *Journal of cellular physiology*, *207*(2), 491-498.

Bidarra, S. J., Barrias, C. C., & Granja, P. L. (2014). Injectable alginate hydrogels for cell delivery in tissue engineering. *Acta biomaterialia*, *10*(4), 1646-1662.

Bidarra, S. J., Barrias, C. C., Fonseca, K. B., Barbosa, M. A., Soares, R. A., & Granja, P. L. (2011). Injectable in situ crosslinkable RGD-modified alginate matrix for endothelial cells delivery. *Biomaterials*, *32*(31), 7897-7904.

Boateng, J. S., Matthews, K. H., Stevens, H. N., & Eccleston, G. M. (2008). Wound healing dressings and drug delivery systems: a review. *Journal of pharmaceutical sciences*, *97*(8), 2892-2923.

Boateng, J., Burgos-Amador, R., Okeke, O., & Pawar, H. (2015). Composite alginate and gelatin based bio-polymeric wafers containing silver sulfadiazine for wound healing. *International journal of biological macromolecules*, *79*, 63-71.

Bott, K., Upton, Z., Schrobback, K., Ehrbar, M., Hubbell, J. A., Lutolf, M. P., & Rizzi, S. C. (2010). The effect of matrix characteristics on fibroblast proliferation in 3D gels. *Biomaterials*, *31*(32), 8454-8464.

Böttcher-Haberzeth, S., Biedermann, T., & Reichmann, E. (2010). Tissue engineering of skin. *Burns*, *36*(4), 450-460.

Bouïs, D., Hospers, G. A., Meijer, C., Molema, G., & Mulder, N. H. (2001). Endothelium in vitro: a review of human vascular endothelial cell lines for blood vessel-related research. *Angiogenesis*, *4*(2), 91-102.

Bowers, S. L., Banerjee, I., & Baudino, T. A. (2010). The extracellular matrix: at the center of it all. *Journal of molecular and cellular cardiology*, *48*(3), 474-482.

Boyd, M., Flasza, M., Johnson, P. A., Roberts, J. S. C., & Kemp, P. (2007). Integration and persistence of an investigational human living skin equivalent (ICX-SKN) in human surgical wounds.

Braccini, I., & Pérez, S. (2001). Molecular basis of Ca2+-induced gelation in alginates and pectins: the egg-box model revisited. Biomacromolecules, 2(4), 1089-1096.

Braccini, I., Grasso, R. P., & Pérez, S. (1999). Conformational and configurational features of acidic polysaccharides and their interactions with calcium ions: a molecular modeling investigation. Carbohydrate Research, 317(1), 119-130.

Bussy, C., Verhoef, R., Haeger, A., Morra, M., Duval, J. L., Vigneron, P., ... & Nagel, M. D. (2008). Modulating in vitro bone cell and macrophage behavior by immobilized enzymatically tailored pectins. *Journal of Biomedical Materials Research Part A*, *86*(3), 597-606.

Butler, David L., Steven A. Goldstein, and Farshid Guilak. "Functional tissue engineering: the role of biomechanics." *Journal of biomechanical engineering*122.6 (2000): 570-575.

Cen, L., Liu, W., Cui, L., Zhang, W., & Cao, Y. (2008). Collagen tissue engineering: development of novel biomaterials and applications. Pediatric research, 63(5), 492-496.

Cevallos, M., Riha, G. M., Wang, X., Yang, H., Yan, S., Li, M., ... & Chen, C. (2006). Cyclic strain induces expression of specific smooth muscle cell markers in human endothelial cells. *Differentiation*, *74*(9-10), 552-561.

Chalupowicz, D. G., Chowdhury, Z. A., Bach, T. L., Barsigian, C., & Martinez, J. (1995). Fibrin II induces endothelial cell capillary tube formation. *The Journal of cell biology*, *130*(1), 207-215.

Chiang, B., Essick, E., Ehringer, W., Murphree, S., Hauck, M. A., Li, M., & Chien, S. (2007). Enhancing skin wound healing by direct delivery of intracellular adenosine triphosphate. *The American journal of surgery*, *193*(2), 213-218..

Choi, S. W., Zhang, Y., & Xia, Y. (2010). Three-dimensional scaffolds for tissue engineering: the importance of uniformity in pore size and structure. *Langmuir*,*26*(24), 19001-19006.

Chrobak, K. M., Potter, D. R., & Tien, J. (2006). Formation of perfused, functional microvascular tubes in vitro. *Microvascular research*, *71*(3), 185-196.

Chunmeng, S., & Tianmin, C. (2004). Skin: a promising reservoir for adult stem cell populations. *Medical hypotheses*, *62*(5), 683-688.

Conn, G., Soderman, D. D., Schaeffer, M. T., Wile, M., Hatcher, V. B., & Thomas, K. A. (1990). Purification of a glycoprotein vascular endothelial cell mitogen from a rat glioma-derived cell line. *Proceedings of the National Academy of Sciences*, *87*(4), 1323-1327.

Cooper, T. P., & Sefton, M. V. (2011). Fibronectin coating of collagen modules increases in vivo HUVEC survival and vessel formation in SCID mice. *Acta biomaterialia*, *7*(3), 1072-1083.

Costa-Almeida, R., Gomez-Lazaro, M., Ramalho, C., Granja, P. L., Soares, R., & Guerreiro, S. G. (2014). Fibroblast-endothelial partners for vascularization strategies in tissue engineering. *Tissue Engineering Part A*, *21*(5-6), 1055-1065.

Cukierman, E., Pankov, R., & Yamada, K. M. (2002). Cell interactions with three-dimensional matrices. *Current opinion in cell biology*, *14*(5), 633-640.

Cukierman, E., Pankov, R., Stevens, D. R., & Yamada, K. M. (2001). Taking cell-matrix adhesions to the third dimension. *Science*, *294*(5547), 1708-1712.

Culver, J. C., Hoffmann, J. C., Poché, R. A., Slater, J. H., West, J. L., & Dickinson, M. E. (2012). Three-Dimensional Biomimetic Patterning in Hydrogels to Guide Cellular Organization. *Advanced materials*, *24*(17), 2344-2348.

Cuono, C., Langdon, R., & McGuire, J. (1986). Use of cultured epidermal autografts and dermal allografts as skin replacement after burn injury. *The Lancet*, *327*(8490), 1123-1124.

Dai, N. T., Williamson, M. R., Khammo, N., Adams, E. F., & Coombes, A. G. A. (2004). Composite cell support membranes based on collagen and polycaprolactone for tissue engineering of skin. *Biomaterials*, *25*(18), 4263-4271.

Daley, W. P., Peters, S. B., & Larsen, M. (2008). Extracellular matrix dynamics in development and regenerative medicine. *Journal of cell science*,*121*(3), 255-264.

Darby, I., Skalli, O., & Gabbiani, G. (1990). a-Smooth muscle actin is transiently expressed by myofibroblasts during experimental wound healing.*Lab Invest*, *63*(1), 21-29.

Dean, D. M., Napolitano, A. P., Youssef, J., & Morgan, J. R. (2007). Rods, tori, and honeycombs: the directed self-assembly of microtissues with prescribed microscale geometries. *The FASEB Journal*, *21*(14), 4005-4012.

Dee, K. C., Andersen, T. T., & Bizios, R. (1999). Osteoblast population migration characteristics on substrates modified with immobilized adhesive peptides. *Biomaterials*, *20*(3), 221-227.

DeVolder, R., & Kong, H. J. (2012). Hydrogels for in vivo-like three-dimensional cellular studies. *Wiley Interdisciplinary Reviews: Systems Biology and Medicine*,*4*(4), 351-365.

Discher, D. E., Janmey, P., & Wang, Y. L. (2005). Tissue cells feel and respond to the stiffness of their substrate. *Science*, *310*(5751), 1139-1143.

Drury, J. L., & Mooney, D. J. (2003). Hydrogels for tissue engineering: scaffold design variables and applications. *Biomaterials*, *24*(24), 4337-4351.

Durand, D., Bertrand, C., Clark, A. H., & Lips, A. (1990). Calcium-induced gelation of low methoxy pectin solutions—Thermodynamic and rheological considerations. *International journal of biological macromolecules*, *12*(1), 14-18.

Dzamba, B. J., & Peters, D. M. (1991). Arrangement of cellular fibronectin in noncollagenous fibrils in human fibroblast cultures. *Journal of cell science*,*100*(3), 605-612.

Eastwood, M., McGrouther, D. A., & Brown, R. A. (1994). A culture force monitor for measurement of contraction forces generated in human dermal fibroblast cultures: evidence for cell-matrix mechanical signalling. *Biochimica et Biophysica Acta (BBA)-General Subjects*, *1201*(2), 186-192.

Eckermann, C. W., Lehle, K., Schmid, S. A., Wheatley, D. N., & Kunz-Schughart, L. A. (2011). Characterization and modulation of fibroblast/endothelial cell co-cultures for the in vitro preformation of three-dimensional tubular networks. *Cell biology international*, *35*(11), 1097-1110.

Edelman, E. R., Mathiowitz, E., Langer, R., & Klagsbrun, M. (1991). Controlled and modulated release of basic fibroblast growth factor. *Biomaterials*, *12*(7), 619-626.

Ehrbar, M., Sala, A., Lienemann, P., Ranga, A., Mosiewicz, K., Bittermann, A., ... & Lutolf, M. P. (2011). Elucidating the role of matrix stiffness in 3D cell migration and remodeling. *Biophysical journal*, *100*(2), 284-293.

Elsner, J. J., & Zilberman, M. (2010). Novel antibiotic-eluting wound dressings: An in vitro study and engineering aspects in the dressing's design. *Journal of tissue viability*, *19*(2), 54-66.

Engler, A. J., Sen, S., Sweeney, H. L., & Discher, D. E. (2006). Matrix elasticity directs stem cell lineage specification. *Cell*, *126*(4), 677-689.

Esser, S., Lampugnani, M. G., Corada, M., Dejana, E., & Risau, W. (1998). Vascular endothelial growth factor induces VE-cadherin tyrosine phosphorylation in endothelial cells. *Journal of cell science*, *111*(13), 1853-1865.

Fang, Y., Al-Assaf, S., Phillips, G. O., Nishinari, K., Funami, T., & Williams, P. A. (2008). Binding behavior of calcium to polyuronates: comparison of pectin with alginate. Carbohydrate Polymers, 72(2), 334-341.

Folkman, J., & D'Amore, P. A. (1996). Blood vessel formation: what is its molecular basis?. *Cell*, *87*(7), 1153-1155.

Folkman, J., & Haudenschild, C. (1980). Angiogenesis in vitro.

Folkman, J., & Hochberg, M. (1973). Self-regulation of growth in three dimensions. *The Journal of experimental medicine*, *138*(4), 745-753.

Fonseca, K. B., Bidarra, S. J., Oliveira, M. J., Granja, P. L., & Barrias, C. C. (2011). Molecularly designed alginate hydrogels susceptible to local proteolysis as three-dimensional cellular microenvironments. *Acta biomaterialia*, *7*(4), 1674-1682.

Fonseca, K. B., Gomes, D. B., Lee, K., Santos, S. G., Sousa, A., Silva, E. A., ... & Barrias, C. C. (2013). Injectable MMP-sensitive alginate hydrogels as hMSC delivery systems. *Biomacromolecules*, *15*(1), 380-390.

Foubert, P., Matrone, G., Souttou, B., Leré-Déan, C., Barateau, V., Plouët, J., ... & Tobelem, G. (2008). Coadministration of endothelial and smooth muscle progenitor cells enhances the efficiency of proangiogenic cell-based therapy.*Circulation research*, *103*(7), 751-760.

Fraeye, I., Duvetter, T., Doungla, E., Van Loey, A., & Hendrickx, M. (2010). Fine-tuning the properties of pectin–calcium gels by control of pectin fine structure, gel composition and environmental conditions. Trends in food science & technology, 21(5), 219-228.

Fuchs, S., Hofmann, A., & Kirkpatrick, C. J. (2007). Microvessel-like structures from outgrowth endothelial cells from human peripheral blood in 2-dimensional and 3-dimensional co-cultures with osteoblastic lineage cells. *Tissue engineering*, *13*(10), 2577-2588.

Gerhardt, H., Golding, M., Fruttiger, M., Ruhrberg, C., Lundkvist, A., Abramsson, A., ... & Betsholtz, C. (2003). VEGF guides angiogenic sprouting utilizing endothelial tip cell filopodia. *The Journal of cell biology*, *161*(6), 1163-1177.

Ghajar, C. M., Chen, X., Harris, J. W., Suresh, V., Hughes, C. C., Jeon, N. L., ... & George, S. C. (2008). The effect of matrix density on the regulation of 3-D capillary morphogenesis. *Biophysical journal*, *94*(5), 1930-1941.

Ghanaati, S., Fuchs, S., Webber, M. J., Orth, C., Barbeck, M., Gomes, M. E., ... & James Kirkpatrick, C. (2011). Rapid vascularization of starch–poly (caprolactone) in vivo by outgrowth endothelial cells in co-culture with primary osteoblasts. *Journal of tissue engineering and regenerative medicine*, *5*(6), e136-e143.

Giancotti, F. G., & Ruoslahti, E. (1999). Integrin signaling. *Science*, *285*(5430), 1028-1033.

Goldberg, V. M. (1992). Natural history of autografts and allografts. In *Bone implant grafting* (pp. 9-12). Springer London.

Goldberger, A., Middleton, K. A., Oliver, J. A., Paddock, C., Yan, H. C., DeLisser, H. M., ... & Newman, P. J. (1994). Biosynthesis and processing of the cell adhesion molecule PECAM-1 includes production of a soluble form.*Journal of Biological Chemistry*, *269*(25), 17183-17191.

Green, D. W., Mann, S., & Oreffo, R. O. (2006). Mineralized polysaccharide capsules as biomimetic microenvironments for cell, gene and growth factor delivery in tissue engineering. *Soft Matter*, *2*(9), 732-737.

Grellier, M., Ferreira-Tojais, N., Bourget, C., Bareille, R., Guillemot, F., & Amédée, J. (2009). Role of vascular endothelial growth factor in the communication between

human osteoprogenitors and endothelial cells. *Journal of cellular biochemistry*, *106*(3), 390-398.

Grellier, M., Granja, P. L., Fricain, J. C., Bidarra, S. J., Renard, M., Bareille, R., ... & Barbosa, M. A. (2009). The effect of the co-immobilization of human osteoprogenitors and endothelial cells within alginate microspheres on mineralization in a bone defect. *Biomaterials*, *30*(19), 3271-3278.

Grinnell, F. (2000). Fibroblast–collagen-matrix contraction: growth-factor signalling and mechanical loading. *Trends in cell biology*, *10*(9), 362-365.

Grinnell, F., & Petroll, W. M. (2010). Cell motility and mechanics in three-dimensional collagen matrices. *Annual review of cell and developmental biology*, *26*, 335-361.

Groeber, F., Holeiter, M., Hampel, M., Hinderer, S., & Schenke-Layland, K. (2011). Skin tissue engineering—in vivo and in vitro applications. *Advanced drug delivery reviews*, *63*(4), 352-366.

Grzesik, W. J., & Robey, P. G. (1994). Bone matrix RGD glycoproteins: immunolocalization and interaction with human primary osteoblastic bone cells in vitro. *Journal of Bone and Mineral Research*, *9*(4), 487-496.

Guerreiro, S. G., Oliveira, M. J., Barbosa, M. A., Soares, R., & Granja, P. L. (2014). Neonatal Human Dermal Fibroblasts Immobilized in RGD-Alginate Induce Angiogenesis. *Cell transplantation*, *23*(8), 945-957.

Guo, S., & DiPietro, L. A. (2010). Factors affecting wound healing. *Journal of dental research*, *89*(3), 219-229.

Hall, H. (2007). Modified fibrin hydrogel matrices: both, 3D-scaffolds and local and controlled release systems to stimulate angiogenesis. *Current pharmaceutical design*, *13*(35), 3597-3607.

Harholt, J., Suttangkakul, A., & Scheller, H. V. (2010). Biosynthesis of pectin. *Plant physiology*, *153*(2), 384-395.

Hoffman, A. S. (2012). Hydrogels for biomedical applications. *Advanced drug delivery reviews*, *64*, 18-23.

Hofmann, A., Ritz, U., Verrier, S., Eglin, D., Alini, M., Fuchs, S., ... & Rommens, P. M. (2008). The effect of human osteoblasts on proliferation and neo-vessel formation of human umbilical vein endothelial cells in a long-term 3D co-culture on polyurethane scaffolds. *Biomaterials*, *29*(31), 4217-4226.

Hohn, H. P., Grümmer, R., Bosserhoff, S., Graf-Lingnau, S., Reuss, B., Bäcker, C., & Denker, H. W. (1996). The role of matrix contact and of cell-cell interactions in choriocarcinoma cell differentiation. *European journal of cell biology*, *69*(1), 76-85.

Huang, A. H., Yeger-McKeever, M., Stein, A., & Mauck, R. L. (2008). Tensile properties of engineered cartilage formed from chondrocyte-and MSC-laden hydrogels. *Osteoarthritis and Cartilage*, *16*(9), 1074-1082.

Ingber, D. E. (1990). Fibronectin controls capillary endothelial cell growth by modulating cell shape. *Proceedings of the National Academy of Sciences*,*87*(9), 3579-3583.

Ingber, D. E., & Folkman, J. (1989). Mechanochemical switching between growth and differentiation during fibroblast growth factor-stimulated angiogenesis in vitro: role of extracellular matrix. *The Journal of cell biology*, *109*(1), 317-330.

Inngjerdingen, K. T., Patel, T. R., Chen, X., Kenne, L., Allen, S., Morris, G. A., ... & Paulsen, B. S. (2007). Immunological and structural properties of a pectic polymer from Glinus oppositifolius. *Glycobiology*, *17*(12), 1299-1310.

Jackson, C. L., Dreaden, T. M., Theobald, L. K., Tran, N. M., Beal, T. L., Eid, M., ... & Mohnen, D. (2007). Pectin induces apoptosis in human prostate cancer cells: correlation of apoptotic function with pectin structure.*Glycobiology*, *17*(8), 805-819.

Jaffe, E. A., Nachman, R. L., Becker, C. G., & Minick, C. R. (1973). Culture of human endothelial cells derived from umbilical veins. Identification by morphologic and immunologic criteria. *Journal of Clinical Investigation*, *52*(11), 2745.

Janvier, R., Sourla, A., Koutsilieris, M., & Doillon, C. J. (1996). Stromal fibroblasts are required for PC-3 human prostate cancer cells to produce capillary-like formation of endothelial cells in a three-dimensional co-culture system. *Anticancer research*, *17*(3A), 1551-1557.

Johnen, C., Steffen, I., Beichelt, D., Bräutigam, K., Witascheck, T., Toman, N., ... & Gerlach, J. C. (2008). Culture of subconfluent human fibroblasts and keratinocytes using biodegradable transfer membranes. Burns, 34(5), 655-663.

Jones, I., Currie, L., & Martin, R. (2002). A guide to biological skin substitutes. *British journal of plastic surgery*, *55*(3), 185-193.

Kleinman, H. K., & Martin, G. R. (2005, October). Matrigel: basement membrane matrix with biological activity. In *Seminars in cancer biology* (Vol. 15, No. 5, pp. 378-386). Academic Press.

Kogan, G., Šoltés, L., Stern, R., & Gemeiner, P. (2007). Hyaluronic acid: a natural biopolymer with a broad range of biomedical and industrial applications. *Biotechnology letters*, *29*(1), 17-25.

Koh, W., Stratman, A. N., Sacharidou, A., & Davis, G. E. (2008). In vitro three dimensional collagen matrix models of endothelial lumen formation during vasculogenesis and angiogenesis. *Methods in enzymology*, *443*, 83-101.

Kolbe, M., Xiang, Z., Dohle, E., Tonak, M., Kirkpatrick, C. J., & Fuchs, S. (2011). Paracrine effects influenced by cell culture medium and consequences on microvessel-like structures in Co-cultures of mesenchymal stem cells and outgrowth endothelial cells. *Tissue Engineering Part A*, *17*(17-18), 2199-2212.

Korducki, J. M., Loftus, S. J., & Bahn, R. S. (1992). Stimulation of glycosaminoglycan production in cultured human retroocular fibroblasts.*Investigative ophthalmology & visual science*, *33*(6), 2037-2042.

Korff, T., Kimmina, S., Martiny-Baron, George., & Augustin, H. G. (2001). Blood vessel maturation in a 3-dimensional spheroidal Co-culture model: direct contact with smooth muscle cells regulates endothelial cell quiescence and abrogates VEGF responsiveness. *The FASEB Journal*, *15*(2), 447-457.

Kunz-Schughart, L. A., Schroeder, J. A., Wondrak, M., van Rey, F., Lehle, K., Hofstaedter, F., & Wheatley, D. N. (2006). Potential of fibroblasts to regulate the formation of three-dimensional vessel-like structures from endothelial cells in vitro. *American Journal of Physiology-Cell Physiology*, *290*(5), C1385-C1398.

Labat-Robert, J., Bihari-Varga, M., & Robert, L. (1990). Extracellular matrix.*FEBS letters*, *268*(2), 386-393.

Laurens, N., Engelse, M. A., Jungerius, C., Löwik, C. W., van Hinsbergh, V. W., & Koolwijk, P. (2009). Single and combined effects of αvβ3-and α5β1-integrins on capillary tube formation in a human fibrinous matrix.

Lee, J., Cuddihy, M. J., & Kotov, N. A. (2008). Three-dimensional cell culture matrices: state of the art. Tissue Engineering Part B: Reviews, 14(1), 61-86.

Li, X. Y., Wang, T., Jiang, X. J., Lin, T., Wu, D. Q., Zhang, X. Z., ... & Yuan, M. J. (2010). Injectable hydrogel helps bone marrow-derived mononuclear cells restore infarcted myocardium. Cardiology, 115(3), 194-199.

Liu, L., Fishman, M. L., Kost, J., & Hicks, K. B. (2003). Pectin-based systems for colon-specific drug delivery via oral route. Biomaterials, 24(19), 3333-3343.

Lokmic, Z., & Mitchell, G. M. (2008). Engineering the microcirculation. Tissue Engineering Part B: Reviews, 14(1), 87-103.

Lu, X., Dunn, J., Dickinson, A. M., Gillespie, J. I., & Baudouin, S. V. (2004). Smooth muscle α-actin expression in endothelial cells derived from CD34+ human cord blood cells. Stem cells and development, 13(5), 521-527.

Luttun, A., Carmeliet, G., & Carmeliet, P. (2002). Vascular progenitors: from biology to treatment. Trends in cardiovascular medicine, 12(2), 88-96.

MacNeil, S. (2007). Progress and opportunities for tissue-engineered skin.*Nature*, *445*(7130), 874-880.

Maia, F. R., Fonseca, K. B., Rodrigues, G., Granja, P. L., & Barrias, C. C. (2014). Matrix-driven formation of mesenchymal stem cell–extracellular matrix microtissues on soft alginate hydrogels. Acta biomaterialia, 10(7), 3197-3208.

Mani, S. A., Guo, W., Liao, M. J., Eaton, E. N., Ayyanan, A., Zhou, A. Y., ... & Weinberg, R. A. (2008). The epithelial-mesenchymal transition generates cells with properties of stem cells. Cell, 133(4), 704-715.

Mao, J., Zhao, L., de Yao, K., Shang, Q., Yang, G., & Cao, Y. (2003). Study of novel chitosan- gelatin artificial skin in vitro. Journal of Biomedical Materials Research Part A, 64(2), 301-308.

Martin, P. (1997). Wound healing--aiming for perfect skin regeneration. Science,276(5309), 75-81.

Maxwell, E. G., Belshaw, N. J., Waldron, K. W., & Morris, V. J. (2012). Pectin–an emerging new bioactive food polysaccharide. Trends in Food Science & Technology, 24(2), 64-73.

Melero-Martin, J. M., Khan, Z. A., Picard, A., Wu, X., Paruchuri, S., & Bischoff, J. (2007). In vivo vasculogenic potential of human blood-derived endothelial progenitor cells. Blood, 109(11), 4761-4768.

Metcalfe, A. D., & Ferguson, M. W. (2007). Bioengineering skin using mechanisms of regeneration and repair. Biomaterials, 28(34), 5100-5113.

Mohd Hilmi, A. B., Halim, A. S., Jaafar, H., Asiah, A. B., & Hassan, A. (2013). Chitosan dermal substitute and chitosan skin substitute contribute to accelerated full-thickness wound healing in irradiated rats. BioMed research international, 2013.

Mohnen, D. (2008). Pectin structure and biosynthesis. Current opinion in plant biology, 11(3), 266-277.

Momoh, F. U., Boateng, J. S., Richardson, S. C., Chowdhry, B. Z., & Mitchell, J. C. (2015). Development and functional characterization of alginate dressing as potential protein delivery system for wound healing. International journal of biological macromolecules, 81, 137-150.

Montesano, R., Orci, L., & Vassalli, P. (1983). In vitro rapid organization of endothelial cells into capillary-like networks is promoted by collagen matrices.The Journal of cell biology, 97(5), 1648-1652.

Montesano, R., Orci, L., and Vassalli, P. (1983) In vitro rapid organization of endothelial cells into capillary-like networks is promoted by collagen matrices, *J Cell Biol 97*, 1648-1652.

Montesano, R., Vassalli, J. D., Baird, A., Guillemin, R., & Orci, L. (1986). Basic fibroblast growth factor induces angiogenesis in vitro. Proceedings of the National Academy of Sciences, 83(19), 7297-7301.

Morita, T., & Kourembanas, S. (1995). Endothelial cell expression of vasoconstrictors and growth factors is regulated by smooth muscle cell-derived carbon monoxide. Journal of Clinical Investigation, 96(6), 2676.

Morra, M., Cassinelli, C., Cascardo, G., Nagel, M. D., Della Volpe, C., Siboni, S., ... & Ulvskov, P. (2004). Effects on interfacial properties and cell adhesion of surface modification by pectic hairy regions. Biomacromolecules, 5(6), 2094-2104.

Mudera, V., Smith, A. S. T., Brady, M. A., & Lewis, M. P. (2010). The effect of cell density on the maturation and contractile ability of muscle derived cells in a 3D tissue- engineered skeletal muscle model and determination of the cellular and mechanical stimuli required for the synthesis of a postural phenotype.Journal of cellular physiology, 225(3), 646-653.

Munarin, F., Giuliano, L., Bozzini, S., Tanzi, M. C., & Petrini, P. (2010). Mineral phase deposition on pectin microspheres. Materials Science and Engineering: C, 30(3), 491-496.

Munarin, F., Guerreiro, S. G., Grellier, M. A., Tanzi, M. C., Barbosa, M. A., Petrini, P., & Granja, P. L. (2011). Pectin-based injectable biomaterials for bone tissue engineering. Biomacromolecules, 12(3), 568-577.

Munarin, F., Petrini, P., Farè, S., & Tanzi, M. C. (2010). Structural properties of polysaccharide-based microcapsules for soft tissue regeneration. Journal of Materials Science: Materials in Medicine, 21(1), 365-375.

Munarin, F., Petrini, P., Tanzi, M. C., Barbosa, M. A., & Granja, P. L. (2012). Biofunctional chemically modified pectin for cell delivery. *Soft Matter*, *8*(17), 4731-4739.

Mutsaers, S. E., Bishop, J. E., McGrouther, G., & Laurent, G. J. (1997). Mechanisms of tissue repair: from wound healing to fibrosis. *The international journal of biochemistry & cell biology*, *29*(1), 5-17.

Nagel, M. D., Verhoef, R., Schols, H., Morra, M., Knox, J. P., Ceccone, G., ... & Siboni, S. (2008). Enzymatically-tailored pectins differentially influence the morphology, adhesion, cell cycle progression and survival of fibroblasts.*Biochimica et Biophysica Acta (BBA)-General Subjects*, *1780*(7), 995-1003.

Nakatsu, M. N., Sainson, R. C., Aoto, J. N., Taylor, K. L., Aitkenhead, M., Pérez-del-Pulgar, S., ... & Hughes, C. C. (2003). Angiogenic sprouting and capillary lumen formation modeled by human umbilical vein endothelial cells (HUVEC) in fibrin gels: the role of fibroblasts and Angiopoietin-1☆.*Microvascular research*, *66*(2), 102-112.

Nakatsu, M. N., Sainson, R. C., Pérez-del-Pulgar, S., Aoto, J. N., Aitkenhead, M., Taylor, K. L., ... & Hughes, C. C. (2003). VEGF121 and VEGF165 regulate blood vessel diameter through vascular endothelial growth factor receptor 2 in an in vitro angiogenesis model. *Laboratory investigation*, *83*(12), 1873-1885.

Nam, M. H., Lee, H. S., Seomun, Y., Lee, Y., & Lee, K. W. (2011). Monocyte-endothelium-smooth muscle cell interaction in co-culture: proliferation and cytokine productions in response to advanced glycation end products.*Biochimica et Biophysica Acta (BBA)-General Subjects*, *1810*(9), 907-912.

Nehls, V., Herrmann, R., Hühnken, M., & Palmetshofer, A. (1998). Contact-dependent inhibition of angiogenesis by cardiac fibroblasts in three-dimensional fibrin gels in vitro: implications for microvascular network remodeling and coronary collateral formation. *Cell and tissue research*, *293*(3), 479-488.

Neufeld, G., Cohen, T., Gengrinovitch, S., & Poltorak, Z. (1999). Vascular endothelial growth factor (VEGF) and its receptors. *The FASEB Journal*, *13*(1), 9-22.

Neves, S. C., Gomes, D. B., Sousa, A., Bidarra, S. J., Petrini, P., Moroni, L., ... & Granja, P. L. (2015). Biofunctionalized pectin hydrogels as 3D cellular microenvironments. *Journal of Materials Chemistry B*, *3*(10), 2096-2108.

Nichol, J. W., & Khademhosseini, A. (2009). Modular tissue engineering: engineering biological tissues from the bottom up. *Soft matter*, *5*(7), 1312-1319.

Nikkhah, M., Eshak, N., Zorlutuna, P., Annabi, N., Castello, M., Kim, K., ... & Khademhosseini, A. (2012). Directed endothelial cell morphogenesis in micropatterned gelatin methacrylate hydrogels. *Biomaterials*, *33*(35), 9009-9018.

Noseda, M., Fu, Y., Niessen, K., Wong, F., Chang, L., McLean, G., & Karsan, A. (2006). Smooth muscle α-actin is a direct target of Notch/CSL. *Circulation research*, *98*(12), 1468-1470.

Noseda, M., McLean, G., Niessen, K., Chang, L., Pollet, I., Montpetit, R., ... & Karsan, A. (2004). Notch activation results in phenotypic and functional changes consistent with endothelial-to-mesenchymal transformation. *Circulation research*, *94*(7), 910-917.

Novosel, E. C., Kleinhans, C., & Kluger, P. J. (2011). Vascularization is the key challenge in tissue engineering. *Advanced drug delivery reviews*, *63*(4), 300-311.

Palamà, I. E., D'Amone, S., Coluccia, A. M., Biasiucci, M., & Gigli, G. (2012). Cell self-patterning on uniform PDMS-surfaces with controlled mechanical cues.*Integrative Biology*, *4*(2), 228-236.

Park, S. N., Kim, J. K., & Suh, H. (2004). Evaluation of antibiotic-loaded collagen-hyaluronic acid matrix as a skin substitute. Biomaterials, 25(17), 3689-3698.

Pataky, K., Braschler, T., Negro, A., Renaud, P., Lutolf, M. P., & Brugger, J. (2012). Microdrop Printing of Hydrogel Bioinks into 3D Tissue-Like Geometries.*Advanced Materials*, *24*(3), 391-396.

Pepper, M. S., Ferrara, N., Orci, L., & Montesano, R. (1992). Potent synergism between vascular endothelial growth factor and basic fibroblast growth factor in the induction of angiogenesis in vitro. *Biochemical and biophysical research communications*, *189*(2), 824-831.

Pereira, R. F., Barrias, C. C., Granja, P. L., & Bartolo, P. J. (2013). Advanced biofabrication strategies for skin regeneration and repair. *Nanomedicine*, *8*(4), 603-621.

Pereira, R., Carvalho, A., Vaz, D. C., Gil, M. H., Mendes, A., & Bártolo, P. (2013). Development of novel alginate based hydrogel films for wound healing applications. *International journal of biological macromolecules*, *52*, 221-230.

Petrie, T. A., Capadona, J. R., Reyes, C. D., & García, A. J. (2006). Integrin specificity and enhanced cellular activities associated with surfaces presenting a recombinant fibronectin fragment compared to RGD supports. *Biomaterials*,*27*(31), 5459-5470.

Pierschbacher, M. D., & Ruoslahti, E. (1987). Influence of stereochemistry of the sequence Arg-Gly-Asp-Xaa on binding specificity in cell adhesion. *Journal of Biological Chemistry*, *262*(36), 17294-17298.

Pinkney, J. H., Stehouwer, C. D., Coppack, S. W., & Yudkin, J. S. (1997). Endothelial dysfunction: cause of the insulin resistance syndrome. *Diabetes*,*46*(Supplement 2), S9-S13.

Place, E. S., Evans, N. D., & Stevens, M. M. (2009). Complexity in biomaterials for tissue engineering. *Nature materials*, *8*(6), 457-470.

Poliseno, L., Tuccoli, A., Mariani, L., Evangelista, M., Citti, L., Woods, K., ... & Rainaldi, G. (2006). MicroRNAs modulate the angiogenic properties of HUVECs. *Blood*, *108*(9), 3068-3071.

Price, L. S. (1997). Morphological control of cell growth and viability. *Bioessays*,*19*(11), 941-943.

Puliafito, A., Hufnagel, L., Neveu, P., Streichan, S., Sigal, A., Fygenson, D. K., & Shraiman, B. I. (2012). Collective and single cell behavior in epithelial contact inhibition. *Proceedings of the National Academy of Sciences*, *109*(3), 739-744.

Qiu, Y., & Park, K. (2012). Environment-sensitive hydrogels for drug delivery.*Advanced drug delivery reviews*, *64*, 49-60.

Raeber, G. P., Lutolf, M. P., & Hubbell, J. A. (2005). Molecularly engineered PEG hydrogels: a novel model system for proteolytically mediated cell migration. *Biophysical journal*, *89*(2), 1374-1388.

Ratner, B. D., Hoffman, A. S., Schoen, F. J., & Lemons, J. E. (2004).*Biomaterials science: an introduction to materials in medicine*. Academic press..

Ratner, B. D., Hoffman, A. S., Schoen, F. J., & Lemons, J. E. Biomaterials science: an introduction to materials in medicine. 1996. *Academic Press: New York*, *56*, 57-58.

Reilly, G. C., & Engler, A. J. (2010). Intrinsic extracellular matrix properties regulate stem cell differentiation. *Journal of biomechanics*, *43*(1), 55-62.

Reinhart-King, C. A. (2011). How matrix properties control the self-assembly and maintenance of tissues. *Annals of biomedical engineering*, *39*(7), 1849-1856.

Reinhart-King, C. A., Dembo, M., & Hammer, D. A. (2008). Cell-cell mechanical communication through compliant substrates. *Biophysical journal*, *95*(12), 6044-6051.

Ribatti, D., Nico, B., and Crivellato, E. (2011) The role of pericytes in angiogenesis, Int *J Dev Biol* 55, 261-268.

Ribeiro, C. C., Barrias, C. C., & Barbosa, M. A. (2004). Calcium phosphate-alginate microspheres as enzyme delivery matrices. *Biomaterials*, *25*(18), 4363-4373.

Ridley, B. L., O'Neill, M. A., & Mohnen, D. (2001). Pectins: structure, biosynthesis, and oligogalacturonide-related signaling. *Phytochemistry*, *57*(6), 929-967.

Rivron, N. C., Liu, J., Rouwkema, J., Boer, J. D., & Blitterswijk, V. C. (2008). Engineering vascularised tissues in vitro. *European cells & materials*, *15*, 27-40.

Romer, L. H., Birukov, K. G., & Garcia, J. G. (2006). Focal adhesions paradigm for a signaling nexus. *Circulation research*, *98*(5), 606-616.

Rouwkema, J., Rivron, N. C., & van Blitterswijk, C. A. (2008). Vascularization in tissue engineering. *Trends in biotechnology*, *26*(8), 434-441.

Rowley, J. A., & Mooney, D. J. (2002). Alginate type and RGD density control myoblast phenotype. *Journal of biomedical materials research*, *60*(2), 217-223.

Rowley, J. A., Madlambayan, G., & Mooney, D. J. (1999). Alginate hydrogels as synthetic extracellular matrix materials. *Biomaterials*, *20*(1), 45-53.

Ruoslahti, E., & Pierschbacher, M. D. (1987). New perspectives in cell adhesion: RGD and integrins. *Science*, *238*(4826), 491-497.

Ruoslahti, E., & Rajotte, D. (2000). An address system in the vasculature of normal tissues and tumors. *Annual review of immunology*, *18*(1), 813-827.

Saito, M., Hamasaki, M., & Shibuya, M. (2003). Induction of tube formation by angiopoietin-1 in endothelial cell/fibroblast co-culture is dependent on endogenous VEGF. *Cancer science*, *94*(9), 782-790.

Salcedo, R., Wasserman, K., Young, H. A., Grimm, M. C., Howard, O. Z., Anver, M. R., ... & Oppenheim, J. J. (1999). Vascular endothelial growth factor and basic fibroblast growth factor induce expression of CXCR4 on human endothelial cells: in vivo

neovascularization induced by stromal-derived factor-1α. *The American journal of pathology*, *154*(4), 1125-1135.

Santos, M. I., Unger, R. E., Sousa, R. A., Reis, R. L., & Kirkpatrick, C. J. (2009). Crosstalk between osteoblasts and endothelial cells co-cultured on a polycaprolactone–starch scaffold and the in vitro development of vascularization.*Biomaterials*, *30*(26), 4407-4415.

Saunders, R. L., & Hammer, D. A. (2010). Assembly of human umbilical vein endothelial cells on compliant hydrogels. *Cellular and molecular bioengineering*,*3*(1), 60-67.

Schubert, S. Y., Benarroch, A., Ostvang, J., & Edelman, E. R. (2008). Regulation of endothelial cell proliferation by primary monocytes.*Arteriosclerosis, thrombosis, and vascular biology*, *28*(1), 97-104.

Schweigerer, L., Neufeld, G., Friedman, J., Abraham, J. A., Fiddes, J. C., & Gospodarowicz, D. (1987). Capillary endothelial cells express basic fibroblast growth factor, a mitogen that promotes their own growth. *Nature*, *325*(6101), 257-259.

Seghezzi, G., Patel, S., Ren, C. J., Gualandris, A., Pintucci, G., Robbins, E. S., ... & Mignatti, P. (1998). Fibroblast growth factor-2 (FGF-2) induces vascular endothelial growth factor (VEGF) expression in the endothelial cells of forming capillaries: an autocrine mechanism contributing to angiogenesis. *The Journal of cell biology*, *141*(7), 1659-1673.

Seidlits, S. K., Drinnan, C. T., Petersen, R. R., Shear, J. B., Suggs, L. J., & Schmidt, C. E. (2011). Fibronectin–hyaluronic acid composite hydrogels for three-dimensional endothelial cell culture. *Acta biomaterialia*, *7*(6), 2401-2409.

Serini, G., Valdembri, D., & Bussolino, F. (2006). Integrins and angiogenesis: a sticky business. *Experimental cell research*, *312*(5), 651-658.

Shahdadfar, A., Frønsdal, K., Haug, T., Reinholt, F. P., & Brinchmann, J. E. (2005). In vitro expansion of human mesenchymal stem cells: choice of serum is a determinant of cell proliferation, differentiation, gene expression, and transcriptome stability. *Stem cells*, *23*(9), 1357-1366.

Sieminski, A. L., Hebbel, R. P., & Gooch, K. J. (2004). The relative magnitudes of endothelial force generation and matrix stiffness modulate capillary morphogenesis in vitro. *Experimental cell research*, *297*(2), 574-584.

Silva, E. A., & Mooney, D. J. (2010). Effects of VEGF temporal and spatial presentation on angiogenesis. *Biomaterials*, *31*(6), 1235-1241.

Sorrell, J. M., Baber, M. A., & Caplan, A. I. (2007). A self-assembled fibroblast-endothelial cell co-culture system that supports in vitro vasculogenesis by both human

umbilical vein endothelial cells and human dermal microvascular endothelial cells. *Cells Tissues Organs*, *186*(3), 157-168.

Soucy, P. A., & Romer, L. H. (2009). Endothelial cell adhesion, signaling, and morphogenesis in fibroblast-derived matrix. *Matrix Biology*, *28*(5), 273-283.

Sriamornsak, P., Thirawong, N., Weerapol, Y., Nunthanid, J., & Sungthongjeen, S. (2007). Swelling and erosion of pectin matrix tablets and their impact on drug release behavior. *European Journal of Pharmaceutics and Biopharmaceutics*,*67*(1), 211-219.

Stahl, A., Wenger, A., Weber, H., Stark, G. B., Augustin, H. G., & Finkenzeller, G. (2004). Bi-directional cell contact-dependent regulation of gene expression between endothelial cells and osteoblasts in a three-dimensional spheroidal Co-culture model. *Biochemical and biophysical research communications*, *322*(2), 684-692.

Stephen-Haynes, J., Gibson, E., & Greenwood, M. (2014). Chitosan: a natural solution for wound healing. *Journal of Community Nursing*, *28*(1), 48-53.

Stupack, D. G., & Cheresh, D. A. (2003). Apoptotic cues from the extracellular matrix: regulators of angiogenesis. *Oncogene*, *22*(56), 9022-9029.

Talukdar, S., Nguyen, Q. T., Chen, A. C., Sah, R. L., & Kundu, S. C. (2011). Effect of initial cell seeding density on 3D-engineered silk fibroin scaffolds for articular cartilage tissue engineering. *Biomaterials*, *32*(34), 8927-8937.

Tho, I., Kjøniksen, A. L., Nyström, B., & Roots, J. (2003). Characterization of association and gelation of pectin in methanol-water mixtures.*Biomacromolecules*, *4*(6), 1623-1629.

Tibbitt, M. W., & Anseth, K. S. (2009). Hydrogels as extracellular matrix mimics for 3D cell culture. *Biotechnology and bioengineering*, *103*(4), 655-663.

Traphagen, S. B., Titushkin, I., Sun, S., Wary, K. K., & Cho, M. (2013). Endothelial invasive response in a co-culture model with physically-induced osteodifferentiation. *Journal of tissue engineering and regenerative medicine*,*7*(8), 621-630.

Trkov, S., Eng, G., Di Liddo, R., Parnigotto, P. P., & Vunjak-Novakovic, G. (2010). Micropatterned three-dimensional hydrogel system to study human endothelial–mesenchymal stem cell interactions. *Journal of tissue engineering and regenerative medicine*, *4*(3), 205-215.

Unger, R. E., Sartoris, A., Peters, K., Motta, A., Migliaresi, C., Kunkel, M., ... & Kirkpatrick, C. J. (2007). Tissue-like self-assembly in Co-cultures of endothelial cells and osteoblasts and the formation of microcapillary-like structures on three-dimensional porous biomaterials. *Biomaterials*, *28*(27), 3965-3976.

Urb, M., & Sheppard, D. C. (2012). The role of mast cells in the defence against pathogens. *PLoS Pathog*, *8*(4), e1002619.

Velazquez, O. C., Snyder, R., Liu, Z. J., Fairman, R. M., & Herlyn, M. (2002). Fibroblast-dependent differentiation of human microvascular endothelial cells into capillary-like 3-dimensional networks. *The FASEB Journal*, *16*(10), 1316-1318.

Ventre, M., Causa, F., & Netti, P. A. (2012). Determinants of cell–material crosstalk at the interface: towards engineering of cell instructive materials.*Journal of The Royal Society Interface*, *9*(74), 2017-2032.

Wang, C., Varshney, R. R., & Wang, D. A. (2010). Therapeutic cell delivery and fate control in hydrogels and hydrogel hybrids. *Advanced drug delivery reviews*,*62*(7), 699-710.

Wang, T. W., Sun, J. S., Wu, H. C., Tsuang, Y. H., Wang, W. H., & Lin, F. H. (2006). The effect of gelatin–chondroitin sulfate–hyaluronic acid skin substitute on wound healing in SCID mice. Biomaterials, 27(33), 5689-5697.

Wenger, A., Kowalewski, N., Stahl, A., Mehlhorn, A. T., Schmal, H., Stark, G. B., & Finkenzeller, G. (2005). Development and characterization of a spheroidal Co-culture model of endothelial cells and fibroblasts for improving angiogenesis in tissue engineering. *Cells Tissues Organs*, *181*(2), 80-88.

Wu, Y., Chen, L., Scott, P. G., & Tredget, E. E. (2007). Mesenchymal stem cells enhance wound healing through differentiation and angiogenesis. *Stem cells*, *25*(10), 2648-2659.

Yamada, K. M., & Geiger, B. (1997). Molecular interactions in cell adhesion complexes. *Current opinion in cell biology*, *9*(1), 76-85.

Yamamoto, K., Takahashi, T., Asahara, T., Ohura, N., Sokabe, T., Kamiya, A., & Ando, J. (2003). Proliferation, differentiation, and tube formation by endothelial progenitor cells in response to shear stress. *Journal of Applied Physiology*,*95*(5), 2081-2088.

Yao, L., & Swords, G. A. (2001). *U.S. Patent No. 6,268,405*. Washington, DC: U.S. Patent and Trademark Office.

Yapo, B. M. (2011). Pectic substances: From simple pectic polysaccharides to complex pectins—A new hypothetical model. *Carbohydrate Polymers*, *86*(2), 373-385.

Yildirimer, L., Thanh, N. T., & Seifalian, A. M. (2012). Skin regeneration scaffolds: a multimodal bottom-up approach. *Trends in biotechnology*, *30*(12), 638-648.

Yu, J., Gu, Y., Du, K. T., Mihardja, S., Sievers, R. E., & Lee, R. J. (2009). The effect of injected RGD modified alginate on angiogenesis and left ventricular function in a chronic rat infarct model. *Biomaterials*, *30*(5), 751-756.

Yu, L., & Ding, J. (2008). Injectable hydrogels as unique biomedical materials.*Chemical Society Reviews*, *37*(8), 1473-1481.

Zanetta, L., Marcus, S. G., Vasile, J., Dobryansky, M., Cohen, H., Eng, K., ... & Mignatti, P. (2000). Expression of von Willebrand factor, an endothelial cell marker, is

up-regulated by angiogenesis factors: A potential method for objective assessment of tumor angiogenesis. *International journal of cancer*,*85*(2), 281-288.

Zhang, C., Sangaj, N., Hwang, Y., Phadke, A., Chang, C. W., & Varghese, S. (2011). Oligo (trimethylene carbonate)–poly (ethylene glycol)–oligo (trimethylene carbonate) triblock-based hydrogels for cartilage tissue engineering. *Acta biomaterialia*, *7*(9), 3362-3369.

Zheng, Y., Chen, J., Craven, M., Choi, N. W., Totorica, S., Diaz-Santana, A., ... & Stroock, A. D. (2012). In vitro microvessels for the study of angiogenesis and thrombosis. *Proceedings of the National Academy of Sciences*, *109*(24), 9342-9347.

Zöller, N., Valesky, E., Butting, M., Hofmann, M., Kippenberger, S., Bereiter-Hahn, J., ... & Kaufmann, R. (2014). Clinical Application of a Tissue-Cultured Skin Autograft: An Alternative for the Treatment of Non-Healing or Slowly Healing Wounds. Dermatology, 229(3), 190-198.

Annexes

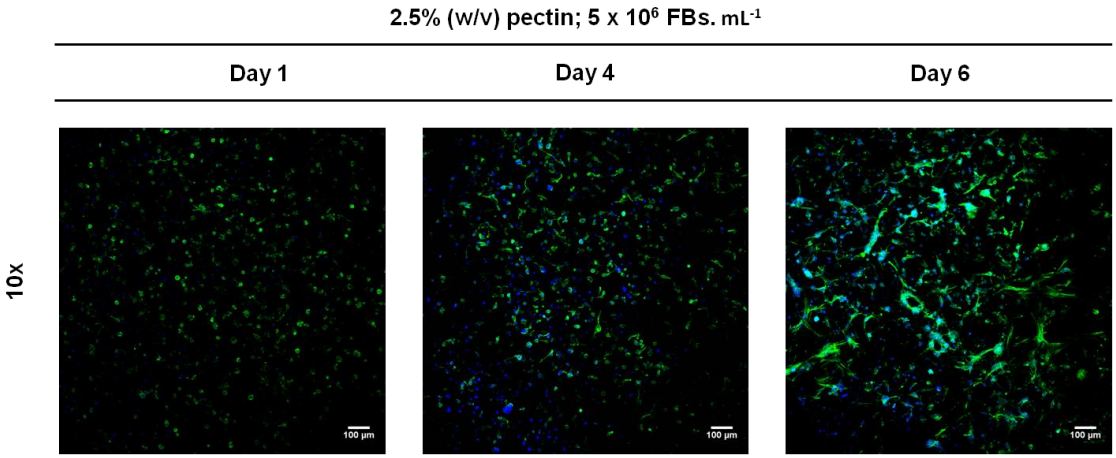

Figure 27. Effect of the initial seeding density on a 2.5% pectin 3D hydrogel on FBs' spatial distibution within a 6 days culture period. Pectin surface view. FBs were stained for F-actin with Alexa Fluor 488 phalloidin (Green) and nuclei were counterstained with DAPI (Blue). Scale bars, 100 µm.